KONINKLIJKE NEDERLANDSE AKADEMIE VAN WETENSCHAPPEN

PROCEEDINGS

SERIES B

PHYSICAL SCIENCES

VOLUME LXIV - No. 5

NORTH-HOLLAND PUBLISHING COMPANY - AMSTERDAM - 1961

The complete Proceedings consist of three Series, viz.:

SERIES A: MATHEMATICAL SCIENCES

SERIES B: PHYSICAL SCIENCES

SERIES C: BIOLOGICAL AND MEDICAL SCIENCES

Articles for these Series cannot be accepted unless formally communicated for publication by one of the members of the Royal Neth. Academy of Sciences.

BIOCHEMISTRY

A SIMPLE METHOD TO DIFFERENTIATE BETWEEN CHOLINE AND ETHANOLAMINE CONTAINING PHOSPHATIDES ON PAPER CHROMATOGRAMS. Ia

BY

H. G. BUNGENBERG DE JONG

(Communicated at the meeting of April 29, 1961)

1. Introduction

In a former communication a spot test for phosphatidyl ethanolamine (cephalin) and lyso phosphatidyl ethanolamine (lysocephalin) has been given, which may be applied to paper chromatograms of phosphatides [1]. It is based on the wellknown reaction of CS_2 with primary amines, followed by decomposition de composition of the dithiocarbamate with acidified $AgNO_3$ solution. The H_2S set free forms brown Ag_2S.

In applying this reaction to cephalin or lyso cephalin one must bear in mind that these compounds have no free NH_2groups, but ionized groups $NH_3^{\bullet}$, which do not react with CS_2.

Hence in principle we must follow the method given by Feigl for salts of primary amines [2], that is one lets react CS_2 in the presence of triethylamine, the latter setting free the undissociated base.

The reagent solution given by Feigl, however, cannot be applied to cephalin or lyso cephalin spots on chromatograms as these phosphatides are dissolved by this solution.

The method developed for chromatograms, therefore, comprises two steps:

a) The formation of the dithiocarbamate by exposure of the dry chromatogram to the vapours of CS_2 and triethylamine.

b) After evaporation of excess reagent in air, the chromatogram is spread out on filter paper thoroughly wetted with an acidified (HNO_3) solution of $AgNO_3$ in water during 15 min., followed by repeated rinsing with distilled water containing some $UO_2(NO_3)_2$.

In the case of chromatograms on silica-impregnated paper, brown spots are obtained when the surface concentration of (lyso) cephalin is not too low. The sensitivity of the reaction is, however, about 3 times lower than the sensitivity of the tricomplex staining (Acid Fuchsin–$UO_2(NO_3)_2$–0.01 N HCl) [1].

A weak cephalin spot, which is still just visible with the tricomplex staining may fail to give a visible brown spot. One might then erroneously

conclude that the spot in question is a choline containing phosphatide.

With chromatograms on low capacity silica-impregnated paper ($SiCl_4$-treated paper) or on non-impregnated paper the brown spots are only visible with difficulty. The method has its inconveniences, which reside in the necessity to perform the second step in the dark and to wash away perfectly all $AgNO_3$ from the paper, lest the paper-background will turn dark later. This intensive washing may also lead to loss of phosphatides from the paper, though in the presence of some $UO_2(NO_3)_2$ the loss is less.

A very simple and convenient method as described in the present communication consists in forming the dithiocarbamate by exposure of the chromatogram to the vapours of CS_2 and triethylamine, after which, as a second step, the treated chromatogram is stained with a suitable solution.

We here use either the tricomplex staining bath, or a similar bath$_t$ containing in addition Brilliant Green. From a comparison of the staining results with those of identical chromatograms, which have not previously been exposed to CS_2 and triethylamine vapours, we may conclude which of the spots on the chromatogram are cephalin or lysocephalin and which are choline-containing phosphatides. The new method is free from the inconveniences and dangers inherent to step b of the original method. Because of its greater sensitivity it allows reliable conclusions in the case of low capacity papers ($SiCl_4$-treated papers). The results will show that even non-impregnated papers may be used in chromatography of phosphatides, the structure of eventual composite spots being revealed by this method.

2. Principle of the new method

It had already been found in [1], that when a chromatogram stained with the dithiocarbamate-$AgNO_3$ method is subsequently stained with the tricomplex staining method, a chromatogram is obtained on which the choline-containing phosphatides are stained red, the ethanolamine-containing phosphatides remain brown. This proves that in the decomposition of the dithiocarbamate with $AgNO_3$ in acid medium the ethanolamine-containing phosphatides are not regenerated.

The decomposition with $AgNO_3$ in acid-medium might be supposed indispensable for the dropping out of the tricomplex staining. This appeared not to be the case. Spots of cephalin or lysocephalin applied on the paper and exposed sufficiently long to the vapour of CS_2 and triethylamine, are thereafter no longer stainable with the tricomplex staining bath. Thus either the dithiocarbamate persists as such in the acid-medium of the tricomplex-staining-bath, or a decomposition occurs in such a way that the original ethanolamine-containing phosphatide is not regenerated.

As a result, the amphoion-structure required for the tricomplex staining [3], is no longer present. We may expect that such spots after treatment with vapours of CS_2 and triethylamine will stain green with a mixed

staining bath containing besides Acid Fuchsin and $UO_2(NO_3)_2$, also Brilliant Green. As in the formation of the dithiocarbamate the phosphate group remains intact, the reaction product must have a strongly acid character and it will stain with a basic dye. It was found indeed that cephalin and lyso-cephalin spots after exposure to vapours of CS_2 and triethylamine are rapidly stained green in the mixed staining bath.

The sensitivity of this green staining equals, and may surpass the sensitivity of the red staining of unchanged cephalin and lyso-cephalin with the tricomplex staining bath.

To apply the new method in either of the two variants to chromatograms of phosphatide mixtures we should compare the staining results with those of identical chromatograms, not previously exposed to CS_2 and triethylamine vapours. A certain spot represents an ethanolamine-containing phosphatide when:

a) With the tricomplex staining method this spot drops out.

b) With the mixed staining bath we obtain a green spot instead of a red spot.

The latter of these two variants is the more sensitive.

To obtain a complete disappearance of the tricomplex staining, all cephalin or lysocephalin in the spot must have reacted. When a spot is not exposed long enough to CS_2 and triethylamine vapour, certain layers of the phosphatide in the spot have not yet reacted and we will observe a more or less strong decrease in the red staining of the spot. We will meet examples of this in the following section.

A much shorter exposure of the spots to the CS_2 and triethylamine vapour suffices already to give the practical green end colouration of the spot.

This resides on the fact that the dithiocarbamate formation begins in the outer layers of the phosphatide in the spot, and when it has proceded to a certain depth it gives already the green end colouration, though the layers further inside may not yet have reacted completely.

3. Remark on serine phosphatides

These phosphatides contain two acidic groups (phosphate and carboxyl) and one basic group (amino).

What should we expect for the tricomplex staining?

If at the pH of the staining bath the carboxylgroup were completely undissociated, the serine phosphatide will have one ionized phosphategroup and one ionized amino group. It would then just as cephalin (phosphatidyl-ethanolamine) stain strongly red, both in the tricomplex staining bath and in the mixed staining bath.

If, to the contrary, the carboxylgroup were to be still completely dissociated, we would have two negative charges against one positive charge. Then no red staining will occur in the tricomplex staining bath, and a green staining will take place in the mixed staining bath.

As the COOH is in amino acids stronger than in fatty acids the carboxylgroup will not be wholly undissociated. Hence serine phosphatides must be expected to

give only a weak red colour with the tricomplex staining bath. Further they will stain green though possibly not at maximum intensity in the mixed staining bath.

We may further expect that after a previous treatment with CS_2 and triethylamine vapour, the weak red staining in the tricomplex staining bath will drop out and the intensity of the green staining in the mixed staining bath will be increased. These expectations could not be tested rigorously as we had not yet at our disposal a pure column fraction of serine phosphatides. Observations in our laboratory, however, support the above expectations. [1])

4. Experimental technique

a) *Phosphatide preparations used for chromatography.*

For the greater part of the chromatograms we have used freshly prepared and reasonably pure column fractions of the following phosphatides:

lecitin (L); cephalin (C); sphingomyelin (S); lysolecithin (LL) and lysocephalin (LC), the latter having been prepared from a cephalin fraction by means of snake venom. [2])

The concentration of the L fraction was known, it was diluted to 0,3 %. The other fractions were diluted until they gave spots of about the same area on chromatograms with $SiCl_4$-treated paper.

These concentrations will have been in the same order of that of L.

b) *Chromatographic papers.*

Throughout the greater part of the investigation we used Schleicher and Schüll paper 2043 B, either as such or silica impregnated. In some experiment also other papers have been used (Whatman nr. 1 and Ederol 208).

Most experiments have been performed with washed $SiCl_4$-treated paper, a kind of silica impregnated paper with a relatively low capacity.

It is easily prepared and has the advantage that even large sheets of the prepared paper show the same chromatographic properties on the whole sheet.

For $SiCl_4$-treated papers see in general the series of communications mentioned in [4]. The variant "washed $SiCl_4$-treated paper" has been described in Part IV Section 2, of the above mentioned series [3]).

In some experiments we have also used another variant, namely "neutralized

---

[1]) F. A. Deierkauf and F. J. M. Heslinga found spots on paper chromatograms of total phosphatides of rat, human and beef brain, of beef spinal chord, of rat-liver and rat-kidney, which are situated where according to the literature serine phosphatides should be expected.

These spots stained weakly red in the tricomplex staining bath and green in the mixed staining bath.

J. Th. Hoogeveen finding the same spots on paper chromatograms of total phosphatide extracts of beef spinal chord, has observed that the weak red spot drops out after previous treatment with CS_2 and triethylamine, further that in such a case the intensity of the green staining of the spot in the mixed staining bath is stronger.

[2]) We thank Mr J. Th. Hoogeveen for placing the column fractions of C, L, S and LL to our disposal, also Dr G. J. M. Hooghwinkel, who prepared the LC-fraction.

[3]) The hope expressed in Part IV that this variant would not markedly change its chromatographic properties with time, has not been fulfilled. In the course of some weeks, when hanging in air, the spot pattern on the chromatograms shifts gradually in upward direction. For comparative studies with small strips (4,5 $\times$ 21 cm) we therefore must always take strips prepared on the same day.

$SiCl_4$-treated paper", the preparation of which has been described in Part I of the above mentioned series of communications.

In a number of experiments we also used silica-impregnated paper prepared in the conventional way (soaking in a silicate solution, coagulation in a 6 N HCl solution and washing first with tap water, then with distilled water and starting from Schleicher and Schüll No 2043 B or Ederol 208 [1]).

c) *Chromatographic apparatus and mobile phase.*

We made use exclusively of the small slit-feeding apparatus (for strips 4,5 × 21,5 cm.) or the large slit-feeding apparatus for larger sheets (for instance of 17 × 27 cm), which have been described in a former communication [5]. As mobile phase was used in most cases di-isobutyl ketone — acetic acid — H_2O = 50:25:5; in some cases in the proportion 40:25:5.

Chromatography was performed in a dark room at constant temperature (20°).

d) *Treatment with* CS_2 *and triethylamine vapours.*

After finishing the chromatographic run, the paper is dried in a stream of warm air and is left hanging in air.

Those small strips or parts of larger sheets which will be treated with CS_2 and triethylamine we suspended in air for at least 1 hour.

We use for the reaction a low empty desiccator or a low cylindrical glass of wide diameter covered with a glass plate.

On the bottom stands a Petri-dish, in which just before use we pipette successively 1 ml triethylamine and 1—2 ml CS_2.

Immediately after the chromatogram is placed in the air space of the desiccator or cylinderglass and it is left there in at least $\frac{1}{2}$ hour.

This time is for non-impregnated paper and $SiCl_4$-treated paper sufficient when we intend to stain with the mixed staining bath.

To observe whether certain spots completely drop out when staining with the tricomplex staining bath, this time is critically short.

A time of 1 hour is in general safer and suffices also for silica papers prepared in the conventional way. Here too a still longer time is necessary to obtain a complete drop out of red spots in the tricomplex staining bath.

Next the paper is removed and is dried in a stream of warm air, for instance by hanging above the central heating to remove excess reagent. A half hour later we may proceed to stain the chromatogram.

e) *Staining procedures.*

The solutions needed for staining and rinsing after staining have been given in the next survey.

formula	Brilliant Green %	Acid Fuchsin %	Uranyl nitrate %	HCl N	Acetic acid N	
A	—	0,02	0,2	0,01	—	Tricomplex-staining [2])
B	—	—	0,2	0,01	—	
C	0,01	0,02	0,04	—	0,1	mixed staining [3])
D	—	—	0,04	0,01	—	
E	—	—	0,04	—	0,1	

Notes on next page.

1) We thank Dr G. J. M. Hooghwinkel for providing us with sheets of silica-impregnated Schleicher and Schüll paper and F. A. Deyerkauf and F. J. M. Heslinga for sheets of silica impregnated Ederol 208.

The staining solutions A and C are stored in the refrigerator to prevent mould growth; the rinsing solutions are kept in store at room temperature.

Tricomplex staining.

This staining is performed at room temperature during $\frac{1}{2}$–$\frac{3}{4}$ hour with solution A. It is then rinsed 10 min. with solution B (eventually for a second time 10 min. with a fresh portion).

After blotting the chromatogram is dried with a stream of warm air, for instance with a hairdryer. Phosphatides of the amphionic type, thus L, C, S, LL and LC are stained red, while acidic phosphatides (for instance inositol-phosphatides) or other acidic substances remain unstained.

Staining with the improved mixed staining bath [6].

It is essential to take a fresh cold portion from the stock in the refrigeration for every staining with this bath. It is stained for 1 hour with bath C; after blotting the chromatogram is rinsed 10 minutes with rinsing bath D, (eventually a second 10 minutes with a fresh portion D), blotted and rinsed 10 min. with rinsing bath E.

After blotting, the chromatogram is dried with a stream of warm air.

Phosphatides of the amphionic type (L. C. S. LL, LC) appear as red or purple spots (purple as a result of green back ground colouration), acidic phosphatides and other acidic substance appear as green spots.

Because of the green background colouration due to acidic contaminations in the paper very weakly by green spots may be masked. The background colouration may be diminished by certain pretreatments of the paper before chromatography, for details of which see [6].

Such preliminary treated papers, however, have not been used in the present investigation.

EXPERIMENTAL PART

5. Application of the detection method to chromatograms on silica-impregnated paper

a) *Impregnated Schleicher and Schüll No 2043 b paper*

On the two halves of the prepared sheets (13×20 cm) are three starting points a, b, and c.

The sheets are run in the large slit-feeding apparatus with di-isobutylketone – acetic acid – $H_2O = 50:25:5$, allowing the front to rise to about 18 cm above the immersion line (i), which took about $4\frac{1}{2}$ hours.

On the starting points situated on a line 2 cm above the immersion line, we applied various mixtures of lecithin (L), cephalin (C), their lyso products (LL and LC) and sphingomyelin (S). For instance when we wish a chromatogram of a mixture of L + C + S, we apply 5 mm³ of the 0.3 % L solution and after evaporation of the solvent (chloroform-methanol = 4 : 1)

---

[2]) In the original communications on tricomplex staining [3] [1], we gave a formula with lower Acid Fuchsin concentration, namely 0,006 %. In our laboratory practice the formula given in the survey has come in practical use, because it results in more rapid staining.

[3]) The original formula of the mixed staining bath [3] [1], has been replaced by the formula given in the survey, which gives better visible green spots on the dry chromatogram than the original formula.

we apply on the same starting point 5 mm³ of the about equal concentrated C solution, and after evaporation of the solvent 5 mm³ of the S solution.

For the chromatogram (fig. 1) we brought up:

L + C + S	on the starting points	a
L + C + S + LC	,, ,, ,, ,,	b
C + LC	,, ,, ,, ,,	c

The left half of the chromatogram was stained with Acid Fuchsin – $UO_2(NO_3)_2$ – 0.01 N HCl. The right half, after preceding exposure to CS_2 and triethylamine vapours, is stained with the mixed staining bath.

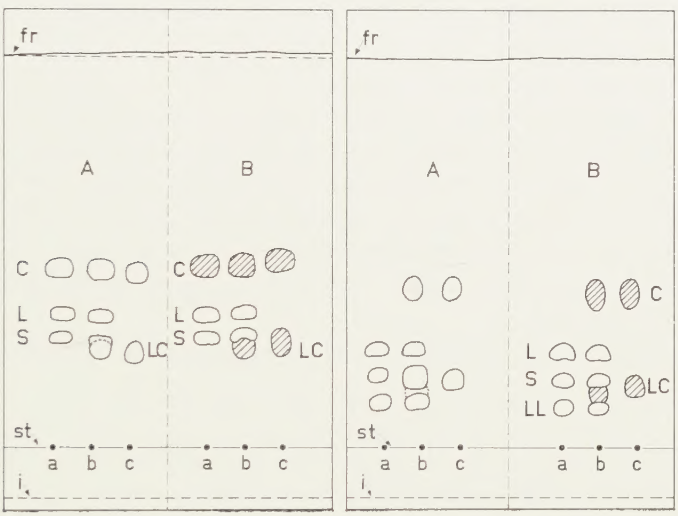

Fig. 1 Fig. 2

Figs. 1 and 2. Chromatograms on silica-impregnated S + S 2043b paper of various mixtures of lecithin (L), cephalin (C), their lyso-products (LL and LC) and sphingomyelin (S). The left halves A of the two chromatograms have been stained with the tricomplex staining bath, the right halves B, after preceding treatment with CS_2 and triethylamine vapour, with the mixed staining bath. As in all further figures, red spots are only circumlined, green spots are also hatched.

On the left half of the chromatogram we obtain only three red spots from the mixture L + C + S + LC. Of the lowest of these spots the base is lower than that of the S spot and about as low as of the LC spot. This suggests that the lower red spot developed from starting point b is a composite spot, containing S + LC. On the right half of the chromatogram the ethanolamine containing phosphatides (C and LC) are stained green, the choline containing phosphatides (L and S) are stained red (as a result of the green background colouration they appear purple). We now see that the lower spot developed from starting point b indeed contains S + LC. These phosphatides are present as a closed group of two spots, the upper spot consisting of S (red) the lower of LC (green).

We now turn to the chromatogram given in fig. 2.

We here applied:

L + S + LL	on the starting points	a
L + C + S + LL + LC	,, ,, ,, ,,	b
C + LC	,, ,, ,, ,,	c

After chromatography with 50:25:5 the left half of the chromatogram was stained with Acid Fuchsin – $UO_2(NO_3)_2$ – 0.01 N HCl, the right half, after preceding exposure to CS_2 and triethylamine vapours, with the mixed staining bath. On the left half of the chromatogram we obtain only three red spots from the mixture L + C + S + LL + LC. The elongated shape, and the occurrence of an upper and lower maximum intensity of of the red colouration of the lowest spot, suggests already that we have here a composite spot, containing S + LL + LC.

On the right half of the chromatogram the ethanolamine containing phosphatides (C and LC) are stained green, the choline containing phosphatides (L, S, LL) are stained red. We now see that the lower spot developed from starting point b indeed contains S + LL + LC, but once more not as a homogeneous mixture. The composite spot consists of a closed group of the three spots, namely S (upper), LC (middle) and LL (lower).

We find thus for the sequence on silica impregnated S + S 2043 B paper:

(upper) C – L – S – LC – LL (lower).

b) *Impregnated Ederol 208 paper*

On the two halves of the impregnated paper sheets (15 × 27.5) are four starting points: a, b, c, d.

The sheets are run in the large slit feeding apparatus with di-isobutylketone – acetic acid – H_2O = 50:25:5 or 40:25:5 allowing the front to rise to about 24 cm above the immersion line, which took about 16–17 hours.

For both chromatograms we applied:

L + C + S + LL	on the starting point	a
L + S + LL + LC	,, ,, ,, ,,	b
L + C + S + LL + LC	,, ,, ,, ,,	c
C + LC	,, ,, ,, ,,	d

The left halves of the chromatograms have been stained with Acid Fuchsin – $UO_2(NO_3)_2$ – 0.01 N HCl and the right halves, after preceding exposure to CS_2 and trietylamine vapours, with the mixed staining bath.

The staining results of the chromatogram run with 40:25:5 (fig. 3) and with 50:25:5 (fig. 4) being equal, we will in the following discussion make no appeart mention of fig. 3 and fig. 4.

On the left halves we find that the lower red spot developed from the

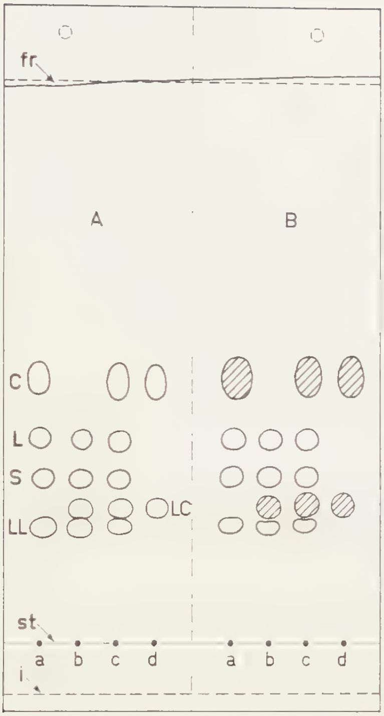

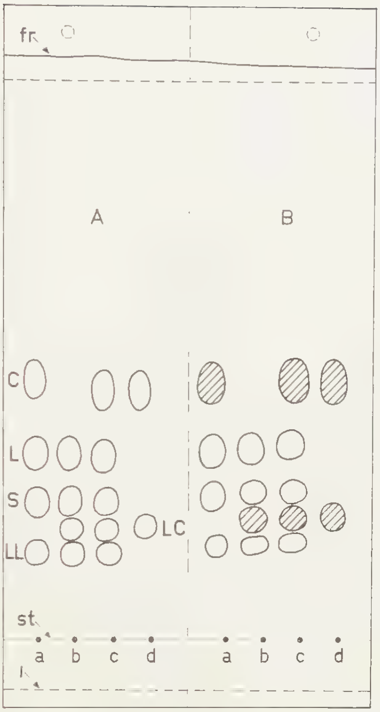

Fig. 3 Fig. 4

Figs. 3 and 4. Chromatograms on silica-impregnated Ederol 208 paper of various mixtures of L, C, LL, LC and S run with 40:25:5 (fig. 3) and 50:25:5 (fig. 4) respectively. Further captions as in fig. 1 and 2.

starting points b and c, has a shape which suggests that it is a composite spot, consisting of a closed group of LC+LL.

On the right halves, the ethanolamine containing phosphatides are stained green and the choline containing phosphatides red (LL) or purple (L and S). We find indeed that the composite spot originated from the starting points b and c consists of a closed group of two spots, the upper spot (green) being LC and the lower spot (red) obviously consisting in LL.

We find thus for the sequence on silica impregnated Ederol 208 paper, both with 40:25:5 and 50:25:5 the sequence:

(upper) C – L – S – LC – LL (lower).

This sequence is the same as on silica-impregnated S+S 2043 B (with 50:25:5) found in paragraph a.

c) *Remark on silica-impregnated papers.*

Apart from the chromatograms given in the figures, we have run others. From this we got the impression that it is difficult too make silica-impregnated papers, which have quantitatively the same chromatographic properties. Compare fig. 1 and 2, which apparently have been impregnated in exactly the same way. Though

both chromatograms have been run with the same mobile phase, and to the same front line, corresponding spots lie in fig. 1 much higher than in fig. 2. Besides, there are indications that even on one chromatogram the chromatographic properties differ from place to place. Compare fig. 1, on which the corresponding spots lie not on exactly horizontal lines. We had the same experiences by comparing chromatograms on silica-impregnated Ederol 208. The above mentioned lack of reproducible preparation is not or to a lesser extent present with $SiCl_4$-treated papers.

6. The sequence of lecithin (L), cephalin (C), their lysoproducts (LL and LC) and sphingomyelin (S) on chromatograms, obtained with non-impregnated paper

a) *Mixture of L and C*

On the starting points of three strips (4.5×22.5 cm) of Schleicher and Schüll 2043 B was brought up 5 mm³ of the L fraction and after evaporation of the solvent 5 mm³ of the C fraction. After running with our mobile phase (50:25:5) in small slit-feeding apparatus, one of the strips (A in fig. 5) was stained with the Acid Fuchsin – $UO_2(NO_3)_2$ – 0.01 N HCl bath, the two others were first subjected to the vapours of CS_2 and triethylamine and there after stained with Acid Fuchsin – $UO_2(NO_3)_2$ – 0.01 N HCl

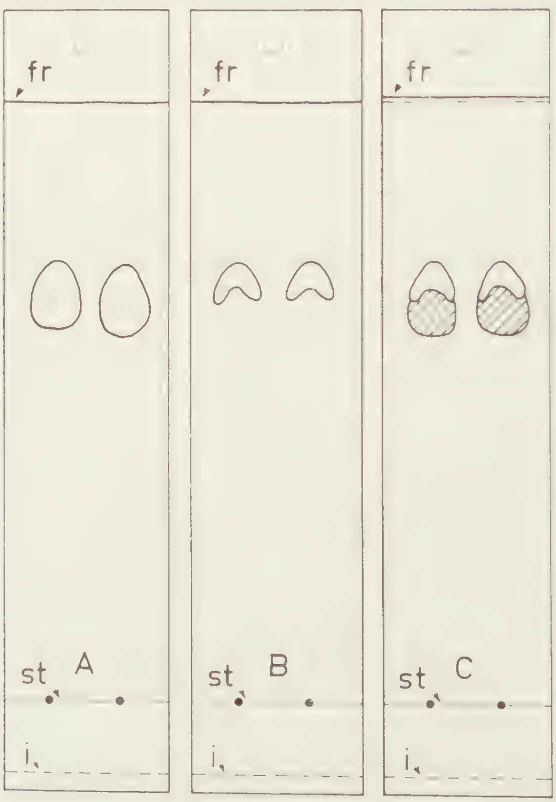

Fig. 5. Chromatograms of a mixture of L and C on non-impregnated S + S 2043b. Explanation see text.

(strip B in fig. 5) and with the mixed staining bath respectively (Strip C in fig. 5).

On strip A only one red spot appears, but as we have brought up L+C, this spot may be called a composite spot. The staining results of strips B (the red staining of the lower part of the composite spot drops out) and of strip C (upper part of the composite spot stains red, but the lower part green) shed light on the nature of the composite spot of strip A.

In this composite spot L and C are not present as a mixture, but as a closed group of two spots, the upper spot consisting of L, the lower of C. Similar experiments have been made with non-impregnated Whatman No 1 and with Ederol 208. The results where quite the same as obtained above with S+S 2043 B, the composite L+C spot consisting of a closed groupe of a L spot (upper) and a C spot (lower).

b) *Mixture of LL and LC*

We use here S+S 2043 b. Two chromatograms have been made in the same way as mentioned in paragraph a. One strip has (fig. 6 B), the

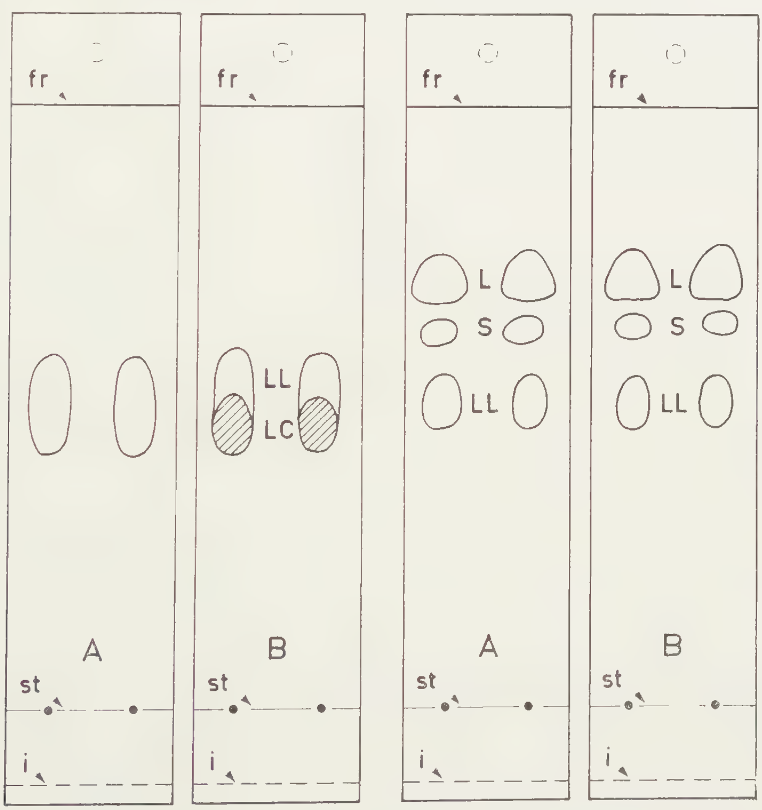

Fig. 6 Fig. 7

Fig. 6. Chromatograms of a mixture of LL and LC on non-impregnated S + S 2043b.
Fig. 7. Chromatogram of a mixture of L, S and LL on non-impregnated S + S 2043b. Explanation see text.

other has not been treated with CS_2 and triethylamine vapours (fig. 6 A) previous to staining with the mixed staining bath. The results are analogous to those in the preceding paragraph.

The composite LL+LC spot is built up of a LL spot (upper) and a LC spot (lower), the two spots forming a closed group.

c) *Mixture of L, S and LL*

Once more we used here two strips of S+S 2043 b, running chromatograms with 50:25:5 in small slit-feeding apparatus. We obtain here three spots: L (upper), S (middle) and LL (lower). (Compare fig. 7.)

The appearance after staining with the mixed staining bath of the chromatogram, which had previously been exposed to CS_2 and triethylamine vapour (strip B) was exactly the same as of the chromatogram (strip A) which had been stained without such exposure. In both cases we obtained three red spots.

We had not expected otherwise as L, S and LL are choline-containing phosphatides and hence do not give di-thiocarbamates with CS_2 and triethylamine.

d) *LC and various mixtures formed out of L, C, S and LC*

In this and the following paragraph we use sheets (17 × 27 cm) of non-impregnated S+S 2043 b paper, on the two halves of which are four starting points: a, b, c and d.

The sheets are run in the large slit-feeding apparatus with 50:25:5, allowing the front to rise here higher above the immersion line (22 cm) than in the preceding paragraphs (18 cm).

In the present paragraph we brought up:

L+C+S	on the starting points	a
L+ S+LC	,, ,, ,, ,,	b
L+C+S+LC	,, ,, ,, ,,	c
LC	,, ,, ,, ,,	d

The left half of the chromatogram was stained with Acid Fuchsin – $UO_2(NO_3)_2$ – 0.01 N HCl (fig. 8 A). The right half was first exposed to CS_2 and triethylamine vapours and subsequently stained with the mixed staining bath (fig. 8 B).

The results show that the composite spot containing L, C and S is a closed group of three spots, consisting in L (upper spot), C (middle spot) and S (lower spot). Of course the staining results with Acid Fuchsin – $UO_2(NO_3)_2$ – 0.01 N HCl of the left half of the chromatogram (fig. 8 A) already suggest that the spot originating from starting point a, and also the upper spot originated from starting point c, consists of a closed group of three spots, consisting in L (upper), C (middle) and S (lower). But this inference is possible only because it is known which mixtures of components have been applied on the starting points a, b, c and d.

If we had only applied the phosphatide mixture of the starting points c and if its components were unknown to us from the number of red spots after tri-complex-staining (left half of fig. 8), we would only be able to conclude that at least two phosphatides of the amphionic type were present. The staining result of the spots from starting point c on the right half of the chromatogram then informs us that in the phosphatide mixture applied four amphionic phosphatides were present, two of which are ethanolamine containing phosphatides and two are choline containing phosphatides. Further, as we know that LL and LC lie on non-impregnated

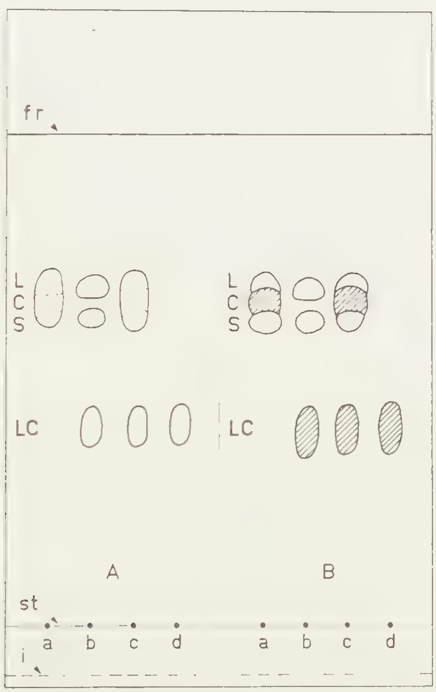

Fig. 8. Chromatogram of various mixtures formed out of L, C, S and LL, on non-impregnated S + S 2043b. Explanation see text.

paper always much lower than L and C, we conclude from the green staining of the lower spot, that LC is present and that the middle green spot of the closed group of three represents C. Knowing further that L and C form a closed group, in which L lies higher than C (fig. 5), the red stained upper spot of the closed group of three must represent L. From fig. 7 we know that S lies lower than L, from which we draw the conclusion that the red stained lower spot of the closed group of three represents S. Thus, without the use of a reference mixture we may conclude that very probably the mixture of phosphatides brought up on starting points c contained L, C, S and LC.

e) *Various mixtures formed out of L, C, S, LL and LC*

In a similar way as in the preceding paragraph we now investigate chromatograms, on the two halves of which has been brought up:

L+C+S+LL	on the starting points	a
L+ S+LL+LC	,, ,, ,, ,,	b
L+C+S+LL+LC	,, ,, ,, ,,	c
C+ LC	,, ,, ,, ,,	d

Two such chromatograms have been run with 50:25:5.

The left halves were stained with Acid Fuchsin $- UO_2(NO_3)_2 -$ 0.01 N HCl. The right halves were first exposed to CS_2 and triethylamine vapours; thereafter one of them was stained with Acid Fuchsin $- UO_2(NO_3)_2 -$ 0.01 N HCl, the other with the mixed staining bath.

We first consider fig. 9, giving the chromatogram the two halves of which have been stained with the tricomplex staining bath. The red staining of the C and LC spots should have dropped out on the right half of the chromatogram. This indeed applies for C. The free C spot originated from starting point d is no longer present.

The composite spot L+C+S originating from starting points a or c, which on the left half of the chromatogram appeared as an elongated red spot, has changed on the right half of the chromatogram into two single red spots L and S as a result of dropping out of the staining of the C spot of the closed group of three spots (L upper, C middle and S lower).

On the contrary, the single LC spot originated from starting point d has not completely dropped out on the right half of the chromatogram, though the intensity of red staining is distinctly smaller than on the left half of the chromatogram. Obviously the time of exposure to the CS_2 and triethylamine vapours ($\frac{1}{2}$ hour), which sufficed for the complete conversion of C into its dithiocarbamate, did not suffice for the complete conversion of LC into its dithiocarbamate. As a result the lower red spots originated from starting points b and c have about the same contours on the right half of the chromatogram as on the left. Thus with the tricomplex staining we did not succeed in demonstrating the composite nature of the LL+LC spots.

We now turn to chromatogram fig. 10, the right half B of which has been exposed during the same time to CS_2 and triethylamine vapours as the right half of the chromatogram fig. 9. Despite the incomplete conversion of LC in its dithiocarbamate, the staining results of the right half with the mixed staining bath are here as one would expect for complete conversion of LC into its dithiocarbamate.

The single LC spot originating from starting point d is now coloured green and the lower spot originated from starting points b and c consists of a closed group of two spots, the upper red spot representing LL and the lower green spot LC. Compare already fig. 6.

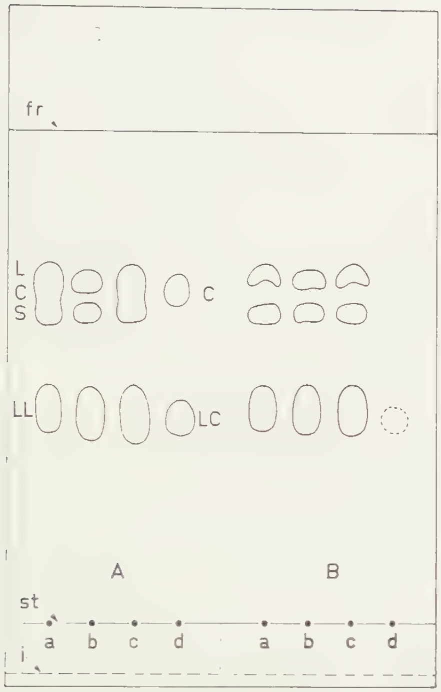

Fig. 9

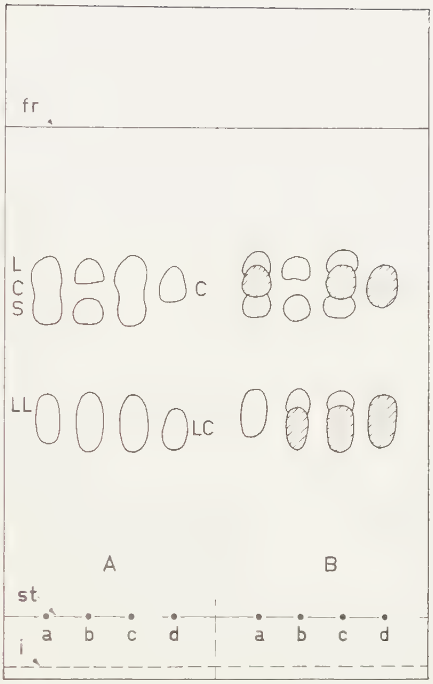

Fig. 10

Fig. 9. Chromatogram of various mixtures formed out of L, C, S, LL and LC on non-impregnated S + S 2043b. In this case both halves of the chromatogram have been stained with the tricomplex staining bath. The right half, which had previously been exposed to CS_2 and triethylamine vapours shows the complete disappearance of the C spot and the much decreased intensity of the red colour of the LC spot (contour given with a broken line). Explanation see text.

Fig. 10. Same as fig. 9, only the right half of the chromatogram having been stained with the mixed staining bath. Both C and LC are stained strongly green. Explanation see text.

f) *The sequence of amphoionic phosphatides on non-impregnated paper*

When we take the results of the preceding paragraphs together, we obtain the following sequence:

(upper) L – C – S – LL – LC (lower).

Relatively close together lie L, C and S, much lower are situated LL and LC, which latter lie also close together.

With the quantities of each of the components brought up in this section (5 mm^3 of an about 0.3 % solution, that is about 15 γ) the capacity of the non-impregnated paper is too low to prevent formation of closed groups of L, C and S, and also of LL and LC. When only L and S are present, the capacity is just sufficient for a resolution of the L and S spot. Compare fig. 7 and in fig. 8, 9 and 10 the train of spots developed from starting point b.

If lower quantities are applied, one may resolve L+C+S into a composite L+C spot and a free S spot. This was for instance the case with the chromatography of the $\frac{1}{2}$ % reference-mixture on non-impregnated paper in former investigations. Compare Parts III and IV of the series of communication mentioned in [4]. The Reference mixture contained L, C, S, LL and LC in roughly equal proportion, thus with 5 mm^3 of this mixture we bring up a quantity of roughly 5 γ per component. But with these smaller quantities L and C still give a composite spot, and equally LL and LC.

(To be continued)

A SIMPLE METHOD TO DIFFERENTIATE BETWEEN CHOLINE AND ETHANOLAMINE CONTAINING PHOSPHATIDES ON PAPER CHROMATOGRAMS. IB

BY

H. G. BUNGENBERG DE JONG

(Communicated at the meeting of April 29, 1961)

7. Application of the detection method to chromatograms on washed $SiCl_4$-treated paper

The phosphatide mictures investigated here are the same as in the case of non-impregnated papers in section 6 (we ommitted only the mixture L+S+LL). All experimental details being the same (S+S 2043 b; mobile phase 50:25:5) and the same dimensions of strips and chromatographic apparatus and methods of staining having been used for the same phosphatide mixtures, we will not repeat all details here for each mixture.

a) *Mixture of L and C*

The results are given in fig. 11. The left strip A (which had not been exposed to CS_2 and triethylamine vapours) has been stained with the tricomplex staining bath. Two red spots are obtained here. The two other strips have been exposed to the vapours of CS_2 and triethylamine before staining. The middle strip B in fig. 11 has been stained with the tricomplex staining bath, which shows that the staining of the upper spot drops out. The strip to the right C has been stained with the mixed staining bath. The upper spot is now stained green, the lower red.

Conclusion: The upper spot represents an ethanolamine containing amphoionic phosphatide, the lower spot a choline containing one.

As a mixture of L+C has been brought up, the upper spot is C and the lower is L.

b) *Mixture of LL and LC*

The results are given in fig. 12.

Only the right strip has previously been exposed to CS_2 and triethylamine vapours. Both strips have been stained in the mixed staining bath. The left strip shows only one red(purple) spot. The right strip shows that the abovementioned spot is a closed group of two spots, the upper being LC (stained green) and the lower LL (stained purple).

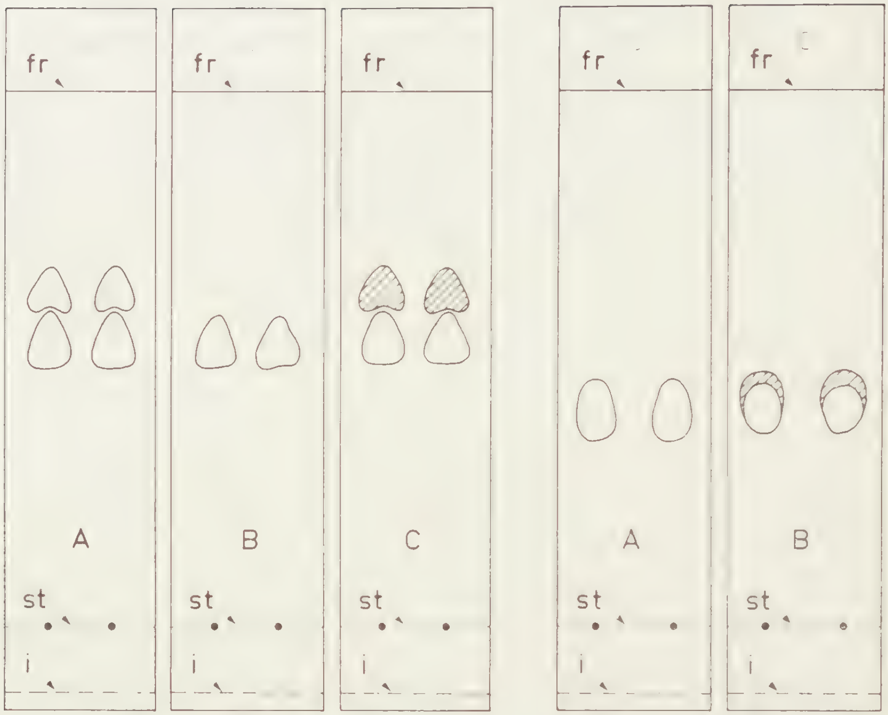

Fig. 11 Fig. 12

Figs. 11 and 12. Chromatograms on washed $SiCl_4$-treated Schleicher and Schüll 2043b paper of a mixture of L and C (fig. 11) and of a mixture of LL and LC respectively (fig. 12). Explanation see text.

c) *LC and various mixtures formed out of L, C, S and LC*

On the chromatogram given in fig. 13 we applied:

L + C + S	on the starting points	a
L + S + LC	,, ,, ,, ,,	b
L + C + S + LC	,, ,, ,, ,,	c
LC	,, ,, ,, ,,	d

The left half A has been stained with Acid Fuchsin – $UO_2(NO_3)_2$ – 0.01 N HCl, the right half B, after preceding exposure to CS_2 and triethylamine vapours, with the mixed staining bath.

We first consider the left half of the chromatogram and draw attention to the lower spot, developed from the starting points b and c.

Its shape and position relative to the S spot to the left and the LC spot to the right of the chromatogram, suggests that it is a composite spot formed by S and LC. We find this confirmed by the staining results of the right half of the chromatogram: The lower spot developed from the starting points b and c is a closed group, consisting of two spots, the upper spot (stained purple) being S and the lower spot (stained green) consisting in LC.

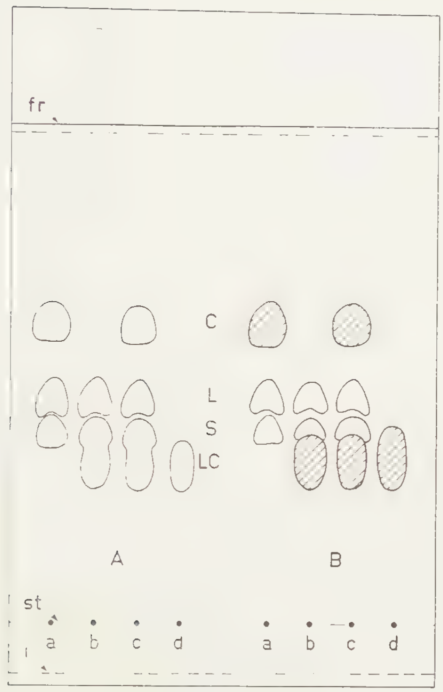

Fig. 13. Chromatogram on washed $SiCl_4$-treated Schleicher and Schüll 2043b paper of various mixtures of L, C, S and LL. Explanation see text.

d) *Various mixtures formed out of L, C, S, LL and LC*

On the chromatograms in fig. 14 and 15 we applied:

L+C+S+LL	on the starting points	a
L+ S+LL+LC	,, ,, ,, ,,	b
L+C+S+LL+LC	,, ,, ,, ,,	c
C+ LC	,, ,, ,, ,,	d

The left halves of both chromatograms were stained with Acid Fuchsin $-UO_2(NO_3)_2-0.01$ N HCl. The right halves were first exposed to CS_2 and triethylamine vapours, thereafter one of them was stained with Acid Fuchsin $-UO_2(NO_3)_2-0.01$ N HCl, the other with the mixed staining bath. We first consider fig. 14, which gives the chromatogram, both halves of which had been stained with the Acid Fuchsin $-UO_2(NO_3)_2-0.01$ N HCl bath. On the right half (B) of the chromatogram the ethanolamine-containing amphoionic phosphatides C and LC_3 should have dropped out.

We see that this indeed applies for the C spots, but the LC spot, though distinctly weaker coloured red, is still to be seen. The time of exposure to CS_2 and triethylamine vapours ($\frac{1}{2}$ hour) has obviously been too short to convert the slower reacting LC completely into its dithiocarbamate. We saw the same already with the analogous chromatogram on non-impregnated paper (compare fig. 9).

We now consider the lower red spots developed from the starting points b and c on the left half of the chromatogram. Its shape and position compared to the free S and LL spots to the left of this elongated spot suggests that it is a composite spot. This suggestion is much enforced by the fact that on the right half of the chromatogram we have here two distinctly red spots (obviously S and LL) connected by a faint red zone (obviously LC, the tricomplex staining of which has not completely dropped out).

Fig. 14 Fig. 15

Fig. 14. Chromatogram on washed $SiCl_4$-treated Schleicher and Schüll 2043b of various mixtures of L, C, S, LL, LC. The right half B (after preceding exposure to CS_2 and triethylamine vapours) has been stained also with the tricomplex staining bath. It shows the complete disappearance of the C spot and the much decreased intensity of the red LC spot (contour given by a broken line). Explanation see text.

Fig. 15. Same as fig. 14, only the right half of the chromatogram having been stained with the mixed staining bath. Both C and LC are here stained strongly green. Explanation see text.

Quite as in the case of the analogous chromatogram on not impregnated paper (fig. 10), staining of the CS_2 + triethylamine treated half with the mixed staining bath gives a clear answer at once. Compare the chromatogram given in fig. 15. The elongated red stained lower spot on the left half of the chromatogram, appears on the right half as a closed group of three spots, which consists in S (upper spot), LC (middle spot) and LL (lower spot).

e) *The sequence of amphoionic phosphatides on washed $SiCl_4$-treated paper Comparison with silica impregnated paper*

Combining the results of the preceding paragraphs, we obtain the following sequence for washed $SiCl_4$-treated paper:

(upper) C – L – S – LC – LL (lower).

This sequence is the same as applies to silica-impregated paper (see section 5).

8. Application of the detection method to chromatograms on neutralized $SiCl_4$-treated paper

In former communications neutralized $SiCl_4$-treated papers have been used for many investigations regarding the mechanism of the chromatography of phosphatides with diisobutylketone — acetic acid — H_2O = 50:25:5 [4]. From our Reference mixture containing L, C, S, LL and LC we always obtained on chromatograms four distinctly visible spots.

By means of the dithiocarbamate reaction followed by acidified $AgNO_3$ solution it seemed that the third spot (reckoned from above) contained LC.

As after this reaction this spot still stained red with Acid Fuchsin — $UO_2(NO_3)_2$ — 0,01 N HCl, we concluded that this spot is a composite spot, consisting in S and LC.

As the above detection method for ethanolamine containing phosphatide is not very sensitive, it was decided to apply our new detection method also to chromatograms on neutralized $SiCl_4$-treated paper.

On the starting points on both halves of the chromatograms applied:

L + C + S + LL	on the starting points a
L + S + LL + LC	on the starting points b
L + C + S + LL + LC	on the starting points c
C + LC	on the starting points d

We have run four chromatograms on neutralized paper; the right halves of which (stained with the mixed staining bath after previous exposure to CS_2 and triethylamine vapours) are given as A, B, C and D in fig. 16. The neutralized papers used differ in the following ways:

A = Neutralized $SiCl_4$-treated Ederol 208, just one year after preparation

B = Neutralized $SiCl_4$-treated Schleicher and Schüll 2043 b, also one year after preparation

C = Freshly prepared neutralized $SiCl_4$-treated Schleicher and Schüll 2043 b, three days after preparation

D = The same as C, but directly after neutralization two times washed 10 minutes with distilled water; chromatography also three days after preparation.

The results show that the relative position of C, L, S and LL is always the same, but that the position of LC may vary:

With very old neutralized $SiCl_4$-papers (fig. 16, A and B) the LC spot is found between L and S, the sequence here being:

(upper) C — L — LC — S — LL (lower).

With freshly prepared neutralized $SiCl_4$-paper (fig. 16, C) the centres of the LC and S spots more or less coincide. The sequence thus becomes:

(upper) C — L — LC + S — LL (lower).

Fig. 16. Right halves of chromatograms of various mixtures of L, C, S, LL and LC on different kinds of neutralized $SiCl_4$-treated paper, stained with the mixed staining bath after preceding exposure to CS_2 and triethylamine vapours. *A.* and *B.* neutralized $SiCl_4$-treated Ederol 208 (A) and S + S 2043b (B), both used one year after preparation. *C.* freshly prepared neutralized $SiCl_4$-treated S + S 2043b. *D.* washed freshly prepared neutralized $SiCl_4$-treated S + S 2043b. Explanation see text.

With washed freshly prepared neutralized $SiCl_4$-paper (fig. 16, D) LC is found between S and LL. The sequence here is:

(upper) C — L — S — LC — LL (lower).

We draw attention to the fact that the sequence found on washed neutralized $SiCl_4$-treated paper is quite the same as on washed $SiCl_4$-treated paper. Compare D in fig. 12 with figs. 14 and 15.

Remembering that in the act of neutralization NH_4Cl is formed [1]), and taking

---

[1]) The preparation of neutralized $SiCl_4$-treated paper has been given in Part I of [4]. It comprises two steps:

1) The air-dry chromatographic paper is drawn evenly in about 10 seconds through a 2 % solution of $SiCl_4$ in CCl_4 and is then hung in air to let evaporate the solvent (CCl_4) and eventual excess of $SiCl_4$.

2) After hanging in air for 30 minutes the $SiCl_4$-treated paper is exposed to vapour of ammonia for 10 minutes and there after is again suspended in air.

During the first step "hygroscopic" water in the paper reacts with $SiCl_4$ in a heterogeneous reaction, as a result of which the cellulose fibres are coated with a thin layer of silica. Compare Part III of [4].

In the second step the HCl formed in the first step, which after 30 minutes is still present in the prepared paper is neutralized by NH_3 under formation of NH_4Cl.

into account that washing will remove the NH_4Cl present in the paper, it may be infered that the divergent sequences found in A, B and C of fig. 16 are correlated with the presence of NH_4Cl in the paper.

Most remarkable and difficult to explain is the relative position of LC and S in the case of freshly prepared neutralized $SiCl_4$-treated paper.

Two tentative explanations may follow:

1) The LC preparation is not one single component, but consists of two components (or groups of components), with slightly different adsorbabilities. The latter are not manifest when the NH_4Cl has been washed out (D in fig. 16), but in the presence of NH_4Cl (which influences adsorption) they come to the fore, resulting in part of the LC being found between the LL and S spot, part between the S and L spot.

The fact that on old neutralized paper the whole of the LS lies between L and S, may be ascribed to altered properties of the adsorbent (SiO_2) during sufficient long ageing, the small difference in adsorbability of the two components of LC no longer coming to the fore.

2) For some unknown reason LC as a whole has a decreased adsorbability, which especially comes to the fore in the presence of NH_4Cl. Only part of the LC stops below the S spot, here by adsorption replacement causing a deeper incision in the S spot than is present in the S spot developed from starting point a.

The other part of LC flows over the S spot and is here sufficiently adsorbed to remain below the L spot.

The altered position of the LC spot in very old neutralized $SiCl_4$-treated paper may be due to ageing of the adsorbent.

9. Some further examples of the use of the new detection method

a) *Chromatograms of total egg phosphatides on washed $SiCl_4$-treated S+S 2043 b paper*

On the two halves of a sheet (17×27 cm) of impregnated paper are four starting points a, b, c and d.

With a self-filling capillary pipet of 5 mm^3 capacity we applied a 0.3 % solution of a commercial preparation ("Lezithin ex ovo, pur., from Merck) in chloroform-methanol (4:1), and this once on starting point d, two times on c, four times on b and six times on a.

After chromatography to a front height of 18 cm above the immersion line, the left half of the chromatogram was stained with Acid Fuchsin $-UO_2(NO_3)_2-0.01$ N HCl, the right half, after previous exposure to CS_2 and triethylamine vapours, with the mixed staining bath. Compare fig. 17.

The contours of faintly visible spots on the chromatogram, have been given with a broken line. One observes that the visibility of the LL and S spots on the left half (A) is better than on the right half (B). This results from the green background colouration present on the right half. Here the S spot developed from the starting point a even is invisible.

For far the greater part the phosphatide mixture consists in L.

We see on the left half A, that with increase of the total amount applied, it is the L spot which rapidly gains in height and above starting points b and a it forms already a composite spot with the C spot.

That we have to do with a closed group is suggested by the fact that the greatest intensity of red staining is not present along the upper limit

of the C+L spot, but on a line given approximately by the broken line somewhat below the top, (compare fig. 17, A).

On the right half of the chromatogram the upper spot stains green; the large spot and the lower situated spots stain red (purple as a result of the green background colouration).

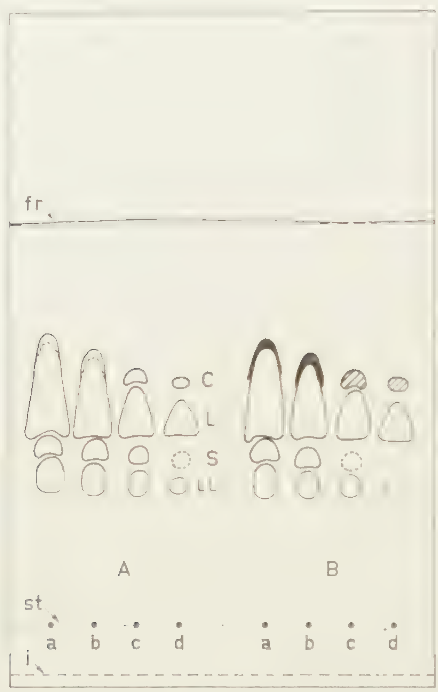

Fig. 17. Chromatogram of an egg phosphatide preparation on washed, $SiCl_4$-treated S + S 2043b. The amount brought up on the starting points increases from d, over c and b to a. Explanation see text.

We conclude that in our phosphatide mixture are present C, L, S and LL.

We mentioned above certain details of the distribution of the red colour in the composite L+C spot on the left halve of the chromatogram, which suggests this composite spot to represent a closed group of two spots. On the right half of the chromatogram this is confirmed with supreme clearness (compare fig. 17, B). The top of the red (purple) lecithin spot is covered with a intense green stained cap of cephalin, its intense green though narrow wings stretching considerably far downwards along both flanks of the L spot. In the case of starting point b the lower end of the wings still aproximately reach the horizontal level characteristic for the base of free C spots.

In the case of starting point a the wings end on a higher level.

Obviously the adsorption displacement by L did not allow the end of the wings of the C spot to maintain its characteristic place.

b) *Chromatograms of total soybean phosphatides on non-impregnated and on washed $SiCl_4$-treated S+S 2043 b paper*

On all preceding chromatograms have been brought up only phosphatides of the ampho-ionic type. We now give an example in which phosphatides of the acidic type and other acidic substances are present.

We take three strips (4.5×21.5 cm) of non-impregnated S+S 2043 B, apply on the starting points 5 mm³ of a 2 % solution of a commercial soybean phosphatide preparation (still containing oil) in chloroform-methanol = 4:1 and run these strips in a small slit-feeding apparatus with our mobile phase 50:25:5. Strip A in fig. 18 has been stained directly with the mixed staining bath. There appear one large red spot and above it three weak green spots α, β and γ. Much lower than the red spot a distinctly green spot δ is found.

The nature of the substances which are stained green here play no role in the following. It may suffice to mention that spot δ is an inositol phosphatide [1]).

Strip B in fig. 18 has first been exposed to CS_2 and triethylamine vapours and there after stained with the mixed staining bath.

Of course spots α, β, γ and δ once more are stained green.

It appears that the lower part of the large red spot on strip A is now strongly stained green, whereas the upper part stains red.

It is concluded that the large red spot on chromatogram A is a closed group of two spots, the upper spot being L and the lower C.

The third strip has been cut lengthwise in two halves C and D. Both have been stained with Acid Fuchsin $-$ $UO_2(NO_3)_2$ $-$ 0.01 N HCl, strip C without pretreatment and strip D after exposure to CS_2 and triethylamine vapours. Strip C shows apart from the red large composite L+C spot a much lower small, weakly coloured red spot. This small red spot was not visible on strip A, obviously because it was masked by the green δ spot. Strip D, in which the ethamolamine containing phosphatides are no longer stained, shows only red the upper part of the red large composite spot on strip C. From the fact that the small, weakly coloured red spot present on strip C appears red on strip D with about the same intensity, we conclude that this weak spot represents LL.

The example given above shows that when an unknown phosphatide mixture is investigated, it is advisable not to restrict ourselves to two chromatograms (or two halves of one chromatogram), one being stained directly with Acid Fuchsin $-$ $UO_2(NO_3)_2$ $-$ 0.01 N HCl, the other, after

---

[1]) Chromatograms of commercial soybean phosphatides have been investigated in former communications. Compare Part I of [4] and [6]. Spot α is probably a fatty acid. Spots β and γ contain phosphorus, but no choline, colamine nor inositol. Spot δ contains phosphorus and inositol but no choline or ethanolamine. On paper which has received a preliminary treatment to diminish the green background colouration, one may observe a still lower situated weak green spot ε containing inositol.

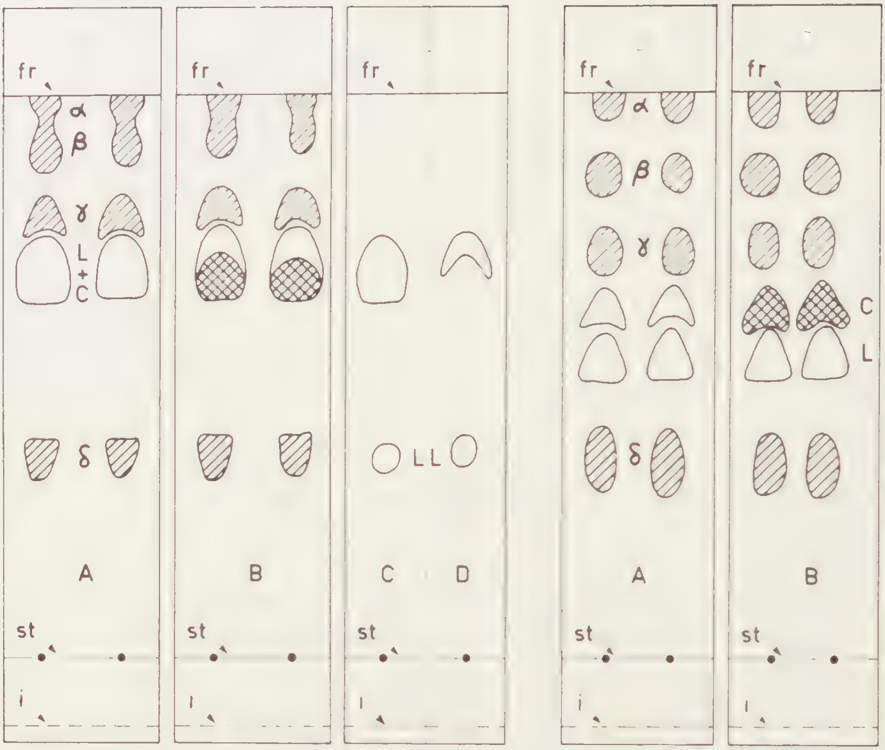

Fig. 18

Fig. 19

Figs. 18 and 19. Chromatograms of a soybean phosphatide preparation on non-impregnated (fig. 18) and on washed $SiCl_4$-treated S + S 2043b (fig. 19). Explanation see text.

preceding exposure to CS_2 and triethylamine, with the mixed staining bath. Had we had only the staining results of the strips C and B at our disposal, we might have concluded erroneously that the lower red spot on strip C represents an ethanolamine containing phosphatide (thus LC), because we find a green spot at the same place on strip B.

In fig. 19 we give two chromatograms of the soybeanphosphatide preparation on washed $SiCl_4$-treated paper, strip A stained directly with the mixed staining bath, strip B after preceding exposure to CS_2 and triethylamine vapours. The spots are now more evenly distributed over the length of the chromatogram than on non impregnated paper (fig. 18). Besides we now obtain two red spots on strip A of fig. 19, instead of the composite red spot on strip A of fig. 18. Strip B in fig. 19 shows that the upper red spot on strip A is now stained intensively green, and thus represents cephalin. The lower red spot remains red on strip C fig. 15, and thus represents lecithin. On the washed $SiCl_4$-treated paper once more the small red spot representing LL is masked by the green δ spot. It may be detected by staining a third chromatogram directly with Acid Fuchsin $-$ $UO_2(NO_3)_2$ $-$ 0.01 N HCl.

Its nature (LL) will then be ascertainable from a fourth chromatogram which is stained with the same staining bath after preceding exposure to CS_2 and triethylamine vapours.

We thank miss J. S. den Boer for her skilfull assistance in the experimental work.

10. Summary

1. A new simple spot test has been given to discern ethnolamine containing amphoionic phosphatides (cephalin, C and lysocephalin, LC) from choline containing amphoionic phosphatides (lecithin, L; sphingomyelin, S and lysolecithin, LL).

2. Spots of L, of C, of S of LL and of LC, brought up on a paper strip and dried, all stain red with the tricomplex staining bath (Acid Fuchsin $- UO_2(NO_3)_2 -$ 0.01 N HCl). Tricomplex staining is based on the amphoionic structure of these phosphatides.

3. When a similar test strip is first subjected to vapours of CS_2 and triethylamine and then is stained with the tricomplex staining bath, only L, S and LL are stained red, and C and LC are stained no longer.

When a third similar test strip is subjected to vapours of CS_2 and triethylamine and then stained with a mixed staining bath (containing besides the ingredients for tricomplex staining also Brilliant Green), the L, S and LL spots are stained red, the C and LC spots are stained green.

4. Choline containing phosphatides do not react with CS_2 and triethylamine and thus their amphoionic structure remains intact. Ethanolamine containing phosphatides form dithiocarbamates. The reaction products have still the phosphate group intact and therefore have now acid character (stain green in the mixed staining bath) and have no amphoionic structure (the tricomplex staining no longer occurs).

5. The new detection method has been applied with success to paper chromatograms of various mixtures out of L, C, S, LL and LC, obtained with non-impregnated paper, washed $SiCl_4$-treated paper and silica impregnated paper, using diisobutylketone – acetic acid – H_2O (50:25:5 or 40:25:5) as mobile phase and a slit-feeding apparatus as chromatographic device.

6. On the left half of a paper sheet are brought up on a number of starting points various mixtures of the abovementioned amphoionic phosphatides and on the corresponding starting point on the right half the same mixtures.

After chromatography the left half is stained with the tricomplex staining bath, the right half is first exposed to the vapours of CS_2 and triethylamine, and thereafter stained with the tricomplex staining bath, or with the mixed staining bath. The staining results are then compared. Red spots on the left half of the chromatogram which are found back as red stained spots on the right half are choline containing phosphatides.

Red spots on the left half, which drop out on the right half with the tricomplex staining bath, or are stained green with the mixed staining bath, indicate ethanolamine containing phosphatides.

7. For a complete dropping out of the tricomplex staining of the ethanolamine containing phosphatides a much longer time of exposure to CS_2 and triethylamine vapours is necessary than for obtaining green colouration of these spots with the mixed staining bath. A simple explanation of this difference has been given.

8. The systematic investigation of phosphatide mixtures, mentioned above sub point 5 allowed to conclude that the succession of the phosphatides on washed $SiCl_4$-treated paper is the same as on silica-impregnated paper:

(upper) C – L – S – LC – LL (lower).

9. With neutralized $SiCl_4$-treated paper the relative position of LC and S in the above sequence may be different (LC and S coinciding, or after long aging LC before S). When freshly prepared neutralized $SiCl_4$-treated paper is washed, we find the normal sequence. The deviating sequences mentioned above are correlated with the NH_4Cl present in neutralized $SiCl_4$-treated paper.

10. Though with non-impregnated paper no resolution of the mixture of the five phosphatides can be obtained (the chromatograms show only two or three spots), the new detection method allows us to detect the structure of the composite spots. The composite spot of L + C consists of a closed group of two spots, the upper spot being L, the lower C. The composite spot formed by L + C + S, consists in a closed group of three spots, the upper being L, the middle C and the lower S.

Similarly the composite spot of LL and LC consists in a closed group of two spots, the upper being LL and the lower LC.

The sequence of spots on non-impregnated paper is then:

(upper) L – C – S – LL – LC (lower).

11. The detection method has been applied to chromatograms of a commercial egg phosphatide preparation on washed $SiCl_4$ treated paper. The formation of the closed group of C and L with increasing amounts applied could readily be followed with this method.

12. In the case of unknown mixtures to be investigated on the presence of phosphatides it is advisable to use four chromatograms (or four longitudinal parts of a broad chromatogram). Two of them are stained with the tricomplex staining bath and the mixed staining bath respectively. The two remaining, after preceding exposure to the vapours of CS_2 and triethylamine are also stained with the tricomplex staining bath and the mixed staining bath respectively. Using as an illustrative example a commercial soybean phosphatide preparation, it is shown that in this way erroneous conclusions may be avoided.

13. The staining behaviour of serine phosphatides in the tricomplex staining bath and the mixed staining bath, before and after the reaction with CS_2 and triethylamine, appears to confirm our theory regarding the staining reaction.

Serine phosphatides, because of the COOH-group present, do not show ideal ampho-ionic properties, compared with choline and colamine phosphatides, and thus stain weakly with the tricomplex staining bath and stain directly green with the mixed staining bath. After CS_2 and triethylamine treatment tricomplex staining no longer occurs and the green staining in the mixed staining bath is increased.

Department of Medical Chemistry,
University of Leyden

REFERENCES

1. Hooghwinkel, G. J. M., J. Th. Hoogeveen, M. J. Lexmond and H. G. Bungenberg de Jong, these Proceedings, Series B, 62, 222 (1959).
2. Feigl, F., Spot tests in organic analysis, Elsevier, Amsterdam, 257 (1956).
3. Bungenberg de Jong, H. G. and G. R. van Someren, these Proceedings, Series B, 62, 150 (1959).
4. ——— and J. Th. Hoogeveen, I, these Proceedings, Series B, 63, 190 (1960); II, 63, 288 (1960); III, 63, 383 (1960); IV, 64, 1 (1961); V, 64, 167 (1961).
5. ——— and ———, these Proceedings, Series B, 63, 1 (1960).
6. ———, these Proceedings, Series B, 64, 445, 458 (1961).

MECHANICS

A SYSTEMATIC SIMPLIFICATION OF THE GENERAL EQUATIONS IN THE LINEAR THEORY OF THIN SHELLS

BY

W. T. KOITER

(Communicated at the meeting of May 27, 1961)

1. *Basic general equations*

The general equations of the linear theory of thin elastic shells have been discussed by many writers. In view of the approximate character of any shell theory, it is not too surprising that these equations, due to slight variations in the approximating assumptions, appear in a wide variety of forms. We shall base our present discussion on the equations derived in an earlier paper [1, 2].

The tangential displacement of a point on the middle surface of a shell is described by the covariant surface vector u_α (all Greek subscripts and superscripts take the value 1 or 2), and the normal displacement by the surface invariant w. The covariant middle surface strain tensor $\gamma_{\alpha\beta}$ is given by

$$2\gamma_{\alpha\beta} = u_{\alpha|\beta} + u_{\beta|\alpha} - 2wb_{\alpha\beta}, \tag{1.1}$$

where a subscript α preceded by a vertical line indicates the covariant surface derivative with respect to the surface coordinate x^α, and $b_{\alpha\beta}$ is the covariant second fundamental tensor of the undeformed middle surface. The covariant rotation tensor in the middle surface $\omega_{\alpha\beta}$ is given by

$$2\omega_{\alpha\beta} = u_{\beta|\alpha} - u_{\alpha|\beta}, \tag{1.2}$$

and the covariant vector of rotation of the normal to the middle surface φ_α is given by

$$\varphi_\alpha = w_{|\alpha} + u_\varkappa b_\alpha^{\varkappa}. \tag{1.3}$$

The covariant tensor of changes of curvature $\varrho_{\alpha\beta}$ is described by

$$2\varrho_{\alpha\beta} = \varphi_{\alpha|\beta} + \varphi_{\beta|\alpha} + b_\alpha^{\varkappa}\omega_{\beta\varkappa} + b_\beta^{\varkappa}\omega_{\alpha\varkappa}. \tag{1.4}$$

The middle surface strain tensor (1.1) and the tensor of changes of curvature (1.4) are connected by three conditions of compatibility, due to Goldenweiser [3], which may be derived in various manners, e.g. from the equations of Codazzi and Gauss for the deformed middle surface [4, p. 28]. If $\varepsilon^{\alpha\beta}$ denotes the contravariant skew-symmetric ε-tensor, defined by

$$\varepsilon^{12} = -\varepsilon^{21} = \frac{1}{\sqrt{a}}, \quad \varepsilon_{12} = -\varepsilon_{21} = \sqrt{a}, \tag{1.5}$$

where $a = \text{Det}\,|a_{\alpha\beta}|$, and $a_{\alpha\beta}$, $a^{\alpha\beta}$ are the covariant and contravariant metric tensors of the undeformed middle surface, the compatibility conditions are, rewritten in tensor form

$$\text{(A)} \qquad \varepsilon^{\alpha\lambda}\varepsilon^{\beta\mu}[\gamma_{\alpha\beta|\lambda\mu} + b_{\alpha\beta}\varrho_{\lambda\mu}] = 0,$$

$$\text{(B)} \qquad \varepsilon^{\beta\mu}\{[\varrho_{\lambda\mu} + {}^1/_2 b_\lambda{}^\varkappa\gamma_{\varkappa\mu} + {}^1/_2 b_\mu{}^\varkappa\gamma_{\varkappa\lambda}]_{|\beta} + b_\beta{}^\varkappa[\gamma_{\varkappa\lambda|\mu} + \gamma_{\varkappa\mu|\lambda} - \gamma_{\lambda\mu|\varkappa}]\} = 0.$$

It may be verified directly, by straightforward, if somewhat lengthy algebra, that equations (A) and (B) are satisfied identically by (1.1) and (1.4), if appropriate use is made of (1.2), (1.3) and the equations of Codazzi and Gauss for the undeformed middle surface

$$\varepsilon^{\beta\mu}b_{\alpha\beta|\mu} = 0, \tag{1.6}$$

$$b_{\alpha\lambda}b_{\beta\mu} - b_{\alpha\mu}b_{\beta\lambda} = K\varepsilon_{\alpha\beta}\varepsilon_{\lambda\mu}, \tag{1.7}$$

where K is the Gaussian curvature of the undeformed middle surface.

The elastic strain energy per unit area of the middle surface is obtained from Hooke's law for plane stress [1, 2]

$$V = {}^1/_2 h\, E^{\alpha\beta\lambda\mu}\gamma_{\alpha\beta}\gamma_{\lambda\mu} + {}^1/_{24} h^3\, E^{\alpha\beta\lambda\mu}\varrho_{\alpha\beta}\varrho_{\lambda\mu}, \tag{1.8}$$

where

$$E^{\alpha\beta\lambda\mu} = G\left[a^{\alpha\lambda}a^{\beta\mu} + a^{\alpha\mu}a^{\beta\lambda} + \frac{2\nu}{1-\nu}a^{\alpha\beta}a^{\lambda\mu}\right] \tag{1.9}$$

is the tensor of elastic moduli, G is the shear modulus, ν is Poisson's ratio, and h is the shell thickness. It should be noted that the approximate character of our theory is due only to the fact that (1.8) is an approximation [1]). The stress resultants $n^{\alpha\beta}$ and stress couples $m^{\alpha\beta}$ are defined in our energy approach by the symmetric contravariant tensors

$$n^{\alpha\beta} = \frac{\partial V}{\partial\gamma_{\alpha\beta}} = hE^{\alpha\beta\lambda\mu}\gamma_{\lambda\mu}, \tag{1.10}$$

$$m^{\alpha\beta} = \frac{\partial V}{\partial\varrho_{\alpha\beta}} = {}^1/_{12} h^3 E^{\alpha\beta\lambda\mu}\varrho_{\lambda\mu}. \tag{1.11}$$

The equations of equilibrium and boundary conditions may be obtained by variational methods. Let p^α denote the contravariant surface vector of tangential loads per unit area of the middle surface, and let p^3 denote the surface invariant of the normal load per unit area. The equations of equilibrium are now [1, 2]

$$\text{(C)} \qquad m^{\alpha\beta}|_{\alpha\beta} - n^{\alpha\beta}b_{\alpha\beta} - p^3 = 0,$$

$$\text{(D)} \qquad [n^{\beta\alpha} + {}^1/_2 b_\lambda{}^\alpha m^{\beta\lambda} - {}^1/_2 b_\lambda{}^\beta m^{\alpha\lambda}]_{|\beta} + b_\lambda{}^\alpha m^{\beta\lambda}|_\beta + p^\alpha = 0.$$

---

[1]) The relative error of the approximation (1.8) is of order h/R or h^2/L^2, whichever may be critical, where h is the shell thickness, R the smallest principal radius of curvature, and L the "wave length" of the deformation pattern on the middle surface [1, 2].

The boundary conditions are most conveniently expressed by choosing a special coordinate system in which the boundary of the shell is a coordinate line, say an x^2-line (i.e. a line $x^1 = \text{const.}$). Geometric boundary conditions are specified by prescribed values $\bar{u}_\alpha$, $\bar{w}$ and $\bar{\varphi}_1$ for the tangential displacement vector u_α, the normal displacement w and the rotation component φ_1 (specification of the rotation component φ_2 is already implied by specification of the displacements). In the case of dynamic boundary conditions the contravariant vector of tangential edge forces $\bar{n}^\alpha$, the transverse shear force $\bar{q}$ and the edge bending moment $\bar{m}^1$ are specified per unit length, and the boundary conditions are [2]

$$
\left\{
\begin{aligned}
&(n^{1\alpha} + {}^1\!/_2 b_\varkappa{}^\alpha m^{1\varkappa} - {}^1\!/_2 b_\varkappa{}^1 m^{\alpha\varkappa})\sqrt{a} + b_2{}^\alpha m^{12}\sqrt{a} = \bar{n}^\alpha \sqrt{a_{22}}, \\
&m^{\alpha 1}|_\alpha \sqrt{a} + (m^{12}\sqrt{a})_{,2} = -\bar{q}\sqrt{a_{22}}, \\
&m^{11}\sqrt{a} = \bar{m}^1 \sqrt{a_{22}}.
\end{aligned}
\right. \tag{1.12}
$$

In the case of boundary conditions of mixed type either $\bar{u}_\alpha$ or $\bar{n}^\alpha$, either $\bar{w}$ or $\bar{q}$ and either $\bar{\varphi}_1$ or $\bar{m}^1$ are specified.

It is worthwhile to note that the equations of equilibrium (C) and (D) are in complete agreement with the equations resulting from integration of the three-dimensional equations of equilibrium over the shell thickness [5, p. 383]. This is by no means fortuitous. In fact, our equations are based on the definition of stress resultants and stress couples by the internal virtual work expression per unit area of the middle surface

$$
n^{\alpha\beta}\,\delta\gamma_{\alpha\beta} + m^{\alpha\beta}\,\delta\varrho_{\alpha\beta}, \tag{1.13}
$$

and the variations of the middle surface strains and changes of curvature, allowed for in the analysis, are the most general variations which satisfy the equations of compatibility (A) and (B). Hence our equations *must* agree with the rigorous equations of equilibrium of a shell element. Obviously, they also remain valid for non-elastic materials, provided that all displacement gradients remain small in the sense of the classical theory of elasticity.

Our further discussion will be based on the fundamental differential equations (A), (B), (C) and (D), together with the simple (finite) stress-strain relations (1.10) and (1.11). It will be noted that the approximate character of our basic equations is due only to the approximate nature of the stress-strain relations.

2. *Criteria for simplification of equations*

The eighth-order system of partial differential equations (A)–(D) is extremely complicated and some simplification is obviously desirable for practical application to a particular problem.

In some cases the simplicity of the middle surface geometry may enable us to simplify the basic equations. A notable example of this type of simplification is the spherical shell, for which the basic equations may

be reduced to two simultaneous fourth-order equations for the normal displacement w and a stress function Φ [6, p. 225].

A different type of simplification for shells of arbitrary shape and constant thickness was achieved by NOVOZHILOV (cf. [4], where references to original papers may be found) by the introduction of complex combinations of stress resultants and stress couples; the order of the system of equations is halved in this process. For POISSON's ratio equal to zero NOVOZHILOV's simplification is rigorous. For arbitrary values of POISSON's ratio it is claimed that no loss in accuracy is involved in the neglection of certain small terms, provided that the surface loads are sufficiently smooth, but this claim is open to some doubt. In fact, when NOVOZHILOV's simplified equations are applied to the problem of a helicoidal shell under uniform normal load, the resulting distribution of the sum of the bending moments, divided by $(1+\nu)$, is independent of POISSON's ratio, in contradiction to COHEN's well-established rigorous solution [7, 8].

In most cases a simplification can indeed only be achieved by neglecting certain "small" terms in one or more of the quations (A)–(D), and *it depends on several circumstances, in particular on the shell geometry, the external loads and the boundary conditions, which terms may be considered negligible.* Moreover, it often happens that some terms are negligible in a large part of the shell but significant in other regions; the well-known edge effect is a striking example of this phenomenon. Finally, the neglection of "small" terms in differential equations is a notoriously tricky business, which may lead to unexpectedly large errors; the application of NOVOZHILOV's simplified equations for arbitrary values of POISSON's ratio to the helicoidal shell is a good example of the dangers involved. *It is strongly recommended always to check a posteriori whether the solution obtained for the simplified equations is indeed a satisfactory approximation to the desired solution of the basic, unsimplified equations.*

An important parameter in the classification of shell problems with respect to the possibility of simplifying the basic equations in a certain region is the order of magnitude in this region of the ratio of maximum (absolute) flexural strain to maximum (absolute) extensional strain. Denoting this ratio by $h\varrho/\gamma$, we have to distinguish between three possibilities, viz.

$$\frac{h\varrho}{\gamma} \ll 1, \quad \frac{h\varrho}{\gamma} = O(1), \quad \frac{h\varrho}{\gamma} \gg 1. \tag{2.1}$$

In the first case the membrane stresses and strains dominate, in the last case the bending stresses and strains dominate, and in the intermediate case the membrane stresses and strains and the bending stresses and strains are of equal order of magnitude.

In order to discuss the order of magnitude of the various terms in the basic equations, it is convenient to employ surface coordinates for which

$$a_{11} = O(1), \quad a_{22} = O(1), \quad a = O(1). \tag{2.2}$$

The minimum principal radius of curvature in the shell region under consideration is denoted by R. Finally, we introduce the concept of "wave length" L of the deformation pattern on the middle surface by the definitions

(2.3) $$|\gamma_{\alpha\beta|\lambda}| = O\left(\frac{\gamma}{L}\right), \quad |\varrho_{\alpha\beta|\lambda}| = O\left(\frac{\varrho}{L}\right).$$

If we now examine our basic equations, we may estimate the order of magnitude of the various extensional and flexural terms

(2.4) $$\text{in (A):} \quad \frac{\gamma}{L^2}, \qquad \frac{\varrho}{R};$$

(2.5) $$\text{in (B):} \quad \frac{\gamma}{LR}, \qquad \frac{\varrho}{L};$$

(2.6) $$\text{in (C):} \quad Gh\,\frac{\gamma}{R}, \quad Gh^3\frac{\varrho}{L^2};$$

(2.7) $$\text{in (D):} \quad Gh\,\frac{\gamma}{L}, \quad Gh^3\frac{\varrho}{LR};$$

It appears that the ratio of the order of magnitude of the terms with middle surface strains to the order of magnitude of the bending terms in each equation depends on *two* parameters, i.e. $h\varrho/\gamma$ (the ratio of flexural strain or stress to extensional strain or stress) and on L^2/hR. We may now expect that we may neglect in (A) all flexural terms if

$$\frac{\varrho h}{\gamma}\cdot\frac{L^2}{hR} \ll 1.$$

It is convenient to denote equation (A), simplified by dropping all bending terms, by (A_γ). Hence our first simplification is

(2.8) $$(A) \to (A_\gamma) \text{ if } \frac{\varrho h}{\gamma} \ll 1, \frac{L^2}{hR} \leqq O(1) \text{ or } \frac{\varrho h}{\gamma} = O(1), \frac{L^2}{hR} \ll 1.$$

Likewise, we denote equation (A), simplified by dropping all membrane terms, by (A_ϱ). This simplification is suggested if

$$\frac{\varrho h}{\gamma}\cdot\frac{L^2}{hR} \gg 1.$$

Hence our second simplification is

(2.9) $$(A) \to (A_\varrho) \text{ if } \frac{\gamma\varrho}{h} \gg 1, \frac{L^2}{hR} \geqq O(1) \text{ or } \frac{\varrho h}{\gamma} = O(1), \frac{L^2}{hR} \gg 1.$$

Equations (B), (C) and (D) may be discussed in an entirely similar way, and the result of our process of simplification is given in table 1, where a subscript γ (or ϱ) to the letters A, B, C or D indicates that only the

membrane terms (or bending terms) in the corresponding equation are retained. If no subscript is attached both bending and membrane terms should be retained in the equation.

Out of the nine combinations of orders of magnitude of our two parameters, five are of major physical importance. These cases all occur in the two diagonals of our table. The equations of generalized plane stress and the equations of bending of plates apply to shells of negligible curvature. The equations of the membrane theory of shells are too well-known to require a further discussion here. The equations of (nearly) inextensional bending of shells govern e.g. the helicoidal shell under normal loads, which has been investigated in detail by means of the complete equations [7, 8]; it has been verified that the simplified equations A_ϱ, B_ϱ, C, D yield the same stress distribution. Finally, the equations of shallow shells are applicable e.g. to a discussion of the edge effect in shells.

TABLE 1

Simplified shell equations

If an equation (A), (B), (C) or (D) may be simplified by dropping the terms involving flexural stresses or strains, this equation is denoted by A_γ etc; conversely, if the terms involving extensional stresses or strains may be dropped, the equation is denoted by A_ϱ.

	$\frac{L^2}{hR} \ll 1$	$\frac{L^2}{hR} = O(1)$	$\frac{L^2}{hR} \gg 1$
$\frac{\varrho h}{\gamma} \ll 1$	Eqs. A_γ, B, C, D_γ *Equations of generalized plane stress*	Eqs. A_γ, B, C_γ, D_γ *Exceptional case*, in which the equations of generalized plane stress and the equations of the membrane theory of shells are satisfied simultaneously	Eqs. A, B, C_γ, D_γ *Equations of membrane theory of shells*
$\frac{\varrho h}{\gamma} = O(1)$	Eqs. A_γ, B_ϱ, C_ϱ, D_γ *Superposition* of the equations of generalized plane stress and the equations of bending of flat plates	Eqs. A, B_ϱ, C, D_γ *Equations of shallow shells*	Eqs. A_ϱ, B_ϱ, C_γ, D_γ *Superposition* of the equations of the membrane theory of shells and the equations of (nearly) inextensional bending of shells
$\frac{\varrho h}{\gamma} \gg 1$	Eqs. A, B_ϱ, C_ϱ, D *Equations of bending of flat plates*	Eqs. A_ϱ, B_ϱ, C_ϱ, D *Exceptional case*, in which the equations of bending of flat plates and the equations of (nearly) inextensional bending of shells are satisfied simultaneously	Eqs. A_ϱ, B_ϱ, C, D *Equations of (nearly) inextensional bending of shells.*

Two cases are marked "exceptional" in our table because their realisation requires that the *three* extensional strain components in one case, and the *three* flexural strain components in the other case satisfy simultaneously a set of *four* independent equations. This will only be possible under exceptional circumstances.

A further simplification of the equations is permissible in the cases $L^2/hR \leqq O(1)$ by observing that the sequence of covariant differentiation may be interchanged in these cases. The general formula for repeated covariant differentiation of a vector is

$$u_{\alpha|\lambda\mu} - u_{\alpha|\mu\lambda} = R^{\varkappa}_{.\alpha\lambda\mu} u_{\varkappa}, \tag{2.10}$$

where the tensor of RIEMANN–CHRISTOFFEL of the middle surface is given by

$$R^{\varkappa}_{.\alpha\lambda\mu} = a^{\varkappa\varrho} R_{\varrho\alpha\lambda\mu} = K a^{\varkappa\varrho} \varepsilon_{\varrho\alpha} \varepsilon_{\lambda\mu}, \tag{2.11}$$

and K is the GAUSSIAN curvature of the middle surface. The terms in the left-hand member of (2.10) are both of order of magnitude u/L^2, whereas the right-hand member is at most of order u/R^2. Hence it is no more than consistent in our approximations to neglect the right-hand member if $L^2/hR \leqq O(1)$. This simplification implies in the cases $\varrho h/\gamma \leqq O(1)$ that the stress resultants $n^{\alpha\beta}$ can be expressed in a single invariant stress function Φ, and in the case $\varrho h/\gamma \geqq O(1)$ that the changes of curvature can be expressed in a single invariant displacement $\bar{w}$, which may be identified with the normal displacement w.

It seems appropriate to end with a repeated word of caution. Many pitfalls lie on the path of an unsuspecting investigator in shell theory, and our recommendation can hardly be overstressed that a careful check a posteriori should always be made, in order to verify that the solution of the simplified equations is indeed a satisfactory approximation to the solution of the original basic equations (A) to (D).

REFERENCES

1. KOITER, W. T., A consistent first approximation in the general theory of thin elastic shells. Proc. I.U.T.A.M. Symposium on the Theory of Thin Elastic Shells (Delft, August 1959), North-Holland Publishing Company, Amsterdam (1960), 12–33.
2. ———, A consistent first approximation in the general theory of thin elastic shells, Part 1, Foundations and linear theory. Report of Laboratorium voor Toegepaste Mechanica, Delft (1959); this report is a more detailed version of [1].
3. GOLDENWEISER, A. L., The equations of the theory of shells (in Russian), Prikl. Mat. Mekh., **4**, Nr. 2 (1940).
4. NOVOZHILOV, V. V., The theory of thin shells. Translated from the Russian 1951 edition by P. G. Lowe (edited by J. R. M. Radok), P. Noordhoff Ltd., Groningen (1959).

5. Green, A. E. and W. Zerna, Theoretical Elasticity, Oxford University Press, Oxford (1954).
6. Wlassow, W. S., Allgemeine Schalentheorie und ihre Anwendung in der Technik. Ubersetzt aus der Russischen Herausgabe (1949) unter Redaktion von A. Kromm, Akademie–Berlag, Berlin (1958).
7. Cohen, J. W., On stress calculations in helicoidal shells and propeller blades. Thesis Delft (1955).
8. ———, The inadequacy of the classical stress-strain relations for the right helicoidal shell. Proc. I.U.T.A.M. Symposium on the Theory of Thin Elastic Shells (Delft, August 1959), North-Holland Publishing Company, Amsterdam (1960), 415–433.

PALEONTOLOGY

LEPIDOCYCLINA RADIATA (K. MARTIN), 1880

BY

I. M. VAN DER VLERK *)

(Communicated at the meeting of June 24, 1961)

ABSTRACT

In 1880, K. MARTIN described a new species of *Lepidocyclina* from the south coast of western Java, and named it *L. radiata*. Although practically nothing was known of its internal structure and although this specimen was the sole representative of the type, various authors have given the name *L. radiata* to *Lepidocyclinae* found elsewhere. For this reason, the author had an equatorial section and a "peel" of part of the vertical section made from the type-specimen, which belongs to the "Rijksmuseum van Geologie en Mineralogie" at Leyden. In the author's opinion, both stratigraphic and palaeontological evidence indicates that the layer at Sindangbaran (JUNGHUHN's locality "K"), in which the type-specimen of *L. radiata* was found, has been formed during the final part of the Tertiary-f.

In 1880, K. MARTIN published the results of his examination of the fossils collected in Java by FR. JUNGHUHN. Among these fossils was a foraminifer to which he gave the name *Orbitoides radiata* (plate I, fig. 1). The rock, in which this "*Orbitoides*" had been found, was a clayey, calcitic vitreous tuff. In this rock, MARTIN also found other foraminifera. Among these was a *Cycloclypeus*, which he called *C. communis*. The presence of molluscs in the deposit, situated near the south coast of western Java, led to its assignment to the Late Miocene. MARTIN based this age determination on the fact that 30 % of the molluscs encountered by JUNGHUHN in this deposit were still to be found in the present-day fauna (K. MARTIN, 1880).

The specimen on which MARTIN based the new species is now in the possession of the "Rijksmuseum van Geologie en Mineralogie" at Leyden. This unique specimen, if it was not to be damaged, could only be studied externally. Nevertheless, the edges were slightly broken already, so that part of the equatorial plane was visible, and the structure thereby exposed to view convinced R. D. M. VERBEEK that "*Orbitoides*" *radiata* was in fact a *Lepidocyclina* (R. D. M. VERBEEK and R. FENNEMA, 1896, p. 809 and p. 1116). By having two thin sections of a part of a specimen made, MARTIN (1900, p. 211) was able to confirm this: the equatorial chambers

*) Koninklijke/Shell Exploratie en Produktie Laboratorium (Shell Internationale Research Maatschappij N.V.) Rijswijk (Z.H.), The Netherlands.

were found to be clearly hexagonal in shape. Fig. 2 of plate I is a photograph of one of these thin sections, which are likewise in the possession of the above-mentioned museum.

The fact that the type-specimen has been far from adequately described has not restrained certain authors from giving the name *L. radiata* to *Lepidocyclinae* found at other localities.

Thus H. DOUVILLÉ (1916) described as *L. radiata Lepidocyclinae* taken from the Rembang strata of eastern Java. These specimens had a maximum diameter of 5 mm and were characterised by a central boss surrounded by a flange on which stood about 10 radiating ridges. H. DOUVILLÉ did not hesitate to consider them as belonging to the species *L. radiata*. By studying the equatorial plane it appeared that the Rembang *Lepidoyclinae* had a nucleoconch that was identical with that of *Lepidocyclina limbata*, which had been found at the same locality and described in the same work (H. DOUVILLÉ, 1916, plate IV, figs. 8–9). This meant that the specimens from eastern Java described by DOUVILLÉ as *Lepidocyclina radiata* possessed a so-called eulepidine nucleoconch.

Apparently MARTIN (1919) was prepared to accept the synonymy between the type-specimen from the JUNGHUHN collection on the one hand and the *Lepidocyclinae* from Rembang on the other. This would at any rate explain why he assumed that the type-specimen must likewise possess a eulepidine nucleoconch. What is more, this conclusion led him to revise the age of the deposit in which JUNGHUHN had found the *Lepidocyclina*. Since *Lepidocyclinae* with a eulepidine nucleoconch could not, according to DOUVILLÉ, be younger than Early Miocene, and since the molluscan fauna of the Rembang strata likewise suggested an Early Miocene age, MARTIN considered it possible that the deposition of the sediments situated on the south coast of western Java and containing the foraminifera and mollusca collected by JUNGHUHN had already begun, at any rate in part, in the Early Miocene.

Another author who identified *Lepidocyclinae* from a different locality with MARTIN's type-specimen of *L. radiata* was G. LESLIE WHIPPLE (1934, p. 148). When describing a foraminiferal fauna collected by Dr. HARRY S. LADD on the island of Vitilevu (Fiji), he found several *Lepidocyclinae* that outwardly showed considerable resemblance to MARTIN's type-specimen. He too does not seem to have felt that the fact that the type's internal structure was practically unknown constituted an obstacle to his giving the name *L. radiata* to these radiate *Lepidocyclinae*. Horizontal sections of these specimens revealed that they too possessed a typically eulepidine nucleoconch.

A third author who was not deterred from identification by the incomplete description of the type-specimen was W. STORRS COLE, who likewise gave the name *L. radiata* to a number of *Lepidocyclinae* originating from the Lau Islands (Fiji) (COLE, 1945, p. 292). He states most emphatically (COLE, 1960, p. 137): "the specimens from Vitilevu, Fiji, illustrated

by WHIPPLE (1934, plate 19, figs. 3, 6) are identical with the illustration given by MARTIN of *L. radiata*".

For some time now, I have been wondering whether it would be justifiable to sacrifice the type-specimen at the "Rijksmuseum van Geologie en Mineralogie" at Leyden in the cause of learning something about its internal structure. My doubts were finally dispelled, however, on reading an interesting publication by W. STORRS COLE, published in 1960 and entitled "Variability in embryonic chambers of *Lepidocyclina*". In numerous publications, COLE has shown that he has a talent for describing accurately the material set before him. His clear illustrations give a good picture not only of the external features but also, as a result of skillful preparation, of the internal structures.

I have always been under the impression that COLE was more apt to be numbered among the "splitters" than among the "lumpers". It is therefore all the more surprising to find that in the above-mentioned publication he has a strong tendency to indulge in "lumping". Under the name *Lepidocyclina radiata* (K. MARTIN, 1880) he includes no less than eight other species, viz.:

Lepidocyclina borneensis PROVALE, 1909
Lepidocyclina luxurians TOBLER, 1928
Lepidocyclina transiens UMBGROVE, 1929
Lepidocyclina irregularis HANZAWA, 1932
Lepidocyclina suvaensis WHIPPLE, 1934
Lepidocyclina gerthi CAUDRI, 1939
Lepidocyclina fijiensis COLE, 1945
Lepidocyclina oneataensis COLE, 1945

After which COLE then adds the hopeful remark: "There may be other synonyms of this variable species, but the listing of these names will be sufficient for the time." (COLE, 1960, p. 137.)

I myself am at present engaged on a study of material collected in the Far East, in which these forms possessing an abnormally large nucleoconch occur. For that reason, I prefer not to express my opinion of COLE's views for the time being. So that those who do wish to express an opinion in the near future may be able to base their arguments on as wide a range of evidence as possible, however, I should like to give here a revised and illustrated description of K. MARTIN's original specimen.

Type description

Test polygonal, with central boss 2 mm in diameter from which radiate 9 ribs. These ribs are less than ½ mm in width, 2 mm or more in length and do not reach the periphery. Horizontal diameter: 8 mm. Thickness

Fig. 1. *L. radiata* before section was made ($\times$ 10).

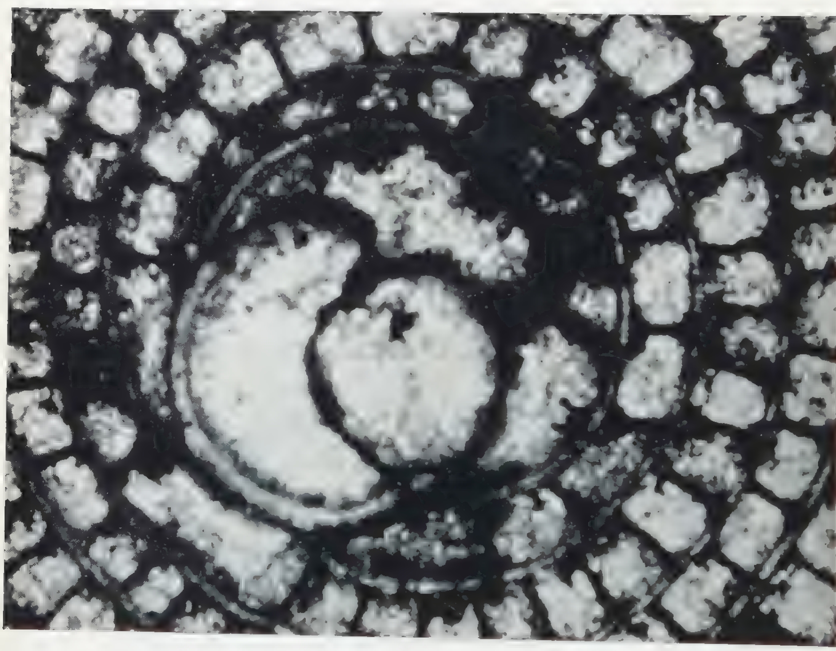

Fig. 2. Horizontal section of *Cycloclypeus* from same rock as that in which *L. radiate* was found. Section shows that this *Cycloclypeus*, which has 3 nepionic chambers, belongs to the Subsectio *carpenteri* (× 100).

at centre: ca. 2 mm, close to periphery ca. 0.25 mm. Small pillars about 50 μ in width are scattered over the whole surface.

The protoconch is more or less oval in horizontal section, measures ca. 275 μ in length and has a maximum breadth of ca. 160 μ. Since the two ends of the protoconch touch the sides of the deuteroconch, which is also oval, the short axis of the deuteroconch likewise measures ca. 275 μ, while its long axis measures ca. 450 μ. There is only one PA (primary auxiliary chamber), which is thus a combination of the two primary auxiliary chambers usually found. There are 9 Ads (adauxiliary chambers).

The hexagonal equatorial chambers are arranged in polygons. In the radii, close to the periphery, they have a radial diameter of 90 μ and a tangential diameter of 50 μ. In the interradii, close to the periphery, their radial diameter is 60 μ, and their tangential diameter 30 μ. The thickness of the walls of the equatorial chambers is 10 μ. The height of the equatorial-chamber plane close to the nucleoconch is 70 μ and close to the periphery also 70 μ.

On either side of the equatorial plane lie, in the centre, about 7 lateral chambers which, close to the periphery, have a horizontal diameter of about 100 μ and a height of 25 to 30 μ. Their walls are 7 μ thick. The lateral chambers do not have curved horizontal walls; they are quadrilaterals with rounded corners.

Type level: Uppermost part of Tertiary-f.

Type locality: The hills north of Sindangbaran, near the south-east coast of western Java (=Junghuhn's locality "K").

Type-specimen: "Rijksmuseum van Geologie en Mineralogie", Leyden, No. 3448.

The type level given above, the uppermost part of the Tertiary-f, requires further clarification.

There are three reasons for my considering the *Lepidocyclina* described here as one of the last to have existed, if not the last.

The first reason is stratigraphic. In 1939, the geologists J. Duyfjes (†) and K. A. F. R. Musper, accompanied by the geomorphologist A. J. Pannekoek, made a reconnaissance of the Djambang area on the south coast of western Java. The original record of this expedition has been lost, but short reports dealing with it appeared in the "Algemeen gedeelte" of the "Jaarboek van het Mijnwezen, 1939" and in the "Tijdschrift van het Koninklijk Nederlandsch Aardrijkskundig Genootschap" (Pannekoek, 1946). With the article published in the latter journal, there appeared a simplified geological sketch map. Although the locality at which *L. radiata* was found, lies just outside the southeastern part of the mapped area, the map does nevertheless permit us to assume that this species of *Lepidocyclina* existed during the formation of the so-called Bentang series. As can be seen from the geological map and the accompanying profiles, the Bentang series is younger than the Tjimandiri series, the clayey deposits

of which are known under the name Njalindoeng beds. The latter largely owe their fame to the rich variety of molluscs they contain. These have been described in detail by K. MARTIN (1891–1922). This work led MARTIN to the conclusion that this fauna must have lived during the Early Miocene and that it was older than the molluscan fauna from the Tji Lanang beds, further to the east, which he considered to be Late Miocene. Observations in the field have shown, however, that this age difference is not very likely (OOSTINGH, 1938). Both sets of beds are now combined under the name "Preangerian". BEETS (1950, p. 279) considers them, on the basis of his numerous studies of the Tertiary molluscan fauna of the Far East, to belong to the last part of the Tertiary-f (f3). It is this that leads me to conclude that *Lepidocyclina radiata*, which almost certainly occurs in the even younger Bentang series, must have lived during the very last part of the Tertiary-f.

The second basis for this conclusion is paleontological. In 1880 (p. 154), MARTIN had already mentioned the presence in the sample containing *L. radiata* of a *Cycloclypeus*, which he called *Cycloclypeus communis*. As TAN SIN HOK later remarked (1932, p. 82), however, MARTIN's *Cycloclypeus communis* was a problematic species that deserved to be re-examined. This has since been done. It is found that the *Cycloclypei* of Sindangbaran are characterised by a horizontal diameter of 2–8 mm and bij pillars that, near the centre, are arranged more or less irregularly and, at the periphery, in concentric rows. Three horizontal sections show that the proloculum has a diameter of 230 μ and that the second protoconchal chamber has a maximum width of about 400 μ (plate II, fig. 2). The ana-nepionic substage is represented by the undivided first nepionic chamber. There are three or, at the most, four nepionic chambers. From these facts it can be concluded that the *Cycloclypeus* of Sindangbaran must be assigned to the Sectio *carpenteri*, Subsectio *carpenteri*. This too is an indication that a late Tertiary-f age is probable.

The third argument in support of the supposition that *L. radiata* was one of the last *Lepidocyclinae* to have lived, if not the last, is derived from the internal structure of the only known specimen (plate II, fig. 1). The shape of the nucleoconch might be characterised as extremely *trybliolepidine*. If this is compared with that of the *Lepidocyclina* occurring in the, older, Njalindoeng beds (VAN DER VLERK, 1924, p. 4, fig. 8), several marked differences can be observed. For example, the shape of the protoconch in the Sindangbaran specimen is so stretched out that its two short sides form part of the wall of the surrounding deuteroconch. Consequently, in horizontal section, the nucleoconch appears to be divided into three parts. A second characteristic is the small width of the basal part of the protoconch. The remarkable consequence of this is that only one primary auxiliary chamber is formed, instead of the usual two. This chamber is formed, however, as the position of the stolons shows and as is normally the case, by the deuteroconch.

When I derive from the construction of this nucleoconch an argument to support my placing *L. radiata* in the very last part of the *Lepidocyclina* containing Tertiary, I am basing it on the very high grade of evolution to which this species has attained. A couple of years ago, I indicated (VAN DER VLERK, 1959) that this degree of evolution could be determined by the combination of two factors. The tendency for the deuteroconch increasingly to enclose the protoconch during the course of evolution was designated factor A. Factor B was the tendency for an increasing number of adauxiliary chambers to be formed. Combination of these factors should enable the age of a *Lepidocyclina*-containing bed to be stated in terms of the degree of evolution – expressed as a number – of the *Lepidocyclinae* occurring in it. The numbers presented in the above-mentioned publication are not, however, by any means definitive, as I was at pains to point out at the time. Before such can be the case, a great deal more material will have to be examined than has been hitherto. Yet, although the figures are still to some extent unreliable, they do possess a certain limited value. If, when examining various specimens of *Lepidocyclina* from the Preangerian (= Tjamandiri series), I find an average degree of evolution of 137.1, whereas the horizontal section of the nucleoconch and periembryonic chambers of *L. radiata* illustrated here is found to have a degree of evolution of 157.9 (plate II, fig. 1), it does not seem to me to be unduly daring to assume that this *L. radiata* must have existed later than the *Lepidocyclinae* from the Preangerian.

I should like, in conclusion, to express my thanks to Dr. P. C. ZWAAN, the acting director of the "Rijksmuseum van Geologie en Mineralogie", who gave me permission to examine the type-specimen more closely, to the staff of "Koninklijke/Shell Exploratie en Produktie Laboratorium" for facilities given, to Mr. W. R. BURKE, who has been so kind as to translate this text into English and to Messrs. J. J. F. HOFSTRA, R. W. TOORENS, B. F. M. COLLET and J. H. H. VAN GIGCH for making preparations, drawings and photographs.

LITERATURE

BEETS, C., On probably young Miocene fossils from the coal concession Batoe Panggal near Tenggarong (Samarinda), Eastern Borneo. Leidse Geol. Med., **XV**, 265–281 (1950).

COLE, W. S., "Larger Foraminifera" in: LADD, H. S. and J. E. HOFFMEISTER, Geology of Lau, Fiji. Bernice P. Bishop Museum, Bull. 181, 227–297 (1945).

———, Variety in embryonic chambers of *Lepidocyclina*. Micropaleontology, **6**, 2, 133–144 (1960).

DOUVILLÉ, H., Les foraminifères des couches de Rembang. Sammlungen des Geologischen Reichsmuseums in Leiden, Serie I, **X**, 19–35 (1916).

———, Révision des Lépidocyclines. Mémoires de la Société Géologique de France, nouvelle série, tome **2**, 2, 51–123 (1924).

Jaarverslag 1939 van den Dienst van den Mijnbouw, Jaarb. Mijnwezen, 68e jaarg., Algemeen Gedeelte, Systematische Kaarteringen Java, 16–27 (1939).

MARTIN, K., Die Tertiärschichten auf Java, nach den Entdeckungen von FR. JUNGHUHN. E. J. BRILL, Leiden (1880).

———, Die Eintheilung der Versteinerungsführenden Sedimente von Java. Sammlungen des Geologischen Reichsmuseums in Leiden, Serie I, **VI**, 135–245 (1900).

———, Unsere palaeozologische Kenntnis von Java. E. J. BRILL, Leiden (1919).

———, Die Fossilien von Java. Sammlungen des Geologischen Reichsmuseums in Leiden, N.F., I (1891–1922).

OOSTINGH, C. H., Mollusken als gidsfossielen voor het Neogeen in Nederl. Indië. Handel. 8e Nederl. Ind. Natuurwetensch. Congres, Soerabaja, 508–516 (1938).

PANNEKOEK, A. J., Geomorphologische waarnemingen op het Djampang-plateau in West Java. Tijdschr. Kon. Ned. Aardrijksk. Gen., 2e reeks, **LXIII**, 3 (May 1946).

TAN SIN HOK, On the genus *Cycloclypeus Carpenteri*, part I. Wetensch. Meded. Dienst Mijnbouw in Nederl. Indië, No. 19 (1932).

VERBEEK, R. D. M. and R. FENNEMA, Geologische beschrijving van Java en Madoera. Amsterdam (1896).

VLERK, I. M. VAN DER, Foraminiferen uit het Tertiair van Java. Wetensch. Meded. Dienst Mijnbouw, No. 1 (1924).

———, Modification de l'ontogenèse pendant l'évolution des Lépidocyclines. Bull. Soc. Géol. de France, 7e sér., **I**, 669–673 (1959).

WHIPPLE, G. L., "Larger Foraminifera from Vitilevu, Fiji" in: LADD, H. S., Geology of Vitilevu, Fiji. Bernice P. Bishop Museum, Bull. **119**, 141–154 (1934).

PALEONTOLOGY

SOME NEW OSTRACODA OF THE CARIBBEAN TERTIARY

BY

W. A. VAN DEN BOLD

(Comm. by Prof. Dr. G. H. R. von Koenigswald at the meeting of May 27, 1961)

Abstract. Seven new and two insufficiently known species of Ostracoda are described from Tertiary deposits of various places in the Caribbean.

Introduction

Reviewing earlier collections, it appeared necessary to redescribe some of the Ostracoda published in my thesis (van den Bold, 1946). New figures are added as well as more detailed data on the localities (fig. 1). D and S numbers refer to the collections of the Paleontological Department of the State University of Utrecht.

I. Miocene, Guatemala

1: "Pliocene" of Sapper, 1937, p. 84, Pl. IV, N. of Chinaja mountains.
T 107: Rio Salinas, N 16°03′, W 90°38′.

2: Rio Dulce limestones. Sapper, 1937, p. 83, 101, Pl. VI.
W 66: N 15°44′, W 88°45′.
W 124: Rio Ciénaga, N 15°44′, W 89°00′.
W 132: Rio Ciénaga, N 15°45′, W 89°07′.

II. Oligocene, Cuba

H 428: E. Oriente, Maquay formation, Keijzer, 1945, map.

P 28: Matanzas, sample of soft buff marl from waterwell on Finca Adelina, about 9.5 km E of Colón, 500 m N of Central highway. Palmer & Bermudez, 1935, p. 227.

III. Middle and Upper Eocene, Cuba

Globorotalia cerroazulensis zone.

F 93: marl with sandy layers, near road from Los Cristales (between Ciego de Avila and Sancti Spiritus, about 6 km N of km 432.8) at about 10 km along the road.

K 206; E. Oriente, outcrop near road from Palmarito to the north, about 13 km due NW from Palmarito, about 8 km W of the serpentine massif of the Sierra de Nipe and about 3 km due N from the Río Cauto. Keijzer, 1945, p. 48, 49.

Fig. 1. Sample map of Central Guatemala. On the latest maps the Rio Chixoy and the Rio Cancuén are both drawn about 6–8 km further west, but even in these maps details of the course of the rivers show strong differences.

IV. **Lower Eocene, Guatemala**

D 160: Caribe anticline, N 16°07′, W 90°19′.
T 88: Río Salinas at El Caribe, N 16°11′, W 90°26′.
T 111: Río Salinas–Cancaná, N 16°03′, W 90°39′.
T 114: Caribe anticline, N 16°11′, W 90°25′.
V 199: Caribe anticline, N 16°11′, W 90°25′.
V 141: Caribe anticline, N 16°10′, W 90°25′.
V 243: West of Setoc, N 16°17′, W 90°11′.

V. **Lower Eocene, British Honduras**

D 211: Golden Stream, N 16°19′, W 88°46′.
D 227: Sunday Wood Creek, N 16°01′, W 89°01′.

SYSTEMATICS

Genus **Paracypris** Sars, 1866

Paracypris sapperi n.sp.

fig. 2a, b

Paracypris aff. limburgensis v. Veen, v. d. Bold, 1946, p. 65, pl. 4, fig. 1a, b.
Not *Paracypris limburgensis* v. Veen, 1934, p. 2, pl. 1, fig. 1–18.
Not *Paracypris aff. limburgensis* v. Veen, v. d. Bold, 1957a, p. 5, pl. 2, fig. 11.

Carapace elongate, highest in the middle, but giving the impression of being higher in the posterior portion than in the anterior. Anterior end low, narrowly rounded, posterior end ventrally rounded, almost subacute; dorsal margin arched with almost straight posterior slope, ventral outline weakly convex. Left valve overlapping the right along the entire periphery except for a very short distance at either end. Overlap strongest in antero- and posterodorsal part, where the dorsal margin of

Fig. 2. *Paracypris sapperi* v. d. Bold n.sp., holotype, from T 88, Lower Eocene, Guatemala. a) right valve view, b) dorsal view. × 45.

the right valve is slightly concave. Dorsal view spindle-shaped, regularly convex throughout, widest in the middle.

Dimensions: Holotype: L: 1.10; H: 0.45; W: 0.40.

Apart from resembling *Paracypris limburgensis* this species bears a slight resemblance to *Paracypris strecca* Schmidt (1948, p. 408, pl. 63, figs. 21, 22), but there the greatest height lies more anteriorly, and the whole anterior end is higher.

Holotype: A complete carapace from T 88 (S 13132), Lower Eocene of Guatemala. Paratypes: same locality (S 14243).

The figured specimen in v. d. Bold, 1946, came from T 111, also Lower Eocene Guatemala.

Genus **Costa** Neviani, 1928

Costa maquayensis n.sp.

figs. 3a–b, 4

Cythereis polytrema (Brady) v. d. Bold, 1946, p. 89, pl. 10, fig. 6 (not pl. 9, fig. 4 (= *Costa* sp., young molt)); v. d. Bold, 1950, p. 108.
Not *Cythere polytrema* Brady 1878, p. 363, pl. 66, fig. 1.

Carapace elongate subquadrate, highest at the anterior cardinal angle, where the left valve strongly overlaps the right. Greatest width behind the middle at the posterior end of the ventral ridge. Anterior end obliquely rounded in the left valve, almost evenly rounded in the right, heavily rimmed and denticulate; dorsal margin straight, partly obscured by a dorsal ridge; it converges posteriorly slightly towards the ventral margin, which is regularly convex and partly obscured by a ventral rim; posterior end angled just below the middle, concave above, convex, and bearing a few stout spines below. The posterior cardinal angle is pronounced in the left valve and bears a short denticle, pointing upward and backward, on its posterior slope.

Carapace heavily reticulate and ridged. There are three longitudinal ridges, and the reticulations in between are of two types: one with large meshes and heavy ribs and a secondary reticulation with smaller meshes and thinner ribs subdividing the large primary type. Dorsal ridge runs forward from in front of the posterior cardinal angle, partly obscuring the dorsal margin; it is arched upward, 4 large meshes long and ends below and behind the anterior cardinal angle; it is highest at the third mesh from behind.

Median ridge starts about the centre of the valve at a rather vaguely defined subcentral tubercle and extends backward about parallel to the dorsal ridge, convex upward, and ends in front of a spot vertically below the posterior end of the dorsal ridge. Sometimes it continues further backwards as a weakly developed ridge in the direction of the middle of the ventral part of the posterior margin. From the subcentral tubercle forward runs a short convex ridge curved downward, starting below the median one. Ventral ridge starts behind the anterior rim and is separated from it by a deep depression, which continues between ventral ridge and ventral rim, which is a continuation of the anterior rim; this depression becomes shallower posteriorly. The ventral ridge extends less far backward than the median ridge and ends in a strong spine. The reticulate surface of the valves is strongly depressed behind the anterior rim and below the anterior median ridge. In the anterior end the ridges of the reticulation appear to radiate from the subcentral tubercle and are convex downward. In this respect they resemble the anterior ridges in *Cythereis rutteni* v. d. Bold.

Interior of the valves fairly shallow; marginal area broad in anterior end, line of concrescence and inner margin coincide; radial porecanals numerous, long, thin and slightly sinuous. Hinge in the left valve consists of an anterior round socket, which is separated from the interior by a low rim, the posterior socket is open to the interior. Median element consists of a strong bar with anterior, attached tooth.

Musclescars: a vertical row of 4 adductor scars of which the second one from the bottom has the tendency to become subdivided. Antennal scars form a more or less cloverleaf-shaped group.

Dimensions: L: 0.87; H: 0.49; W: 0.35 (holotype).

In the structure of the anterior median ridge the species bears some resemblance to *Costa variabilocostata* (v. d. Bold) (1957b, p. 241, pl. 2, fig. 4) and *Costa meka* v. d. Bold (1960, p. 167, pl. 4, figs. 7a, b).

Occurrence: Lower Oligocene of Cuba (F 93, H 428, P 28, Bermudez 209 (v. d. Bold 1950). Oligocene of Venezuela, together with *Costa meka*, the range of which is in Trinidad U. Eocene–L. Oligocene. In Trinidad it has been found in a sample containing: *Krithe hiwanneensis* Howe & Lea, *Munseyella minuta* (v. d. Bold), *Cytherella stainforthi* v. d. Bold, *Xestoleberis moriahensis* v. d. Bold, and *Loxoconcha wagneri* v. d. Bold. The ranges of these species suggest that the sample should be placed in

the Oligocene section, in the *Globigerina ampliapertura* or the *Globorotalia ciperoensis ciperoensis* zone.

Holotype: a complete carapace from H 428 (S 13123). Paratypes (S 14244) from H 428, P 28 and F 93, Oligocene, Cuba.

The species referred to *Cythereis polytrema* (Brady) from T 1479, Lower Miocene, should be referred to as *Costa* sp., as should be the one from G 12, Upper Eocene of Bonaire.

Genus **Hermanites** Puri, 1955

Hermanites setocensis n.sp.

figs. 6a, b

Cythereis collei Gooch?, v. d. Bold, 1946, p. 94, pl. 11, fig. 4a (not fig. 4b, c = *Cythereis collei* Gooch var. *extrema* v. d. Bold).

Not *Cythereis collei* Gooch, 1939, p. 585, pl. 67, fig. 19.

Not *Cythereis collei* Gooch?, v. d. Bold, 1957a, p. 9, pl. 2, fig. 6a, b (= *Hermanites ulrichi* n. sp.).

Hermanites bassleri (Ulrich) var. 1, Drooger, 1960, p. 462, pl. 3, fig. 8a, b.

Carapace subquadrangular, highest at the anterior cardinal angle, where the left valve very largely overlaps the right. Widest about the middle, at the subcentral tubercle. Anterior end very broadly rounded, almost truncate in the left valve, with anterior rim, and very finely denticulate. Glassy eyespot just below the anterior cardinal angle at the dorsal end of the anterior rim. Dorsal margin straight, partly obscured by a parallel dorsal ridge; ventral margin straight behind a sinuation in front of the middle, converging slightly towards the dorsal margin posteriorly; posterior end angled below the middle, concave above, strongly so in the right valve, convex below, and bearing a few small blunt spines. Surface reticulate with rather rounded meshes. Dorsal ridge slightly nodose, curving over the meshes of the reticulation, very wide in dorsal view at its posterior end, in front of the posterior cardinal angle. Ventral ridge short, starting behind the anterior rim, ending about 1/3 from posterior end, well in front of the end of the dorsal ridge. Subcentral tubercle strongly developed, placed nearly in the centre, only slightly anterior to it.

Dorsal view shows the sides parallel behind the bulging subcentral tubercle with the posterior end of the ventral ridge just sticking out. This dorsal view is reminiscent of *Hermanites thoracophora* (v. d. Bold), but the species differs by its very blunt anterior end in side view.

Dimensions: Holotype: L: 0.61; H: 0.37; W: 0.30.

Sexual dimorphism is very weak and not expressed in measurements as the males are only slightly more slender in the posterior portion.

Occurrence: Guatemala, Lower Eocene and Paleocene: D 160, 221, 230, H 169, T 88, 111, V 113, 128, 150, 178, 179, 199, 243, 321, 341, 342.

Holotype: A complete carapace from V 243 (Paleocene, Guatemala) near Setoc (see map fig. 1), S 13124. Paratypes: V 243 (S 13125).

Fig. 3. *Costa maquayensis* v. d. Bold n.sp., holotype, from H 424, Maquay formation, Oligocene, Cuba. a) right valve view, b) dorsal view. × 55.

Fig. 4. *Costa maquayensis* v. d. Bold n.sp., from P 28, Finca Adelina, Oligocene, Cuba. Interior of left valve. × 55.

Fig. 5. *Hermanites ulrichi* v. d. Bold n.sp., holotype, from T 88, Lower Eocene, Guatemala. a) right valve view, b) dorsal view. × 55.

Fig. 6. *Hermanites setocensis* v. d. Bold n.sp., holotype, from V 243, Paleocene, Guatemala. a) right valve view, b) dorsal view. × 52.5.

Fig. 7. *Quadracythere stadnichenkoae* v. d. Bold n.sp., holotype, from V 141, Lower Eocene, Guatemala. a) right valve view, b) dorsal view. × 57.5.

Fig. 8. *Quadracythere goldenensis* v. d. Bold n.sp., holotype, from D 211, Lower Eocene, British Honduras. a) right valve view, b) dorsal view. × 55.

Hermanites ulrichi n.sp.

figs. 5a, b

Cythereis bassleri (Ulrich)?, v. d. Bold, 1946, p. 94, pl. 6, fig. 20a, b.
Not *Cythere bassleri* Ulrich, 1902, p. 120, pl. 16, fig. 19–21.
Hermanites collei (Gooch)?, v. d. Bold, 1957a, p. 9, 10, pl. 2, fig. 6a, b.

Carapace elongate, subrectangular, highest at the anterior cardinal angle, widest at the posterior end of the ventral ridge, about 1/4 from behind. Anterior end broadly and somewhat obliquely rounded, denticulate and rimmed, the rim ending dorsally in a small eyespot just below the anterior cardinal angle. Left valve overlapping strongly at this place. Dorsal margin straight, converging slightly posteriorly to the equally nearly straight ventral margin; posterior end angled below the middle, rounded and dentate below, concave above. The left valve also shows large overlap in the dorsal portion of the posterior end. Shape in side view fairly similar to *Quadracythere goldenensis* n.sp., but reticulate pattern different. This consists of large and irregular meshes in the posterior portion, in the anterior portion of much smaller meshes. Subcentral tubercle more pronounced than in the *Quadracythere goldenensis* n.sp. Ornamentation with dorsal and ventral ridge. The ventral ridge is more strongly alate than in the species quoted above, while the dorsal ridge is also more pronounced. A median ridge, running obliquely from the subcentral tubercle to just below the posterior end of the dorsal ridge, is also more strongly developed in this species. In dorsal view the very strong compression of the posterior end behind the dorsal ridge is typical of this species. Sexual dimorphism is weak.

Dimensions: ? female: L: 0.87; H: 0.52; W: 0.48.
? male : L: 0.89; H: 0.53; W: 0.44.

Occurrence: top Paleocene and Lower Eocene of Guatemala: T 88, 111, D 160, H 137, V 314, 321, 342 (D 30811).

Holotype: a complete carapace from T 88 (S 13130), Lower Eocene, Guatemala. Paratypes: S 13131, from T 88 and T 111.

Genus **Munseyella** van den Bold, 1957

Munseyella machaquillaensis (v. d. Bold)

figs. 9a, b

Cythereis ? machaquillaensis v. d. Bold, 1946, p. 46, pl. 9, fig. 5 a, b.

Carapace small, elongate quadrangular, highest near anterior cardinal angle, widest in anterior third of the carapace. Anterior end obliquely rounded, heavily rimmed, with 2–3 thick knobby spines projecting anteriorly in the lower half. Dorsal outline almost straight, very gently convex, ventral outline slightly but regularly concave, parallel to the dorsal margin in posterior half, slightly converging in the anterior part. Posterior end almost vertically truncate, exhibiting two short stout spines, one

about 1/3 down posterior margin, the other about 2/3 down from the posterior cardinal angle, which is rounded but nearly 90 degrees.

Surface with an irregular pattern of swellings, the most prominent of which goes vertically down from in front of the posterior cardinal angle to about halfway down the carapace. A ventral ridge ends about 1/4 from the posterior end, the carapace is strongly compressed behind it and below and behind the posterior swelling. Part of the ventral ridge runs forward and slightly upward, diverging from the ventral margin and splits off 2–3 upward ridges before turning upward itself; the other part joins the anterior rim. From the upper end of the posterior ridge a dorsal ridge extends forward, rather ill-defined in side view.

In dorsal view the sides of the carapace are almost parallel, slightly greater width in the anterior third. The anterior rim projects very conspicuously and the carapace is strongly compressed behind it. Posterior end compressed behind the posterior ridge.

Left valve slightly larger than the right, overlapping along part of the dorsal margin and anterior end, strongest overlap at the anterior cardinal angle.

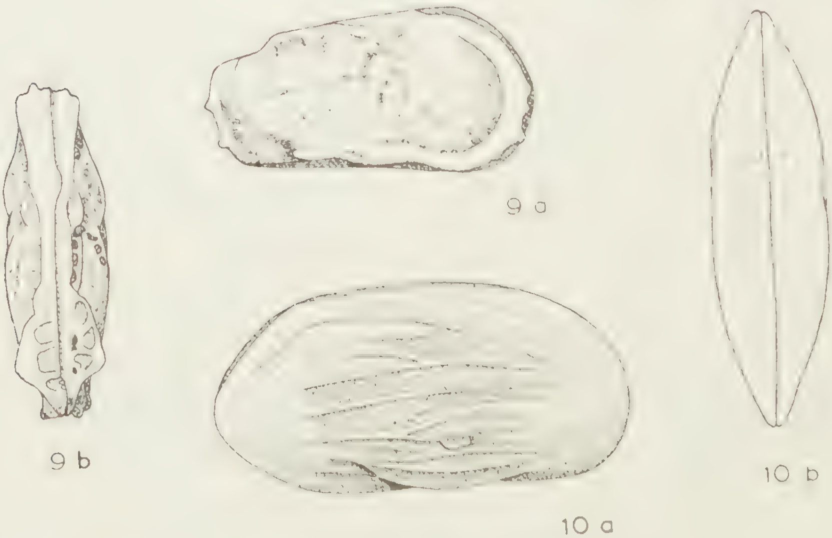

Fig. 9. *Munseyella machaquillaensis* (v. d. Bold), from V 199, Lower Eocene, Guatemala. a) right valve view, b) dorsal view. × 110.

Fig. 10. *Megacythere meridionalis* (v. d. Bold), from W 66, Miocene, Guatemala. a) right valve view, b) dorsal view. × 90.

Dimensions: L: 0.41; H: 0.19; W: 0.13.

The species is very similar in general aspect to *Toulminia hyalokystis* Munsey (1953, p. 6–7, pl. 2, figs. 26–27, textfig. 1), but is much more elongate and the compression of the carapace behind the ventral ridge is much stronger and extends higher up in the valve. Also the posterior

end is relatively higher, and the dorsal and ventral margin are more nearly parallel.

Occurrence: top of the Paleocene and Lower Eocene, Guatemala.

Holotype: a complete carapace from V 199 (S 13031) (v. D. BOLD, 1946, pl. 9, figs. 5a, b) Lower Eocene, Guatemala. Paratypes: same locality (S 13032).

Genus **Quadracythere** HORNIBROOK, 1952

Quadracythere goldenensis n.sp.

figs. 8a, b

Cythereis cf. bursilloides (Stadnichenko), V. D. BOLD, 1946, pl. 6, fig. 19a, b.
Not *Cythere bursilloides* STADNICHENKO, 1927, p. 239, pl. 39, fig. 21–23.

Carapace elongate, subquadrangular, height almost equal throughout, only slightly higher at the anterior cardinal angle. Anterior end broadly rounded, rimmed; dorsal and ventral margin almost straight and parallel, posterior end blunt, angled below the middle, steeply truncate above, rounded, and bearing a few blunt spines below. Dorsal view with almost equal width at the subcentral tubercle and just in front of the posterior end of the ventral ridge at about 1/3 from behind; anterior end wider than posterior one, which is rather strongly compressed. Carapace reticulate, most of the meshes of hexagonal shape; they stand in longitudinal rows which trend slightly upward posteriorly and curve, to become nearly horizontal in the anterior portion. A subcentral tubercle is weakly developed. A dorsal and ventral ridge are present, the dorsal one is slightly nodose. The ventral ridge is stronger in the posterior part. Posterior part of ventral margin slightly denticulate, the size of the denticles increasing posteriorly. Anterior end minutely denticulate.

There are two dimensions of carapaces, one longer than the other. As more specimens of the longer type occur, it is thought to be the female. In the ? male the width at the subcentral tubercle is slightly more than at the ventral ridge, in the ? females the opposite can be observed.

Dimensions: ? female: L: 0.84; H: 0.47; W: 0.40.
? male : L: 0.74; H: 0.46; W: 0.40.

This species is very close to *Quadracythere stadnichenkoae* n.sp. in side view, but more quadrangular and slightly larger; in dorsal view it exhibits a stronger subcentral tubercle, and the shape of the anterior end is different. Also the eyetubercle is larger and the posterior end of the dorsal ridge is much wider.

Occurrence: Lower Eocene of Guatemala and British Honduras: B 257, D 211, 227, V 117, 134, 139.

Holotype: a complete carapace from D 211 (S 13128), Lower Eocene, British Honduras, Golden stream. This locality was erroneously printed as D 311 (v. D. BOLD, 1946, p. 94). Paratypes: S 13129, same locality.

Quadracythere stadnichenkoae n.sp.

figs. 7a, b

Cythereis bursilloides Stadnichenko, v. d. Bold, 1946, p. 94, pl. 12, fig. 2a–c.
Not *Cythereis cf. bursilloides* Stadnichenko, v. d. Bold, 1946, pl. 6, fig. 19a, b (= *Quadracythere goldenensis* n.sp.).
Not *Cythere bursilloides* Stadnichenko, 1927, p. 239, pl. 39, fig. 21–23.
? *Hermanites bassleri* (Ulrich) var. 4 Drooger, 1960, p. 462, 463, pl. 3, fig. 12a, b.

Carapace roundly subrectangular, slightly higher at anterior cardinal angle, widest in the middle. Anterior end broadly rounded, almost evenly, weakly rimmed and with a small eyespot below the anterior cardinal angle at the dorsal end of the anterior rim. Dorsal margin straight, slightly depressed behind the anterior cardinal angle in the left valve, parallel to the ventral margin, which is slightly sinuate in front of the middle and curves upward into the ventral part of the posterior end, which is bluntly angled just below the middle and slightly concave above. Dorsal view spindle-shaped, widest in the middle, ends compressed, posterior end slightly more so than anterior.

Carapace evenly reticulate, the meshes forming curved rows, convex upward in the posterodorsal part, with the upper ridge forming a weak, curved, dorsal ridge; convex downward in the ventral part with the lower row forming a ventral ridge, which is roughly parallel to the ventral margin and more conspicuous in its anterior part. The valves are strongly compressed below this ridge.

Dimensions: ? female: L: 0.72; H: 0.43; W: 0.39.
? male : L: 0.79; H: 0.43; W: 0.39.

Sexual dimorphism rather weak: a small number of slightly longer carapaces are thought to represent the males.

Occurrence: Lower Eocene of Guatemala: D 211, 227, 228, 230, T 111, 114, V 134, 141.

Holotype: a complete carapace from V 141 (S 13126), Lower Eocene, Guatemala. Paratypes: S 13127, same locality.

Genus **Loxoconcha** Sars, 1866

Loxoconcha lienenklausi n.sp.

figs. 11a, b

Loxoconcha dentata (Lienenklaus), v. d. Bold, 1946, p. 111, 112, pl. 15, fig. 8a–e.
Not *Eucytherura dentata* Lienenklaus, 1905, p. 47, pl. 4, fig. 31.
Loxoconcha dentata (Lienenklaus), v. d. Bold, 1950, p. 108.

Carapace subquadrangular; anterior end angled about the middle, straight or slightly concave above and meeting the dorsal margin under a 130° angle, rounded and denticulate or nodular below; dorsal margin straight, ventral nearly straight and parallel in the middle; posterior end protruded above the middle into a short, blunt caudal process, convex below, concave above. Valves covered with a network of fine meshes,

in the greater part without particular orientation; only in the ventral part, in front of a posteroventral lateral process, are they aligned in the direction of this process, slightly downward and backward. A second lateral tubercle lies about halfway between the first and the caudal process. At the posterodorsal angle is a short tubercle just emerging over the dorsal margin and at the anterior cardinal angle is a small eyetubercle. The size of the processes varies slightly in individual carapaces.

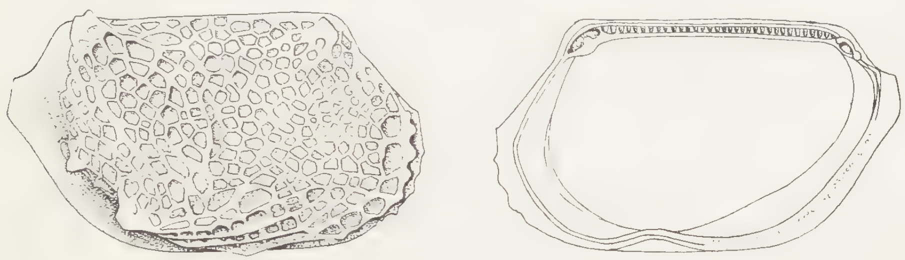

Fig. 11. *Loxoconcha lienenklausi* v. D. BOLD n.sp., holotype, from K 206, Upper Eocene (?), Cuba. a) exterior of right valve, b) interior of right valve. × 110.

Interior of the valves fairly shallow, marginal area broad with few radial porecanals, but difficult to make out because of recrystallization of the shell. Line of concrescence and inner margin do not quite coincide in the anteroventral part. Hinge as described for the genus, median element crenulate.

Dimensions: Holotype: L: 0.48; H: 0.29. Paratype: L: 0.44; H: 0.27.

Holotype: a right valve from K 206 (S 13133), Upper Eocene ? of Cuba. Paratypes: Left and right valves from K 206 (D 27192).

Occurrence: Upper Eocene ?, Cuba, (K 206), Oligocene Cuba (L 940, V 349), U. Eocene Bonaire (G 12).

This is the form, tentatively compared with *Loxoconcha fischeri* (BRADY), which occurs in the Antigua limestone (*Globigerina ciperoensis ciperoensis* zone), (v. D. BOLD, 1958, p. 244). Differences with *Loxoconcha antillea* lie in the shape of the anterior end and the position of the lateral processes.

Genus **Megacythere** PURI, 1960

Megacythere meridionalis (v. D. BOLD)

figs. 10a, b

Cytherura similis Sars var. *meridionalis* v. D. BOLD, 1946, p. 119, pl. 9, fig. 21a, b.
? *Microcythere johnsoni* MINCHER, 1941, p. 344, pl. 47, fig. 4a–d.

Carapace small, elongate. Anterior end slightly obliquely rounded, posterior end somewhat pointed and narrowly rounded in the middle, convex above and below this angulation; dorsal margin straight in the right valve, very slightly convex in the left, ventral margin slightly concave

in the middle, subparallel to the dorsal, very slightly converging anteriorly. Surface ornamented with irregular, longitudinal ribs, which disappear before reaching anterior and posterior margin.

The course of the ribs is slightly different from *Microcythere johnsoni* MINCHER, and the posterior end is more pointed in the left valve. *Microcythere striata* PURI (1953, p. 291, pl. 16, figs. 9, 10, textfigs. 12i, j) is relatively much higher in the posterior portion.

Dimensions: L: 0.58; H: 0.30; W: 0.17.

Holotype: W 66 (S 13068), v. D. BOLD, 1946, pl. 9, figs. 21a, b, Miocene, Guatemala. Paratypes: W 66, 124, 132 (D 30764). Also occurring in T 107, Miocene Guatemala.

REFERENCES

BOLD, W. A. VAN DEN, Contribution to the study of Ostracoda with special reference to the Tertiary and Cretaceous microfauna of the Caribbean Region. Univ. thesis, Utrecht (1946).

———. A checklist of Cuban Ostracoda. Journ. Pal., **24**, 107–109 (1950).

———. Ostracoda from the Paleocene of Trinidad. Micropal., **3**, 1–18 (1957a).

———. Oligomiocene Ostracoda from southern Trinidad. Micropal., **3**, 231–254 (1957b).

———. Ostracoda of the Brasso formation of Trinidad. Micropal., **4**, 391–418 (1958).

———. Eocene and Oligocene Ostracoda of Trinidad. Micropal., **6**, 154–196 (1960).

BRADY, G. S., Monograph of the Ostracoda of the Antwerp Crag. Trans. Zool. Soc. London, **10**, 379–409 (1878).

DROOGER, C. W., Microfauna and age of the Basses Plaines formation of French Guyana. II: Ostracoda. Kon. Ned. Akad. Wetensch. Proc. ser. B, **63**, 460–468 (1960).

GOOCH, D. D., Some Ostracoda of the genus *Cythereis* from the Cook mountain Eocene of Louisiana. Journ. Pal., **13**, 580–588 (1939).

KEIJZER, F. G., Outline of the Geology of the eastern part of the Province of Oriente, Cuba. Univ. thesis, Utrecht (1945).

LIENENKLAUS, E., Die Ostracoden des Mainzer Tertiärbeckens. Ber. Senckenberg. Naturf. Gesell., Frankfurt/Main, 3–68 (1905).

MINCHER, A. R., The fauna of the Pascagoula formation. Journ. Pal., **15**, 337–348 (1941).

MUNSEY, G. C., A paleocene Ostracode fauna from the Coal Bluff member of the Naheola formation of Alabama. Journ. Pal., **27**, 1–20 (1953).

SAPPER, K., Mittelamerika. Handb. d. Region. Geologie, **8**, Abt. 4a, Heidelberg (1937).

STADNICHENKO, M. N., The Foraminifera and Ostracoda of the marine Yegua of the type section. Journ. Pal., **1**, 221–243 (1927).

STEPHENSON, M. B., Review of: van den Bold: Contribution to the study of Ostracoda etc.. Journ. Pal., **21**, 591–595 (1947).

ULRICH, E. O., Ostracoda in: Maryland Geol. Survey, Eocene Recept. 98–130 (1902).

VEEN, J. E. VAN, Die Cypridae und Bairdiidae der Maestrichter Tuffkreide und des Kunrader Korallenkalkes von Sud-Limburg. Nat. Hist. Maandblad, **23**, No. 7, 8, 9, 10 (1934).

PALEONTOLOGY

THE ENAMEL-DENTINE BORDER: A NEW MORPHOLOGICAL FACTOR IN THE STUDY OF THE (HUMAN) MOLAR PATTERN. Ia

BY

C. A. W. KORENHOF

(Communicated by Prof. G. H. R. von Koenigswald at the meeting of June 24, 1961)

INTRODUCTION

Although the oral surface of the enamel layer of the teeth has frequently been subject of morphological and morphogenetical considerations in odontography, it is a striking fact that practically no investigations seem to have been published regarding the interior surface of the enamel cap (enamel-dentine border).

As far as could be ascertained only a single paper on this subject exists in the literature (Kraus, 1952). This author studied the morphological relationship between the enamel and dentine exterior surfaces in the recent human dentition, but confined himself to a metrical analysis of the mutual position of the cuspal tips of both the enamel and the dentine crown of the mandibular first molar. No evolutionary considerations have been given by Kraus (*op. cit.*). The enamel of the crowns had been artificially removed by means of acids. This method has the disadvantage that the enamel layer is lost, while it is difficult to solute it completely – also in deep valleys and fissures – without involving the tips of the dentine cusps. The reverse procedure, the artificial removal of the dentine without affecting the interior surface of the enamel, is quite unknown to me.

Among fossil findings, however, enamel caps as the sole remains of teeth have been known at least since 1898, when Branco (*op. cit.*, pl. I, figs. 6 and 7) illustrated those of *Dryopithecus*. Later, more enamel crowns of a similar nature became known, such as those of *Pongo pygmaeus palaeosumatrensis* from the Pleistocene or early Holocene of Sumatra (coll. Dubois, Rijksmuseum van Natuurlijke Historie, Leyden) and those of *Pongo* cf. *pygmaeus* from the Pleistocene of Java and China (private collection Prof. von Koenigswald, Utrecht). With regard to Man I know of only one instance in the literature that reports a comparable disintegration of the dentine (Walkhoff, 1911). In it material is mentioned from burials of the late Stone- or even of the Bronze age, among which isolated enamel caps occur. These, however, are very brittle, they disintegrate easily and are lustreless. More or less identical material (Rijksmuseum Twente at Enschede) has been found in the Netherlands at Mander (prov. of Overijssel).

This demonstrates the uniqueness of a collection of subrecent human teeth, collected by Professor von Koenigswald at Sangiran (Central Java) between 1935 and 1940. Large parts of the main tuffaceous Trinil-beds here, containing many old graves, are eroded every year by the heavy rains during the wet seasons. As a result the contents of the graves can be found regularly at the foot of the hills.

Of the teeth, which are always found separately, the roots are mostly absent, while in a considerable number of teeth the dentine of the crown has disintegrated as well, due to an unknown factor. In many of these crowns the dentine is fully absent or so loosened that it can be easily removed, leaving a mostly beautifully preserved enamel cap, with—also interiorly—a hard lustrous surface (pl. I, fig. 2).

MATERIAL AND METHODS

By means of an alginate stage plaster casts could be made from the inside of a number of the subrecent Malay enamel caps. The "endocasts" thus obtained represent the enamel-dentine border, the original partition-plane between ameloblasts and odontoblasts. They show the "dentine crown" in positive, the interior of the "enamel crown" in negative (plates II–VI). The types and numbers of the permanent teeth and of their endocasts (with their catalogue numbers) follow from table 1.

Some results illustrating the significance of the enamel-dentine border as an important factor in the understanding of the evolution of the surface pattern will be discussed with the help of the upper molar material. The types according to which this may be distinguished, the number and the catalogue numbers of these types, follow from table 2.

With the material thus obtained it was tried:

a. to distinguish the evolutionary significance of the different component parts of the enamel surface;

b. to determine, whether the characteristic features on the dentine crown, are more conservative or more progressive in relation to the enamel exterior.

To obtain an insight into these problems a study was made of comparative material, both from early Tertiary prosimian stages and fossil and recent hominoid representatives. In an earlier, more extensive paper (Korenhof, 1960), morphogenetical considerations have been based on the pattern of the upper molars of representatives belonging to the following groups:

1. Paleocene and Eocene lemuroid or tarsioid Prosimii, which show many primitive structural features in their molar crown pattern.
2. Pongid Anthropoidea, both fossil and recent, which show many characteristics connecting them structurally with the first group, but

TABLE 1

Number and catalogue numbers of permanent teeth and endocasts of the Malay collection [1]).

Type	Right side			Left side		
	No. of teeth	Cat. numbers	No. of endocasts	No. of teeth	Cat. numbers	No. of endocasts
Upper molars	717	MMSD 1–712, 184A–D, 555A	238	714	MMSS 1–710, 27A, 93A–B, 491A	237
Upper P4	135	MPPSD 1–135	60	140	MPPSS 1–140	65
Upper P3	188	MPASD 1–188	59	190	MPASS 1–190	62
Upper canines	99	MCSD 1– 99	—	91	MCSS 1– 91	—
Upper lat. incisors . . .	38	MLSD 1– 38	—	38	MLSS 1– 38	—
Upper centr. incisors . .	49	MISD 1– 49	—	48	MISS 1– 48	—
Lower molars Y6-pattern	49	MY6D 1– 49	14	55	MY6S 1– 55	10
Lower molars Y5-pattern	70	MY5D 1– 70	20	108	MY5S 1–108	31
Lower molars Y4-pattern	7	MY4D 1– 7	—	7	MY4S 1– 7	—
Lower molars +6-pattern	71	M+6D 1– 70, 57A	25	69	M+6S 1– 69	25
Lower molars +5-pattern	146	M+5D 1–146	53	124	M+5S 1–124	36
Lower molars +4-pattern	57	M+4D 1– 57	15	69	M+4S 1– 69	17
Lower molars X6-pattern	125	MX6D 1–125	54	100	MX6S 1–100	26
Lower molars X5-pattern	193	MX5D 1–193	86	155	MX5S 1–155	42
Lower molars X4-pattern	89	MX4D 1– 89	29	67	MX4S 1– 67	20
Lower P4	185	MPPID 1–185	64	178	MPPIS 1–178	48
Lower P3	147	MPAID 1–147	42	133	MPAIS 1–133	29
Lower canines	81	MCID 1– 81	—	95	MCIS 1– 95	—
Lower incisors	70	MII 1– 70 (dexter and sinister)	—			
Total number . . .	2446 (2516)		759	2381		648

[1]) The catalogue numbers of the endocasts do not always represent continuous series. Therefore their mention in the table is not quite possible owing to lack of space. Moreover, only those of the upper molars are of importance here. These are specified in table 2, p. 642.

TABLE 2

Types and number of maxillary molars and endocasts of the Malayan collection

Type [1])	Right side				Left side			
	No.	Cat. number	Endo-casts	Cat. number	No.	Cat. number	Endo-casts	Cat. number
Carabelli type a	29	MMSD 1–29	10	MMSD 20–29	28	MMSS 1–27, 27 A	14	MMSS 15–27, 27 A
Carabelli type b	121	MMSD 30–150	38	MMSD 113–150	115	MMSS 28–93, 93 A-B 94–140	47	MMSS 94–140
Carabelli type c	28	MMSD 151–178	20	MMSD 154–157, 163–178	24	MMSS 141–164	9	MMSS 142, 157–164
With parastyle	10	MMSD 179–184, 184 A-D	6	MMSD 179–184	5	MMSS 165–169	5	MMSS 165–169
Tritubercular	24	MMSD 185–208	9	MMSD 200–208	41	MMSS 170–210	18	MMSS 193–210
With four cusps	206	MMSD 209–414	53	MMSD 362–414	185	MMSS 211–395	40	MMSS 356–395
With mesial edge tubercles . .	142	MMSD 415–555, 555 A	44	MMSD 573–555, 555 A	143	MMSS 396–491, 491 A, 492–537	46	MMSS 492–537
With distal edge tubercles . .	40	MMSD 556–595	18	MMSD 578–595	46	MMSS 538–583	16	MMSS 568–583
With mesial and distal edge tubercles	117	MMSD 596–712	40	MMSD 673–712	127	MMSS 584–710	42	MMSS 669–710
Total number	717		238		714		237	

1) It appeared later that the specimens cat. nos. MMSD 532 and 583 possessed two very weakly developed pits on the lingual side of the protocone, and accordingly, should have been arranged among the teeth with Carabelli's cusp type c.

which, on the other hand, possess a number of features connecting them with the following group:

3. Hominidae, both fossil and recent; the last category is mainly represented by a description and discussion of the collection of Malay teeth and their endocasts.

In the present paper only those results will be communicated which refer to comparisons between certain structural features of the enamel exterior and interior occlusal surfaces.

DISCUSSION

In particular the following structural features in the occlusal aspect of the upper molar pattern of the Hominidae (and the Pongidae) have been subject, phylogenetically, to morphological alterations and to mutually differing relations:

A. Cusps and ridges:

I. The main cusps of the trigon.
II. The hypocone.
III. The intermediary proto- and metaconule.
IV. The mesial marginal ridge.
V. The crista transversa anterior.
VI. The crista obliqua.
VII. The crista transversa posterior.
VIII. The trigonal hypocone crest.
IX. The distal marginal ridge.

B. Grooves and wrinkles.

X. The central fossa.
XI. The fovea anterior.
XII. The fovea posterior.
XIII. The system of wrinkles.

These features will therefore be considered separately for the Malay material.

A. Cusps and ridges

I. *The main cusps of the trigon*

The nature of the material in the Malay collection makes it impossible to determine the differences in height between the cusps of Gregory's (1922) secondary trigon both in the enamel surfaces and in the endocasts, and to compare these mutually. On the exterior of the enamel cap the shape of the cusps is rather blunt, rounded and with convex slopes.

In the endocasts, however, they appear to be very high and acutely pointed in almost all cases. Though only occlusal views are shown in the illustrations of plates II–VI, this difference in shape of the cusps is very striking. Especially the centrally directed slopes of the cusps usually have a concave character. In these respects the enamel-dentine border represents an aspect which is in far better agreement with early Tertiary relations such as shown in *Teilhardina belgica* (pl. I, fig. 1) and other early Prosimii.

II. *The hypocone*

In the more extensive study, mentioned above, it has been pointed out that the hypocone is the youngest principal cusp of the occlusal surface. Its height in relation to the trigonal plane represents one way of measuring its degree of evolution. A positive trigonal hypocone height (including a tip of the hypocone which is situated more occlusally than the trigonal plane) expresses a very high degree of evolution.

In 49 molars, selected because they did not show any traces of attrition and possessed clear and sharply defined cusps, also in the endocasts, no positive trigonal hypocone height appeared to be present. Nor does the literature seem to make mention of any human group [1]). On the other hand, it was encountered in *Oreopithecus bambolii* and in *Australopithecus a. transvaalensis*, which support the view that in this respect, the upper molar teeth of these genera have attained a higher evolutionary level than those of recent Man.

The measurements on the inside of the Malay enamel crowns resulted in finding six cases with positive trigonal hypocone heights, whereas the significant mean difference between the height on the inside and the outside appeared to be 0.154 mm ($t_{48} = 3.28$; $0.1\% < p < 1\%$).

The fact that the hypocone on the internal side appears to be significantly higher than on the outside is in contrast with the findings in other characteristics of the molar pattern (see below). Three different explanations may be considered for this:

a. the hypocone in recent Man is on its way toward a reduction in height. In that case the endocasts do indeed show primitive situations;
b. the method followed to determine the heights is unreliable;
c. the greater amount of primitivity of the border between enamel and dentine as opposed to that of the outer enamel surface should not be seen as a law which holds good for all morphological characteristics.

III. *Proto- and metaconule*

The study of structural evolutionary stages of the upper molars in representatives of the groups mentioned on pages 640 and 643 shows that, in a

1) The method of measurement on the exterior and interior surfaces of the enamel caps has been exhaustively described and illustrated by the author at an earlier occasion (1960, pp. 198–200 and plate XV).

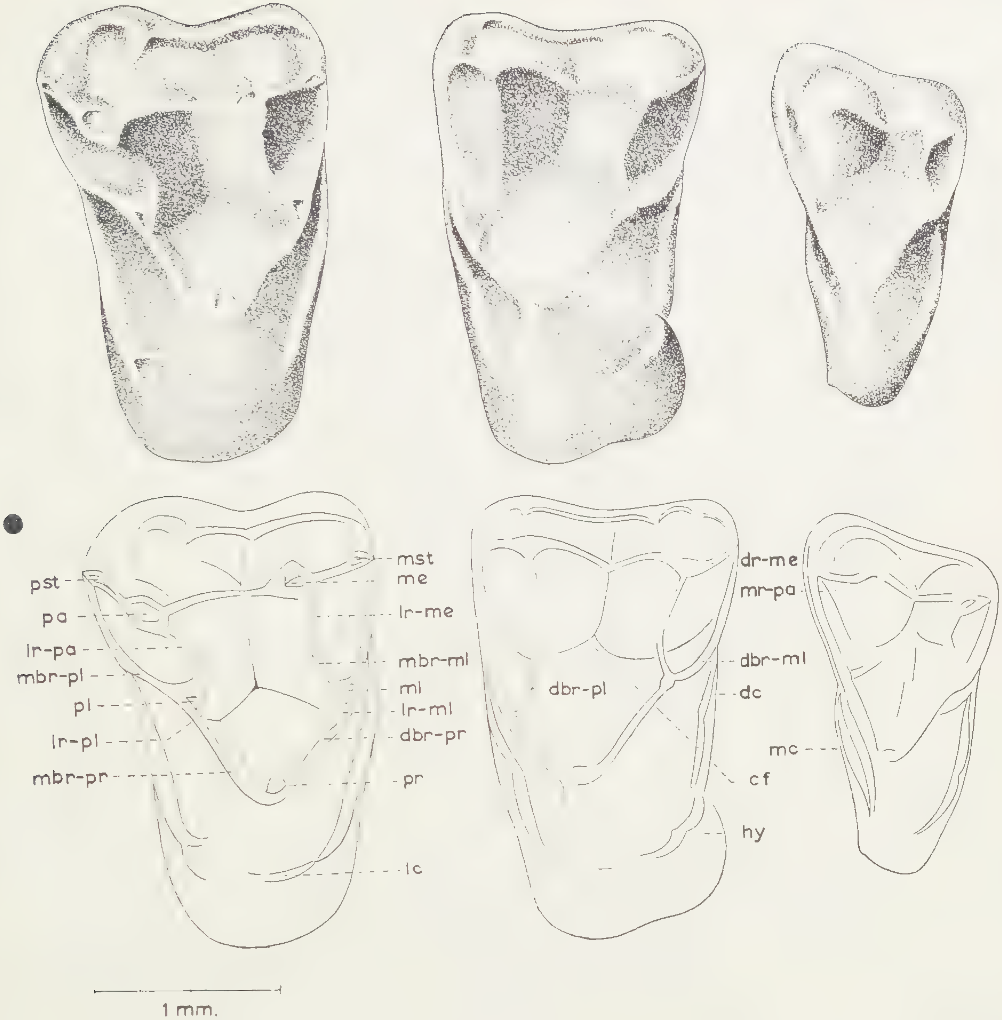

Fig. 1. *Teilhardina belgica.* Upper molars. Coll. Institut royal des Sciences naturelles, Brussels. Cat. nos. Ct. M. 58, Ct. M. 57 and Ct. M. 59 [1]).

---

[1]) The following significance should be accorded to the abbreviations used in the designation of the textfigures:

pa — paracone
me — metacone
pr — protocone
hy — hypocone
pl — protoconule
ml — metaconule
pst — parastyle
bst — buccostyle
tC — tuberculum Carabelli
c — cingulum
mc — mesial cingulum
dc — distal cingulum
bc — buccal cingulum
lc — lingual cingulum

mbr — mesiobuccal ridge
dbr — distobuccal ridge
lr — lingual ridge
mr — mesial ridge
dr — distal ridge
co — crista oblique
cta — crista transversa anterior
ctp — crista transversa posterior
cpc — cingulum-protocone crest
trhc — trigonal hypocone crest
mmr — mesial marginal ridge
fa — fovea anterior
bmg — buccal main groove
cf — central fossa
x — other structural features

A boldly printed point next to one or more molars in a textfigure indicates the mesial side of the dental element(s) in question, after the method of Butler and Mills (1959).

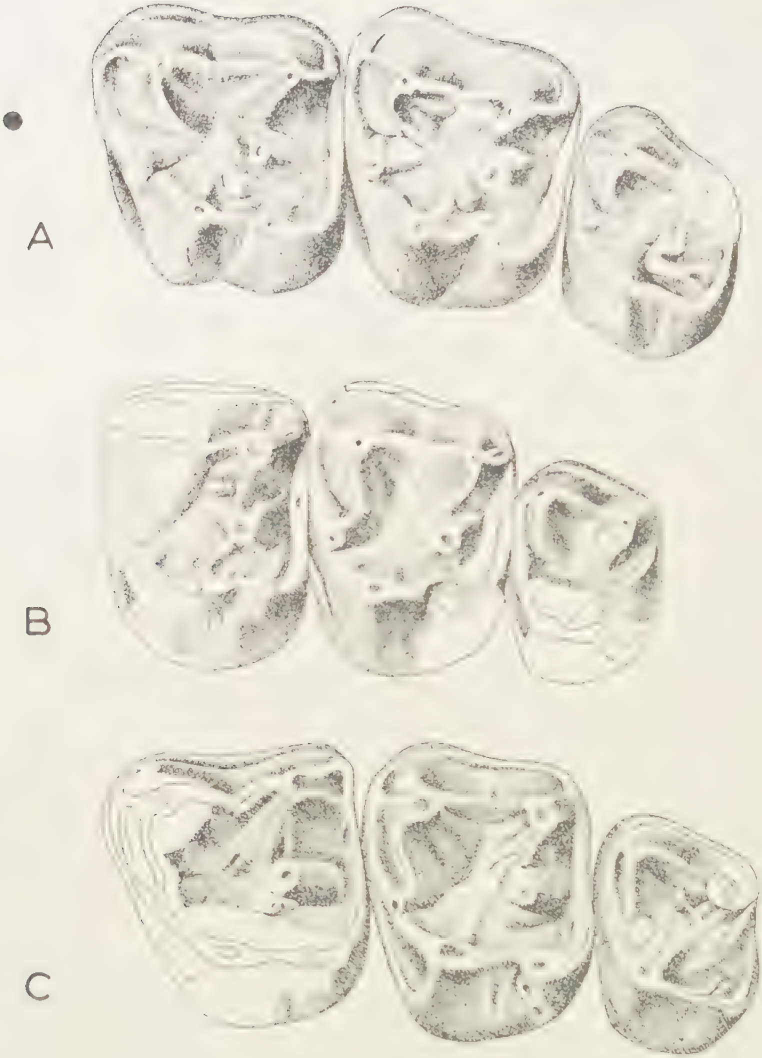

Fig. 2*a*. A. *Necrolemur antiquus*. M^1–M^3 dexter (mirror images). Cat. no. Q.H. 468. B. *Necrolemur* cf. *zitteli*. M^1–M^3 sinister. Cat. no. Ef. 377. C. *Necrolemur* cf. *zitteli*. M^1–M^3 sinister. Cat. no. Ef. 378. Coll. Naturhistorisches Museum, Bâle. Drawn from HÜRZELER (1948), slightly modified.

molar pattern which is as highly evolved as that of recent Man, cusp-like remains of a proto- and especially of a metaconule, are no longer to be expected.

Among the earliest Hominidae nothing or hardly anything can be recovered of the metaconule, which latter element may be strongly developed in early Prosimii (figs. 1 and 2).

In *Pliopithecus* cf. *antiquus* from the Upper Vindobonian of Göriach (Styria) this element, as such, seems to have already disappeared altogether, although traces of its former presence may perhaps still be

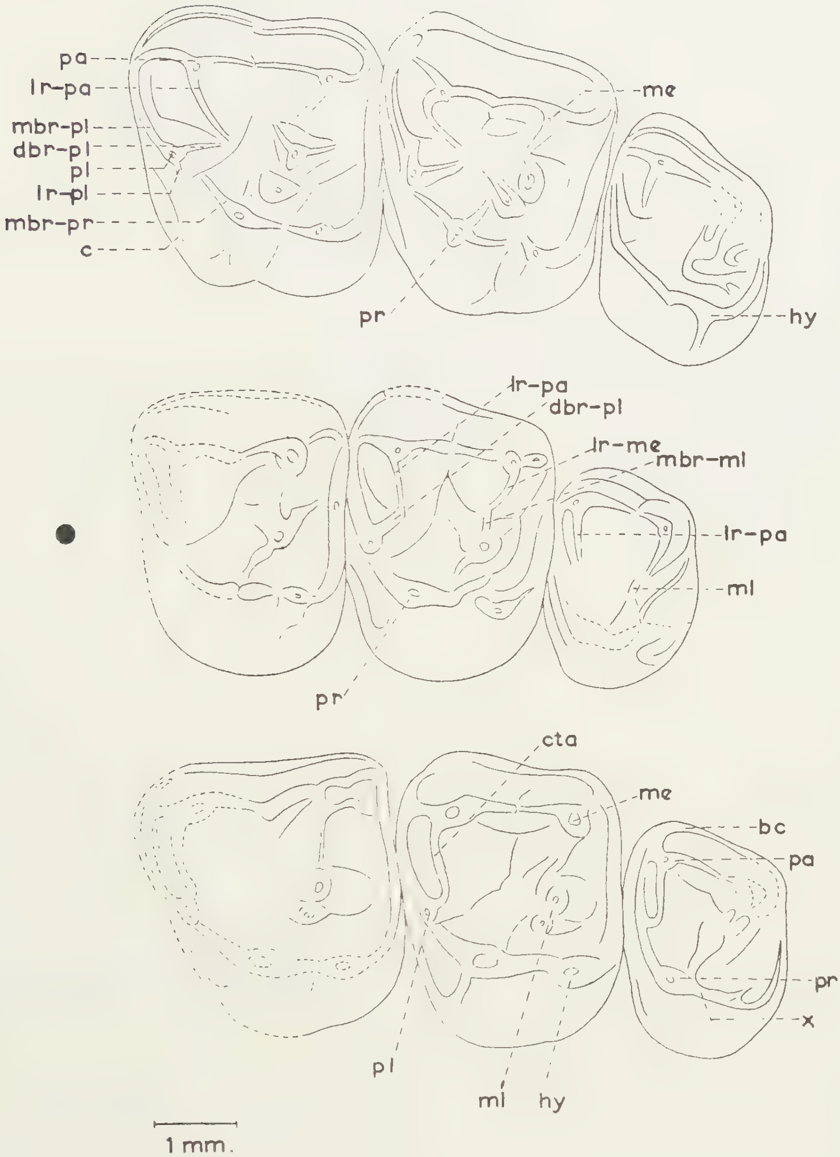

Fig. 2*b*. Schematical representation of the opposite illustrations.

observable on the second molar of the specimen cat. no. 2094 (fig. 3). As far as I know, no indications of the cuspule can be found in *Dryopithecus* and *Sivapithecus* or other related genera (figs. 4 and 5), nor are there any distinctly developed remains of a metaconule among younger Pongidae and Hominidae. In these groups it forms, as has been exhaustively explained in the paper already mentioned earlier, an important constituent part of the crista obliqua (compare fig. 6, A and B, vertically striped areas). As a cusp, however, it is no longer to be found there when the

crest has been formed into a complete formation [1]). In the Malay collection no indications could be observed of a distinct metaconule.

What has been said for the metaconule is also true for the protoconule. In a *Teilhardina* stage (fig. 1) it is clearly developed and possesses three ridges, the distobuccal one of which plays an important part in the construction of the later crista transversa anterior. The cuspule itself, which is still present in certain *Necrolemurinae* (fig. 2) seems to have quite disappeared in *Pliopithecus* (fig. 3). Its occurrence in further evolved

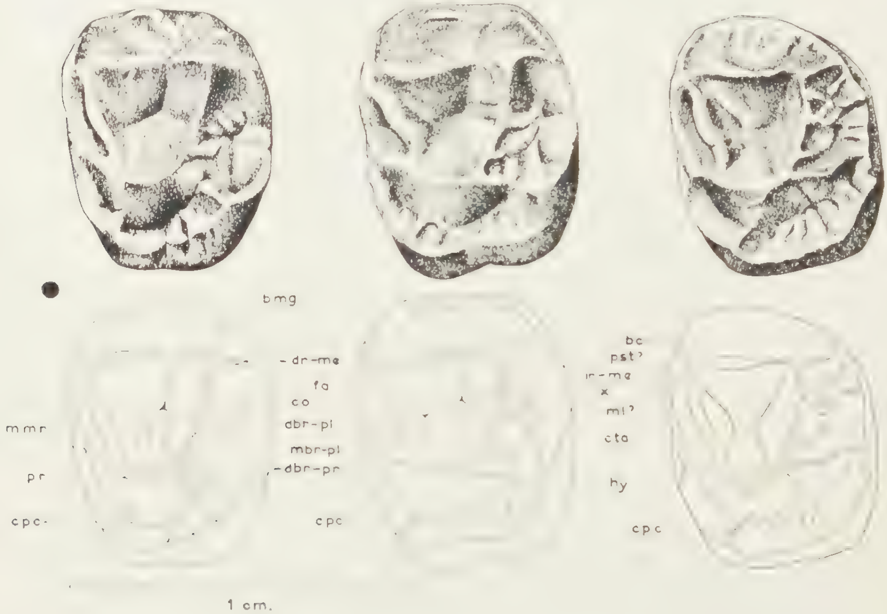

Fig. 3. *Pliopithecus* cf. *antiquus*. M¹–M³ sinister. Coll. of the Joanneum, Graz. Cat. nos. M¹: 2108; M², M³: 2094. Upper row drawn from HÜRZELER (1954), slightly modified.

Hominoidea, including Man, is very dubious and difficult to prove, even in those cases where an extra tubercle is found on the mesial marginal ridge of the occlusal surface at the location of the former protoconule (*Gorilla*, *Pan*, *Pongo*, Man).

Endocasts. In none of the endocasts which are specified in table 2 do extra cusps, which may be considered to represent a proto- or metaconule, occur between protocone and paracone or between protocone and metacone. Edge tubercles are quite often found on the mesial marginal ridge of the enamel exterior. In 49 molars, selected because they showed mesial edge tubercles, and also had endocasts, edge tubercles occurring

[1]) The occurrence of the metaconule as a distinct cusp on *Oreopithecus*, and the lack of a metaconal attachment of the crista obliqua (in certain molars), points to a divergent type of molar.

on these latter only were present in three, doubtful, cases, so that the conclusion seems to be justified that no distinct mesial edge tubercles exist in the endocasts.

IV. *The mesial marginal ridge*

Phylogenetical considerations contain sufficient arguments, in my opinion, for the contention that it is practically certain that the following component parts have originally combined into the construction of the mesial marginal ridge of the human (and other hominoid) upper molars (fig. 6):

a. the mesiobuccal ridge of the protocone;
b. the lingual ridge of the protoconule;
c. the mesiobuccal ridge of the protoconule;
d. the mesial termination of the buccal cingulum;
e. the mesial cingulum.

This can be proved by the conditions which may be encountered in early Primate molars belonging to an only slightly differentiated type, such as is demonstrated by *Teilhardina belgica* (pl. I, fig. 1 and textfig. 1), *Omomys* (see GAZIN, 1958, pl. 6, figs. 1–8), *Pelycodus trigonodus*, *Plesiadapis gervaisi*, *Anchomomys gaillardi*, *Pseudoloris parvulus* (see STEHLIN, 1916, figs. CCCLXXI, CCCLV, CCCXXVIII and CCCXXI, respectively). In these forms the mesial cingulum usually follows a basal course along the mesial crown surface, coming from a lingual direction. During higher evolutionary stages it rise occlusally and reaches the masticatory surface on an arbitrary point of the mesial marginal ridge, adding a fifth component in the primary continuous edge.

Endocasts. Whereas in recent Man the mesial marginal ridge on the crown exterior has been dissolved, in many cases, into a number of edge tubercles (see table 2 and pl. III, figs. 2 and 4), this is never the case

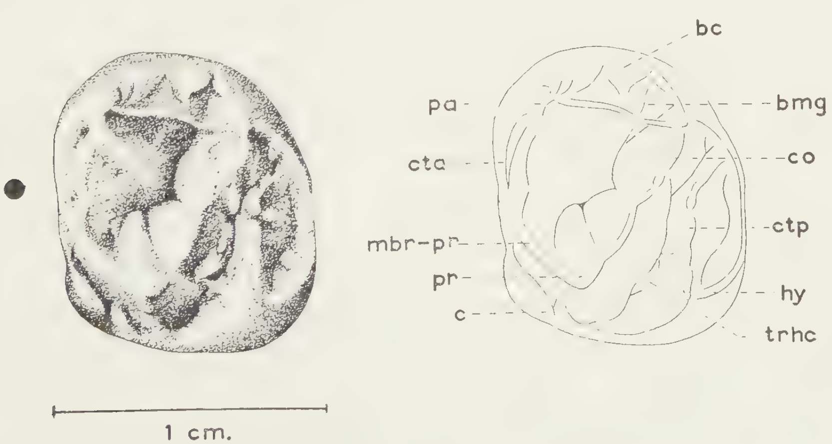

Fig. 4. *Dryopithecus* sp. M1 or M2 sinister. Coll. Prof. CRUSAFONT, Museo de la Ciudad de Sabadell, Spain. Drawn from a cast.

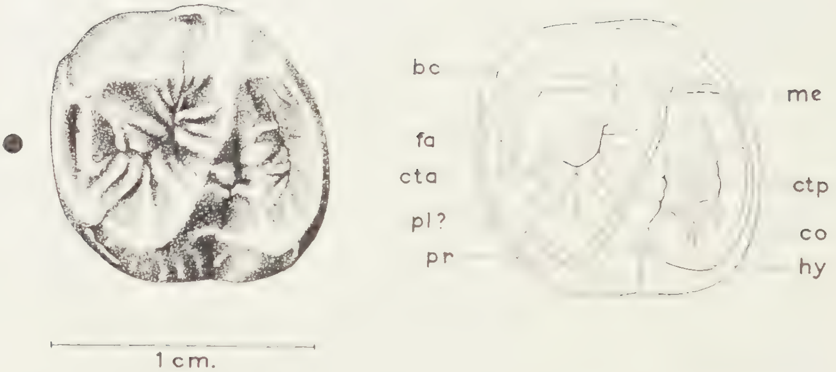

Fig. 5. *Dryopithecus* (*Paidopithex* ?) sp. M^1 or M^2 sinister. Coll. University of Tübingen. Drawn from a cast.

in the endocasts. There appear te be no exceptions to this rule. The feature always has a regular level here, rarely with some small convexities in a mesial direction, which correspond with the tubercles on the outside (pl. III, fig. 4). In several cases they have developed to a multiple of five or six (pl. IV, figs. 3–5).

With regard to the marginal edge under consideration the endocasts show a very primitive stage which is highly reminiscent of the one encountered in *Teilhardina belgica*. They also prove that at least four out of the five components mentioned earlier, with which the mesial ridge must have been constructed, have played a part; at least when it is thought permissible to apply the significance of the structural stages, which have been discussed earlier, also to Man.

The presence of a protoconule in an earlier stage is proved in many endocasts by the existence of a distinct crista transversa anterior (see point V, below). Therefore, the component parts mentioned under *b* and *c* must have had a share in the construction of the marginal ridge in Man.

As regard component *a* the endocasts clearly show that the mesial marginal ridge gradually passes lingually into the mesiobuccal protocone ridge. Here also one may therefore presume, in my view, that a protoconal component must be taken into account for the lingual extremity of the crest. The part played by the buccal cingulum can no longer be demonstrated clearly in the endocasts. For the component mentioned under *e* the reader may be referred to the author's earlier publication on this subject (1960).

The lack of sharply defined criteria and objective standards for the characteristics mentioned above form the reason why it is impossible here to give any statistical data on the Malay material.

Jørgensen's "protoconule groove" (1956) does not occur in any of the endocasts, a fact which provides additional support for my opinion that the feature is unrelated to the protoconule.

V. *The crista transversa anterior*

The phylogenetical considerations with regard to this feature in Prosimii given earlier (1960), and the criticisms to be found there of the views held by REMANE (1921), ECKARDT (1930), GLAESSNER (1931), WEIDENREICH (1937), HÜRZELER (1954) and ROBINSON (1956), or of their naming of the crest in recent Pongidae, *Pongo*, *Dryopithecus darwini*, *Gorilla*, *Pliopithecus* cf. *antiquus*, and *Australopithecus-Paranthropus* (respectively), may show that, in my opinion, the mesial transverse crest in these and other Primates has always been formed out of two component parts:

a. the distobuccal protoconule ridge;
b. the lingual paracone ridge.

A transversal mesial crest with its original course does not occur on the outside of the enamel in any of the 1431 molars of the Malay material, and as far as I know, has not been described as occurring in any other ethnical group of Man, both fossil and recent. It is, however, clearly visible on the M^1 of *Pithecanthropus modjokertensis*, despite the fairly heavy attrition.

The frequency of occurrence of no doubt probable remains of the mesial transverse ridge in the Malay molars is difficult to determine. An attempt at counting and at arranging them according to different types has been made in table 3. The table shows that indications of the crista transversa anterior occur only in a very small percentage (1,5) on the exterior of the enamel layer.

TABLE 3

Types and frequency of occurrence of indications of the crista transversa anterior on the outer and inner surface of the Malay enamel caps.

Type	Definition	Number of cases on the exterior surface (1431 molars)	Number of cases on the interior surface (475 endocasts)
1	Lingual paracone ridge connected with the mesial marginal ridge	8	9
2	Distinct ridge, mesially from the the lingual paracone ridge, not connected with the marginal ridge, and not directed distally	2	16
3	Complete crest from the tip of the paracone-mesial marginal ridge	4	8
4	Uninterrupted connection from the tip of the paracone- the tip of the protocone	1(?)	6
5	C-shaped crest between two localities on the mesial marginal ridge	7	9
	Total number	22(21?)	48

Endocasts. With respect to this structural feature the enamel-dentine border demonstrates more primitive conditions than the external side of the crown (table 3).

It does not appear to be justified to draw any far-going conclusions from a comparison of the data given here because of the small number of cases. The remark may be made, however, that the crista transversa anterior occurs approximately seven times more frequently among the endocasts than among the outsides of the enamel crowns. In this respect the border between enamel and dentine surfaces therefore again shows the more original conditions in the sample.

VI. *The crista obliqua*

The situations which exist in early Prosimii make it necessary to assume, when they are transferred to the Anthropoidea, including Man, that the oblique crest (or ridge) most probably has been constructed with the aid of the following four component parts:

a. a distobuccal protocone ridge;
b. a lingual metaconule ridge;
c. a mesiobuccal metaconule ridge;
d. a lingual metacone ridge.

This implies that its lingual and buccal extremities have to lie on the tip of the protocone and on that of the metacone (respectively), at least when the original conditions have not been subjected to alterations. In the human dentition the crest is nearly always well-developed in every ethnical group; at the least it is still clearly indicated.

From the enumeration of the components given above and a comparison of the figures 6 A and B it may follow that I cannot agree with the fairly common opinion that the crista obliqua represents the distal leg of the

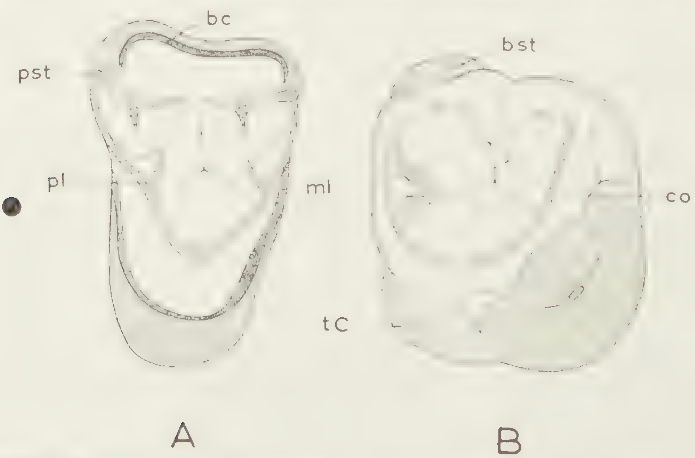

Fig. 6. Homologous structural features in upper molars of (A) Paleocene prosimian Primate and (B) recent Man (generalized pattern). The dotted area represents the cingulum component. Not to the same scale.

TABLE 4

Frequency of occurrence of types of the crista obliqua on the outside and in the endocasts of the Malay collection

Type	Outside of the enamel						Inside of the enamel						Total no.
	Type a		Type b		Type c		Type a		Type b		Type c		
	No.	%	No.	%	No.	%	No.	%	No.	%	No.	%	
With Carabelli's cusp type a	14	58.3	4	16.7	6	25.0	19	79.2	—	—	5	20.8	24
With Carabelli's cusp type b	58	68.2	18	21.2	9	10.6	76	89.4	4	4.7	5	5.9	85
With Carabelli's cusp type c	17	58.6	4	13.8	8	27.6	19	65.5	4	13.8	6	20.7	29
With parastyle	7	63.6	2	18.2	2	18.2	9	81.8	2	18.2	—	—	11
With four cusps	63	67.7	9	9.7	21	22.6	78	83.8	9	9.7	6	6.5	93
With mesial edge tubercles	53	58.9	10	11.1	27	30.0	81	90.0	2	2.2	7	7.8	90
With distal edge tubercles	16	47.1	6	17.6	12	35.3	29	85.3	2	5.9	3	8.8	34
With mesial and distal edge tubercles . .	58	70.7	8	9.8	16	19.5	73	89.0	6	7.3	3	3.7	82
Total number	286	63.9	61	13.6	101	22.5	384	85.7	29	6.5	35	7.8	448

original (GREGORY's, 1922, secondary) trigon (TOPINARD, 1892, in Man; REMANE 1921, in recent Pongidae; GLAESSNER, 1931, in *Dryopithecus darwini*; ROBINSON, 1956, in *Australopithecus* and *Paranthropus* and probably PIVETEAU, 1957, in *Gorilla*).

The measure of development of the crista obliqua in the Malay collection of upper molar teeth may be distinguished into three types:

Type a. A continuous crest between the tip of the protocone and the tip of the metacone, possibly with a vertical notch at the locality of the longitudinal main groove, but never fully cut through by the latter (pl. II, figs. 1–6).

Type b. A similarly situated crest, which, however, is distinctly interrupted by the longitudinal main groove (pl. IV, fig. 3; endocasts: pl. V, fig. 2).

Type c. A total absence of the crista obliqua. Contrary to the situation in type b, the lingual ridge of the metacone and the distobuccal ridge of the protocone have not developed more strongly than those of the paracone (pl. III, fig. 4).

In my opinion type a represents the most primitive conditions, type c the most progressive. The frequency of occurrence of the three types has been expressed in table 4. Only those molars have been considered of which endocasts were present, whereas the group with tritubercular molars has been omitted.

Endocasts. In most cases the oblique ridge has developed more strongly than on the outside of the enamel layer (pl. II, figs. 1–6; pl. III, figs. 1–3, 5, 6; pl. IV, figs. 1–6; pl. V, figs. 1–5; pl. VI, figs. 1–6). It occurs as a sharper crest with a pronounced "line-angle". If it is completely present it is extended between the tips of proto- and metacone. The frequency of occurrence of the three types of the crista among the endocasts follows from table 4. The endocasts appear to show more primitive conditions in a markedly higher percentage than the outside of the enamel. This holds true for all groups of molars.

VII. *The crista transversa posterior*

The feature seems to be a rather late specialisation of the talon and is present in *Dryopithecus* (figs. 4 and 5) and *Sivapithecus*, less clearly in *Gorilla*, *Pan* and *Pongo*. In the Malay human material indications of its presence are weak or completely absent.

Endocasts. No conclusions can be drawn from the few specimens that show weak indications of a possible distal transverse crest (pl. II, fig. 2; pl. III, fig. 3; pl. IV, fig. 1).

VIII. *The trigonal hypocone crest*

This crest, between the tip of the hypocone and a point on the lingual half of the crista obliqua, does not occur distinctly in the human dentition.

As far as known it has never been described in this context. In the exterior view of the Malay crowns its presence can only be deduced from the observation that the occlusolingual groove (distolingual groove) is less deep (pl. II, figs. 2 and 3; pl. IV, fig. 6; pl. V, fig. 5), or is even fully interrupted (pl. III, fig. 3; pl. IV, fig. 1; pl. V, fig. 4) at the locality where the trigonal hypocone crest, present in earlier Primates (*Necrolemur antiquus* and *N.* cf. *zitteli*, fig. 2; *Pliopithecus* cf. *antiquus* from Göriach, fig. 3), would have been expected to be situated.

In the molars of the Malay collection the interruption of the occlusolingual groove, at the height of, or somewhat lingually from, the lingual marginal ridge, is a last indication, in my opinion, of the lost trigonal hypocone crest in Man. This is proved by the findings in the endocasts (see below). Its frequency of occurrence follows from table 5.

TABLE 5

Frequency of occurrence of indications of the trigonal hypocone crest in the different groups of Malay maxillary molars

Type of molar	Type a		Type b		Type c		Total no.
	No.	%	No.	%	No.	%	
With Carabelli's cusp type a	7	14.9	40	85.1	—	—	47
With Carabelli's cusp type b	60	32.1	124	66.3	3	1.6	187
With Carabelli's cusp type c	7	21.9	22	68.7	3	9.4	32
With parastyle	3	15.0	15	75.0	2	10.0	20
With four cusps	57	24.6	158	68.1	17	7.3	232
With mesial edge tubercles	14	8.7	143	88.8	4	2.5	161
With distal edge tubercles	7	15.6	36	80.0	2	4.4	45
With mesial and distal edge tubercles	22	18.6	89	75.4	7	6.0	118
Total number	177	21.2	627	74.3	38	4.5	842

In this table (and in table 6):

type a represents interrupted grooves (conservative),
type b represents continuous grooves (progressive),
type c represents grooves which are no longer distinctly visible lingually from the locality of interruption.

The group of molars having a tribubercular type has not been considered, neither have molars with a too heavy attrition.

Endocasts. The endocasts not only show an important higher percentage of interrupted (conservative) occlusolingual grooves, but also in many cases a nicely pronounced trigonal hypocone crest (plates II–VI). The exact relations follow from table 6. The numbers between brackets indicate the instances in which the discontinuity distinctly consists of a distinct crest. The dominance of type a is very striking in all groups of

TABLE 6

Frequency of occurrence of indications of the trigonal hypocone crest in the endocasts of the different groups of Malay molars

Type of molar	Type a		Type b		Type c		Total
	No.	%	No.	%	No.	%	no.
With Carabelli's cusp type a .	22 (21)	88.0	3	12.0	—	—	25
With Carabelli's cusp type b .	57 (55)	92.0	3	4.8	2	3.2	62
With Carabelli's cusp type c .	8 (8)		1		—		9
With parastyle	5 (4)		3		—		8
With four cusps	55 (49)	69.6	9	11.4	15	19.0	79
With mesial edge tubercles. .	61 (60)	79.2	9	11.7	7	9.1	77
With distal edge tubercles . .	18 (17)	75.0	4	16.7	2	8.3	24
With mesial and distal edge tubercles	38 (35)	80.8	6	12.8	3	6.4	47
Total number	264(249)	79.7	38	11.5	29	8.8	331

molars. Compared with table 5 it appears that in the endocasts a higher percentage of this type exists among all groups than on the exterior of the enamel. In addition the high incidence of cingulum-protocone crests is evident.

IX. *The distal marginal ridge*

The ridge has mainly been built up by the distal cingulum in an early tribubercular-triangular stage of molar type. A very small component may perhaps been supplied by the metacone (distal arm). In the Malay teeth it does not always follow a continuous course on the outside of the crown, but it may be dissolved into one or more edge tubercles (table 2), separated from one another by means of fissures or grooves (pl. II, figs. 2, 4 and 5; pl. III, figs. 4 and 5; pl. IV, fig. 3). A phylogenetical consideration results in the conclusion that they cannot have the slightest evolutionary significance, but represent terminal products.

A second peculiarity of the distal marginal ridge is the cleavage of the longitudinal main fissure, by a distal extension, a situation already encoutered in *Pithecanthropus modjokertensis*, a very common feature in the Malay human collection. Its frequency of occurrence in the latter follows from table 7. In this:

Type a represents a continuous distal marginal ridge.
Type b represents an interrupted ridge without continuity of the groove on the distal surface.
Type c represents an interrupted ridge with a continuity of the groove on the distal surface.

Endocasts. In not a single case did distal edge tubercles occur as circumscript and sharply defined elevations of the distal marginal ridge. The latter is more strongly developed than on the outside of the enamel

TABLE 7

The frequency of occurrence of types according to which the relation between the longitudinal main groove and the distal marginal ridge could be distinguished in the Malay collection

Type	Type a		Type b		Type c		Total no.
	No.	%	No.	%	No.	%	
With Carabelli's cusp type a . .	17	40.5	15	35.7	10	23.8	42
With Carabelli's cusp type b . .	63	41.5	37	24.3	52	34.2	152
With Carabelli's cusp type c . .	13	46.4	4	14.3	11	39.3	28
With four cusps	6		3		1		10
With parastyle	67	44.9	34	22.8	48	22.3	149
With mesial edge tubercles . . .	93	51.3	22	12.2	66	36.5	181
Total number	259	46.0	115	20.5	188	33.5	562

cap, and has a continuous course in all casts (cf. enamel crowns and endocasts in pl. III, figs. 2, 4 and 5; pl. IV, figs. 3 and 4). On the distal surface no fissure was observed in any of the specimens. These findings, compared with those for the exterior enamel surface, given in table 7, illustrate very convincingly, in my opinion, the greater measure of primitiveness of the endocasts in this respect, compared with the morphology of the outside of the enamel layer.

(To be continued)

THE ENAMEL DENTINE BORDER: A NEW MORPHOLOGICAL FACTOR IN THE STUDY OF THE (HUMAN) MOLAR PATTERN. Ib

BY

C. A. W. KORENHOF

(Communicated by Prof. G. H. R. VON KOENIGSWALD at the meeting of June 24, 1961)

B. GROOVES AND WRINKLES

X. *The central fossa*

The original early Tertiary form of the central fossa (fovea centralis) is shown in molar teeth like those of *Teilhardina belgica* (pl. I, fig. 1 and textfigure 1). A primitive central fossa probably possesses only weak indications of grooves. It is situated between the three main cusps of the trigon and has the form of a figure Y (when seen in a buccolingual direction). The three limbs of the Y do not cut through the limbs of the trigon and the buccal marginal ridge.

The conditions in recent Man are sufficiently well known from textbooks on dental anatomy. Secondary obtained characters of the fovea centralis are:

1. deep, fissure-like grooves, sharply separating the main cusps;
2. rupture of the crista transversa anterior, or a sharp separation of the mesial, central parts of paracone and protocone;
3. rupture of the crista obliqua;
4. rupture of the buccal marginal ridge, with possible continuation in the form of the buccal main groove.

No statistical consideration of the characteristics can be given, as no objective criteria could be found to discuss them.

Endocasts. It is a striking fact that the enamel-dentine border nearly always shows a central fossa with less pronounced grooves than on the outside of the enamel crown (pl. II, figs. 1–6; pl. III, figs. 1, 4, 5, 6; pl. IV, figs. 2–6; pl. V, figs. 1–6; pl. VI, figs. 1–6). It is, however, not possible to express the differences in numbers.

The amount of rupture of the crista transversa anterior and the crista obliqua, by means of the central fossa grooves, follows from the pertinent descriptions of these crests (points V and VI, respectively).

XI. *The fovea anterior*

The original fovea anterior is characterized, in its early Tertiary phenotype, by the following marks of identification:

1. it forms the valley between paracone and protoconule and is limited by a part of the lingual slope of the first cusp and the buccal slope of the latter;
2. it is bounded mesially by the mesial marginal ridge;
3. it is bounded distally by the crista transversa anterior, or by structural components forming this crest later.

During its evolution an aperture of the feature follows in two directions:

a. first in a distal direction: breach of the crista transversa anterior
b. later on in a mesial direction: breach of the mesial marginal ridge.

Ad. a. In Necrolemurinae of the Quercy fissure deposits the fovea is still being formed (fig. 2). It is completely present in *Pliopithecus* from the Upper Vindobonian of Styria (fig. 3) and occurs in the same fissure-like way in *Dryopithecus* and *Sivapithecus* (figs. 4 and 5), though not always as clearly as regards its lingual section. This part is first of all subjected to reduction. In further evolved molar teeth, such as in *Sivapithecus* cf. *indicus*, *Gigantopithecus blacki*, *Australopithecus africanus* and *Paranthropus robustus*, a distinct mesial fossa is no longer present.

In the Malay human teeth the fovea is in nearly all cases connected with the central fossa (progressive), or is fully reduced. The presence of (remains of) the crista transversa anterior has been discussed in point V, and is specified in table 3.

In the 22 cases mentioned in this table the following relations appear to exist with regard to the development of the fovea anterior:

Types 1–3: all 14 molars possess a buccal remnant of the fovea anterior, well separated from the rest of the groove system (pl. III, fig. 4; pl. VI, figs. 2 and 4).
Type 4 : the molar possesses a complete and distally closed fovea.
Type 5 : all molars have a complete, but (in a bucco-lingual sense) narrow anterior fossa of the original (distally bounded) type. In one case (cat. no. MMSS 48) the fossa is very small (pit-like).

A fovea, or remnant of a fovea, which is distally well defined from the central fossa, consequently occurs in only 1.5 per cent of the Malay molars (original conditions). In all remaining cases the circumstances are modified.

Ad b. The mesial breach of the fovea anterior seems to have taken place later in its evolution. In none of the non-hominid examples mentioned above has a discontinuity of the mesial marginal ridge taken place (as far as I could verify), except in the highly evolved molars of *Gigantopithecus*. It seems to be a feature of a later (Pleistocene?) evolutionary significance.

In *Gigantopithecus* the fovea may be disclosed in both a mesial and a distal direction (see von Koenigswald, 1952, pl. 49, fig. A). The same

can be said of *Australopithecus* and *Paranthropus* (see ROBINSON, 1956, figs. 24, 26, 28 and figs. 23, 25, 27, respectively). In *Pithecanthropus modjokertensis* (see VON KOENIGSWALD, 1958, figs. 3 and 6), and in *Sinanthropus* (WEIDENREICH, 1937) the conditions are less clear, just as in most neanderthaloid forms.

In recent Man the breach of the mesial marginal ridge, and the disclosure of the fovea anterior in that direction, is an almost constant characteristic. Several authors, in giving a normal type of a generalized first (and second [and third]) molar, depict a breach of the mesial edge of the occlusal surface (DEWEY, 1927: M^1, M^2; VAN DEN BROEK, 1946: M^1; ZEISZ and NUCKOLLS, 1949: M^1, M^2, M^3; WOERDEMAN–DE JONGE, 1950: M^1, M^2; DE JONGE, 1954: M^1). Some of them mention the breach in their descriptions (BLACK, 1902: M^1; DEWEY, 1927: M^1; ZEISZ and NUCKOLLS, 1949: M^1, M^2, M^3).

In the Malay collection only those molars have been considered with regard to this feature of which endocasts were present. In table 8 the frequency of occurrence of three types of the mesial wall of the fovea are considered:

TABLE 8

The frequency of occurrence of types, according to which the mesial wall of the fovea anterior could be distinguished in different groups of Malay teeth

Type of molar	Type a		Type b		Type c		Total
	No.	%	No.	%	No.	%	no.
With Carabelli's cusp type a . .	17	42.5	15	37.5	8	20	40
With Carabelli's cusp type b . .	12	35	21	62	1	3	34
With Carabelli's cusp type c . .	10	67	2	13	3	20	15
With parastyle	2		2		—		4
With four cusps	11	48	10	43	2	9	23
With mesial edge tubercles . . .	7	12.5	28	50	21	37.5	56
With distal edge tubercles . . .	14	87.5	2	12.5	—	—	16
With mesial and distal edge tubercles	6	35.3	8	47.0	3	17.7	17
Total number	79	38.6	88	42.9	38	18.5	205

Type a: no indications of a breach of the mesial wall of the fovea anterior (pl. III, fig. 1).

Type b: the mesial marginal ridge shows a slight groove which does not continue on the mesial surface (pl. III, fig. 5).

Type c: the mesial marginal ridge shows a slight groove which continues on the mesial surface (not visible in the occlusal views of the illustrations).

The number of molars of all groups is too small to permit any separate conclusions. Seen totally it may be inferred that in the Malay sample the fovea anterior is exposed mesially in the greater number of cases.

Endocasts. With regard to the distal enclosure of the fovea, it follows from the discussion under point V, that the enamel-dentine border shows more primitive conditions than the outer enamel coating does. Mesially the foveae of all 475 endocasts show an uninterrupted barrier (see plates II–VI), which demonstrates in no uncertain manner the very original conditions shown by the endocasts with respect to this feature, compared with the exterior of the enamel cap.

XII. *The fovea posterior*

The feature appears to be without a great phylogenetical significance. It is a terminal derivative product. Secondary fissures between the lobes of hypocone and metacone on the one side, and the distal marginal ridge on the other, may show a picture analogous with that of the fovea anterior (pl. III, figs. 2 and 5).

XIII. *The system of wrinkles*

From the Malay molars and their endocasts no decisive conclusions can be drawn regarding the questions whether the phenomenon of the crown wrinkles is a primitive or a secondarily obtained character, and whether the feature is in a progressive or in a regressive stage in Man and other hominoid forms.

As far as is known the wrinkles, in the phylogenetical line(s) which probably lead(s) up to the recent Hominoidea, occur for the first time in *Dryopithecus*. A moderate wrinkling therefore need not necessarily have been obtained terminally, in contrast to the excessive folding which occurs in *Pongo*.

The presence of a more extensive wrinkling on the endocasts of the Malay material, as compared with the external side of the enamel in the same teeth, suggests that the process is following a regressive course in recent Man.

CONCLUSIONS

In the human upper molars from a collection of subrecent Javanese teeth the following morphological features of the occlusal surface of the enamel-dentine border appear to show phylogenetically more original conditions than on the exterior surface of the enamel layer:

1. The shape of the main cusps are higher and more acutely pointed, with concave centrally directed slopes.
2. The hypocone is higher.
3. The mesial marginal ridge is never dissolved into a number of edge tubercles and always shows a continuous course.
4. The crista transversa anterior is of more frequent occurrence.
5. The crista obliqua occurs more sharply pronounced and has a continuous course in a considerable higher percentage (table 4).

LEGENDE OF PLATES

Plate I

1. *Teilhardina belgica.* Upper molars. Collection of the Institut royal des Sciences naturelles, Brussels. Cat. nos. Ct. M. 58, 57 and 59. Enlargement 20 × natural size. The illustration in the right upper corner shows the same teeth in their natural size.

2. Upper molars of the collection of Malay human teeth. Enamel crowns, internal views. Enlargement $2^1/_2$ × natural size.

Plate II

Subrecent Malay upper molars and their endocasts. Enlargement $2^1/_2$ × natural size.

1. Dext., cat. no. MMSD 25
2. Dext., cat. no. MMSD 22
3. Dext., cat. no. MMSD 27
4. Dext., cat. no. MMSD 21
5. Sin., cat. no. MMSS 21
6. Sin., cat. no. MMSS 100

Plate III

Subrecent Malay upper molars and their endocasts. Enlargement $2^1/_2$ × natural size.

1. Sin., cat. no. MMSS 102
2. Sin., cat. no. MMSS 108
3. Sin., cat. no. MMSS 127
4. Dext., cat. no. MMSD 168
5. Sin., cat. no. MMSS 163
6. Dext., cat. no. MMSD 532

Plate IV

Subrecent Malay upper molars and their endocasts. Enlargement $2^1/_2$ × natural size.

1. Dext., cat. no. MMSD 372
2. Dext., cat. no. MMSD 681
3. Sin., cat. no. MMSS 578
4. Sin., cat. no. MMSS 121
5. Sin., cat. no. MMSS 367
6. Dext., cat. no. MMSD 531

Plate V

Subrecent Malay upper molars and their endocasts. Enlargement $2^1/_2$ × natural size.

1. Sin., cat. no. MMSS 167
2. Sin., cat. no. MMSS 165
3. Sin., cat. no. MMSS 166

3. Dext., cat. no. MMSD 579
5. Sin., cat. no. MMSS 164
6. Dext., cat. no. MMSD 583

Plate VI

Subrecent Malay upper molars and their endocasts. Enlargement $2^1/_2$ × natural size.

1. Sin., cat. no. MMSS 369
2. Dext., cat. no. MMSD 525
3. Dext., cat. no. MMSD 526
4. Sin., cat. no. MMSS 573
5. Sin., cat. no. MMSS 365
6. Sin., cat. no. MMSS 510

C. A. W. KORENHOF: *The enamel-denitne border: a new morphological factor in the study of the (human) molar pattern.*

PLATE I

1

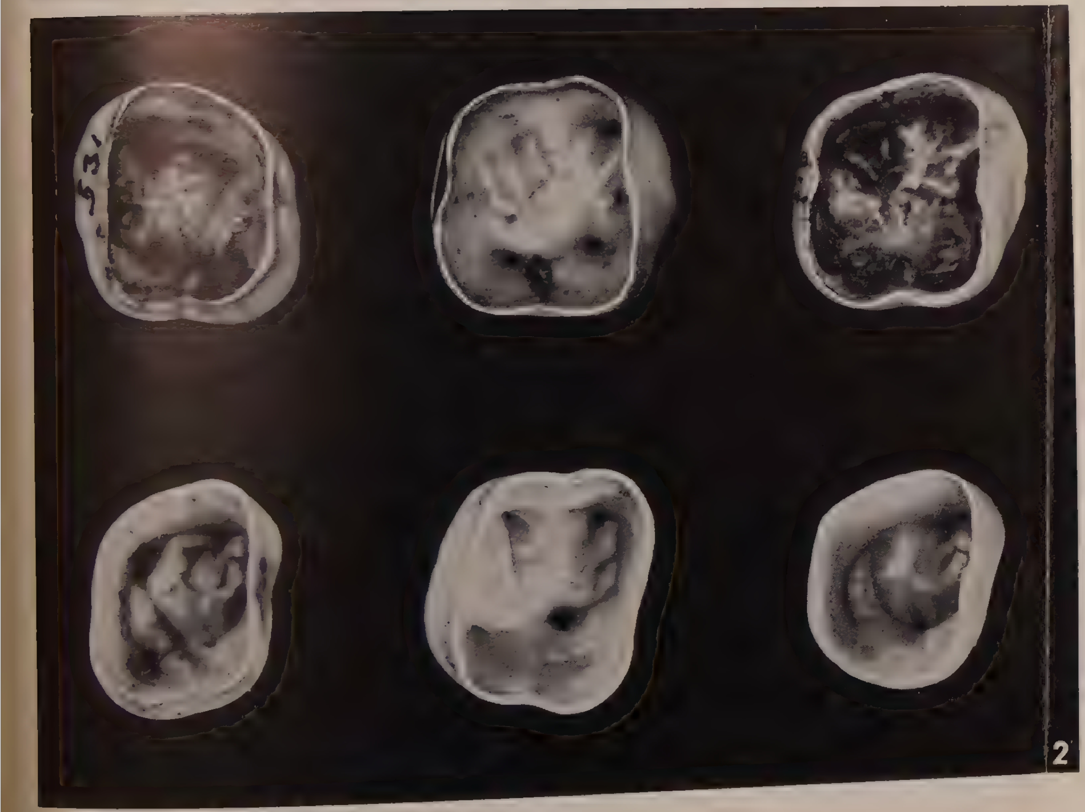

2

PLATE II

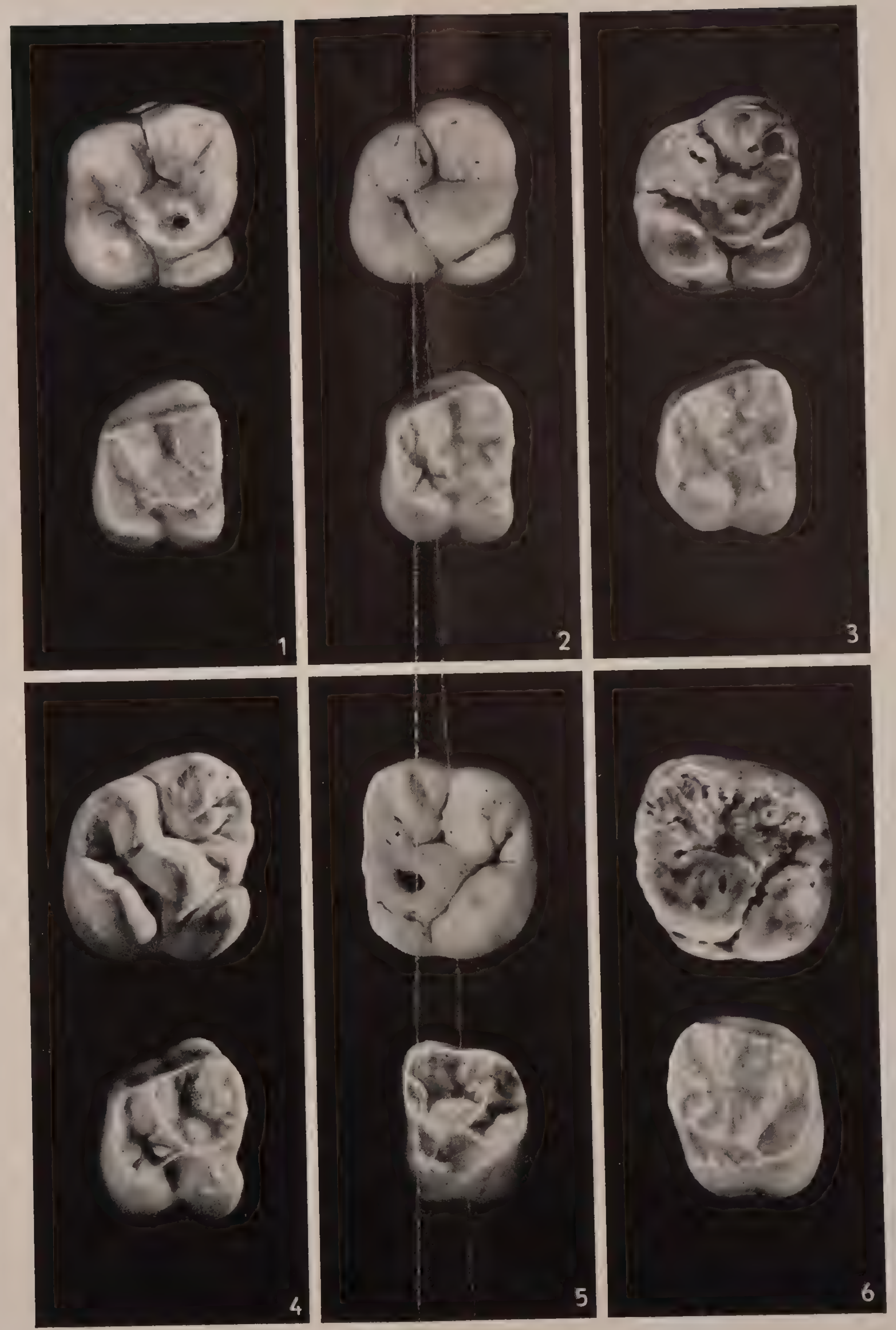

1 2 3

4 5 6

PLATE III

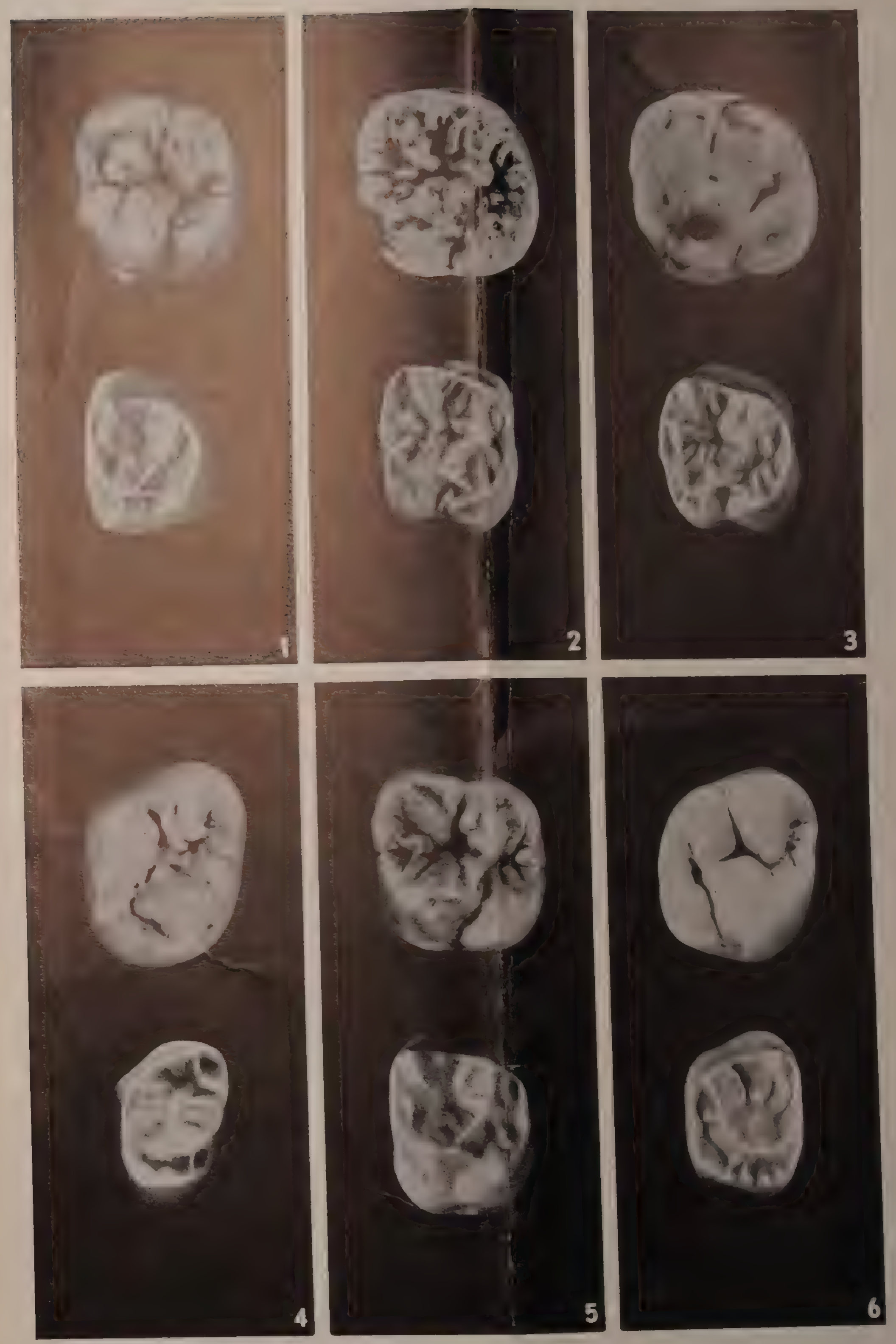

1 2 3

4 5 6

PLATE IV

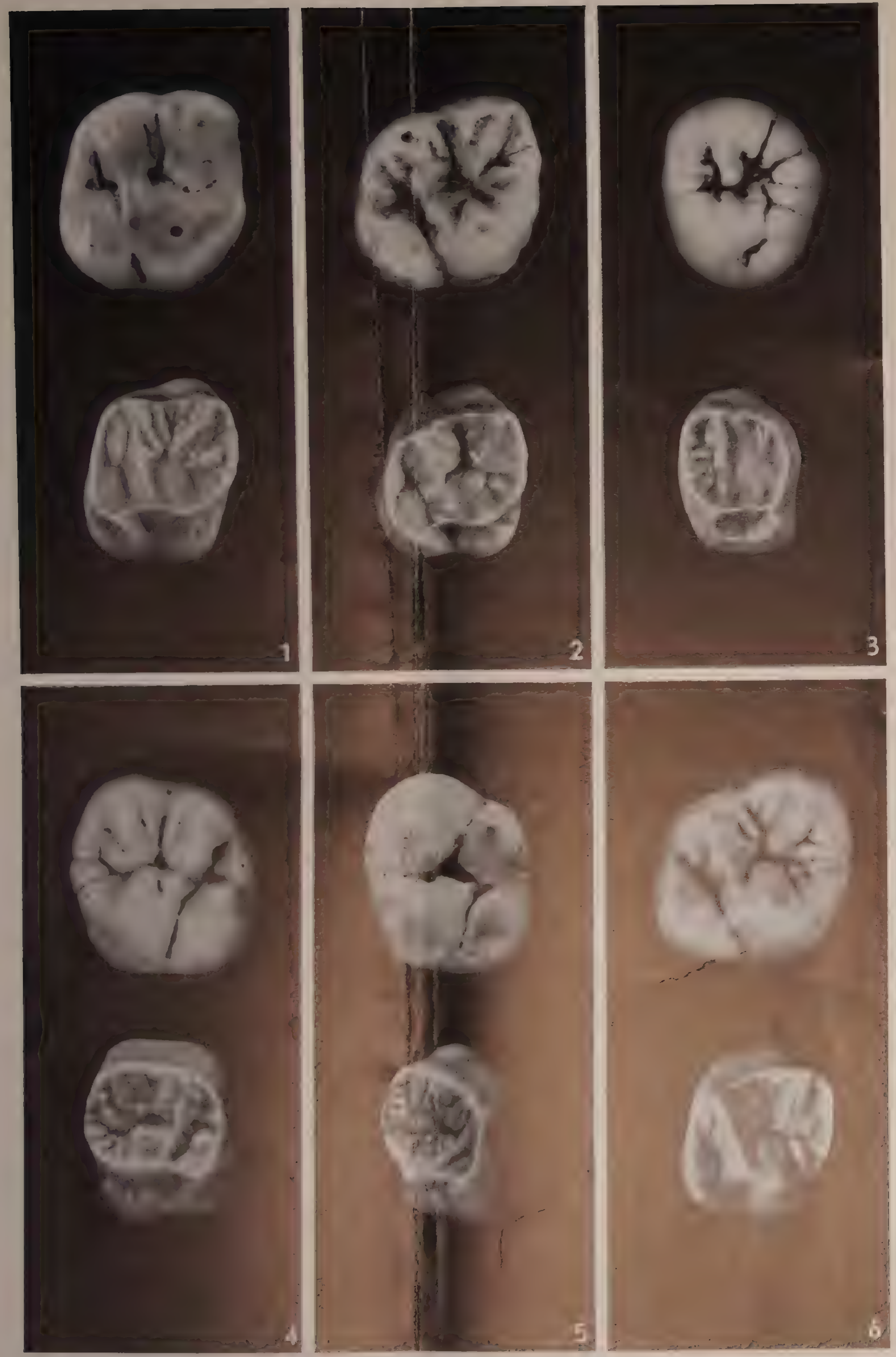

PLATE V

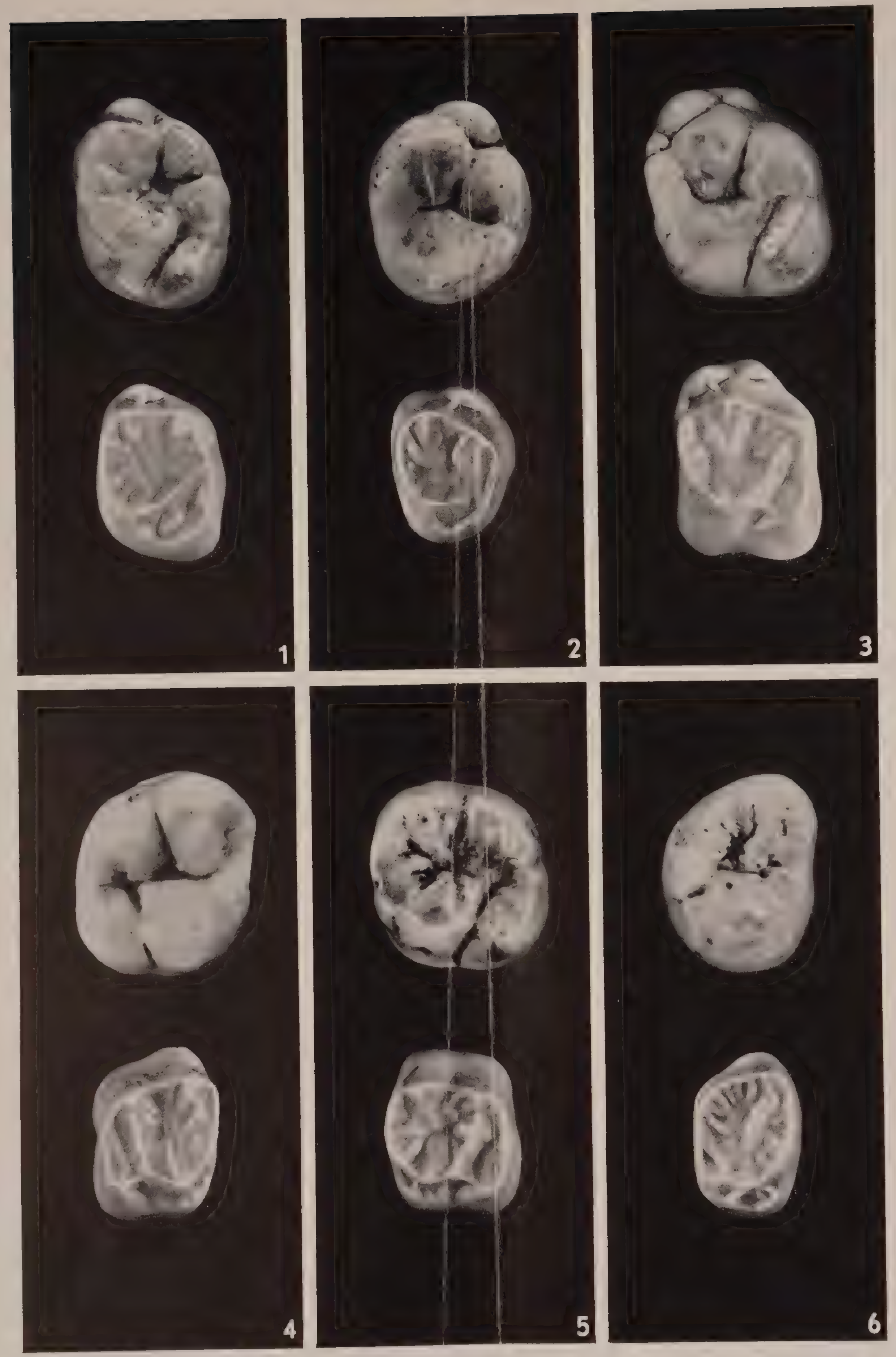

PLATE VI

6. The trigonal hypocone crest, lost in the exterior surface of the enamel, is completely present and sharply pronounced in nearly all endocasts (compare tables 5 and 6).
7. The distal marginal ridge is never dissolved into a number of edge tubercles and always shows a continuous course.
8. The central fossa is less pronounced, with only weak indications of grooves. The three limbs of the Y-pattern of grooves do not cut through the limbs of the trigon and the buccal marginal ridge.
9. The fovea anterior or rests of it is present in a higher percentage (table 3).
10. The crown wrinkles are more extensive.

It seems therefore advisable to look for means which enable us to separate the enamel artificially from the dentine in human and other vertebrate teeth, so as to get a better insight into the evolutionary significance of the structural features of their enamel surface.

LITERATURE CITED

Black, G. V., Descriptive Anatomy of the Human Teeth, 4th ed. Philadelphia: The S.S. White Dental Manufacturing Co. (1902).

Branco, W., Die menschenähnlichen Zähne aus dem Bohnerz der schwäbischen Alb. Jahreshefte des Vereins f. Vaterl. Naturk. in Württemberg, **54**, 1–144 and plates I–III (1898).

Broek, A. J. P. van den, Leerboek der bijzondere ontleedkunde voor tandartsen. Tweede druk. Utrecht: N.V. A. Oosthoek's Uitgevers-Maatschappij, 236 (1946).

Butler, P. M. and J. R. E. Mills, A contribution to the odontology of *Oreopithecus*. Bull. Brit. Museum (Nat. Hist.) Geol., **4** (no. 1): 1–26 and one pl. (1959).

Dewey, M., Dental Anatomy. London: Henry Kimpton; 291 (1927).

Eckardt, H., Vergleichend morphologische Studien an den Molaren des Orang Utan und des Gibbon. Zeitschr. f. Morphol. u. Anthropol., **27**, 225–338 and plates VI–X (1930).

Gazin, C. L., A review of the Middle and Upper Eocene Primates of North America. Smithonian Miscellaneous Collections, **136**, no. 1; 112 pp. and 14 plates (1958).

Glaessner, M. F., Neue Zähne von Menschenaffen aus dem Miozän des Wiener Beckens. Ann. Naturhist. Museum in Wien, **46**, 15–27 and 1 pl. (1931).

Gregory, W. K., The Origin and Evolution of the Human Dentition. Baltimore: Williams & Wilkins Company; 548 (1922).

Hürzeler, J., Zur Stammesgeschichte der Necrolemuriden. Schweiz. pal. Abhandl. **66**, 1–46 (in the reprint) (1948).

———, Contribution à l'odontologie et à la Phylogénèse du Genre *Pliopithecus* Gervais. Ann. de Pal., **40**, 1–63 (in the reprint) (1954).

Jonge, T. E. de, Anatomie der Zähne. Die Zahn-, Mund- u. Kieferheilk., **1**, 169–232 (1954).

Jørgensen, K. D., The deciduous dentition. Acta Odontol. Scand. (suppl.) **14**, 1–202 and 14 tables (1956).

Koenigswald, G. H. R. von, *Gigantopithecus blacki* Von Koenigswald, a giant fossil hominid from the Pleistocene of Southern China. Anthropol. Papers Am. Museum Nat. Hist., New York, **43** (part 4): 297–325 (1952).

——, L'hominisation de l'appareil masticateur et les modifications du régime alimentaire. Colloques internat. du centre national de la recherche scientifique. Sciences humaines. Les processus de l'hominisation. Paris: Centre nat. de la recherche scient., pp. 59–78 (discussion incl.) (1958).

KORENHOF, C. A. W., Morphogenetical aspects of the human upper molar. A comparative study of its enamel and dentine surfaces and their relationship to the crown pattern of fossil and recent primates. Utrecht: Uitgeversmaatschappij Neerlandia; 368 pp. and 15 plates (1960).

KRAUS, B. S., Morphologic Relationships between Enamel and Dentin Surfaces of Lower first molar teeth. Journ. Dent. Res., **31**, 248–256 (1952).

PIVETEAU, J., Vers la forme humaine. Le Problème biologique de l'homme. Les époques de l'Intelligence. Traité de paléontologie, tome VII (Primates-paléontologie humaine). Paris: Masson et Cie.; 675 (1957).

REMANE, A., Beiträge zur Morphologie des Anthropoidengebisses. Archiv. f. Naturgeschichte, **87** (Abt. A), 1–179 (1921).

ROBINSON, J. T., The Dentition of the Australopithecinae. Transvaal Museum, Memoir no. 9; 179 (1956).

STEHLIN, H. G., Die Säugetiere des schweizerischen Eocaens; siebenter Teil, zweite Hälfte. Abh. der Schweiz. pal. Gesellsch., **41**, 1299–1552 (1916).

TOPINARD, P., De l'évolution des molaires et prémolaires chez les primates et en particulier chez l'homme. L'Anthropologie, **3**, 641–710 (1892).

WALKHOFF, Der Zahn von Sondé (ein fossiler Menschenzahn von Java). Pp. 214–221 and pl. 28 in: Die Pithecanthropus-Schichten auf Java. Leipzig: Wilhelm Engelmann (1911).

WEIDENREICH, F., The Dentition of *Sinanthropus pekinensis*. A comparative Odontography of the Hominids. Pal. Sinica. N.S. D, no. 1, Whole S. no. 101. (I): 180 pp., 36 plates and 49 diagr. (1937).

WOERDEMAN, M. W. and T. E. DE JONGE, Dental Anatomy. Extr. from Atlas of human anatomy. Vol. II. Amsterdam: Wetensch. Uitgeverij N.V.; 56 pl. (1950).

ZEISZ, R. C. and J. NUCKOLLS, Dental Anatomy. St. Louis: The C.V. Mosby Company; 486 (1949).

CONTRIBUTION TO THE STUDY OF *MIOGYPSINA* s.l. FROM EGYPT. I

BY

F. J. SOUAYA

(Communicated by Prof. G. H. R. VON KOENIGSWALD at the meeting of June 24, 1961)

ABSTRACT

This work investigates statistically the *Miogypsina* assemblages of a number of samples from the lower part of the Miocene from the Eastern Desert and Sinai.

Miogypsina intermedia DROOGER, *M. cushmani* VAUGHAN and *M.* (*Miogypsinoides*) *complanata* SCHLUMBERGER *mauretanica* BRONNIMANN are reported here for the first time from Egypt. The occurrence of this latter species amongst a comparatively young *Miogypsina* s.s. series is discussed.

Various biometric, biostratigraphic and paleoecologic conclusions follow the statistic investigation.

INTRODUCTION

Until now little work has been done in Egypt on *Miogypsina* although it occurs in several Miocene sections.

CUVILLIER (1938) was first to report the presence of *Miogypsina*, identified by Prof. SILVESTRI as *M. irregularis*, at a locality 3 km West of G. Chahabi and between G. Aouebed and the Cairo-Suez road at km 77.

Later, STAINFORTH (1949), in a brief summary on the distribution of Foraminifera in the Upper Tertiary of Egypt, mentioned *Miogypsina* in his reefal facies.

Miogypsina assemblages from the Eastern Desert and Sinai are here investigated for the first time in detail, using statistics in the study of a number of characters.

This work aims at contributing towards the general knowledge of the Miogypsinidae and to attract attention to the detailed study of their representatives in Egypt, because their careful investigation will certainly help in a better understanding of the Miocene stratigraphy.

Besides the interesting results which were obtained, this work serves to evaluate the technique used, and shows the necessity for improvement in future studies of similar type.

ACKNOWLEDGEMENT

The writer is indebted to Messrs. The Anglo-Egyptian Oilfields Ltd. (Management and Geological Dept.) for putting their laboratory and

library at his disposal, and for allowing him to do part of this research in the Company's time.

To Professor GALLAL EL-DINE HAFEZ AWAD, the writer wishes also to express his gratitude for his supervision of this work, which represents part of a thesis presented for the doctorate degree at the University of Alexandria.

Thanks are also extended to M. A. GHORAB (Palaeontological Dept. A.E.O.) for his constant encouragement and to Dr. C. W. DROOGER (Geological Institute, University of Utrecht) for reading the manuscript critically and for making valuable comments and useful suggestions.

GENERAL STRATIGRAPHY

The Miocene deposits of Egypt cover about 125.000 square kilometers which is about one-eighth of the total area of the country.

They occur in the Northern part: in the Eastern and Western deserts, along the Red Sea, in Sinai and possibly also across the Nile delta to a considerable depth below the alluvial sand. They are unconformable upon older rocks. Faunal affinities of the marine phases of the Miocene are with those of the Vienna Basin and the Mediterranean region specifically Malta, Italy and Cyprus.

In the Eastern desert, the Miocene is present between Cairo and Suez with abundant proof to show that there was a great overlap of the Miocene beds from West to East (BARRON, 1904, pp. 607, 608).

The existence of genuine Lower Miocene beds in the Cairo-Suez Area has been much disputed. DEPÉRET and FOURTAU (1900, pp. 402–403), followed by BARRON (1904, pp. 604–608), HUME (1912, p. 17), BARTHOUX (1922, p. 88), MACFADYEN (1930) and CUVILLIER (1938) gave evidence for the Lower Miocene. BLANCKENHORN (1901, pp. 52–59), on the other hand, was of the opinion that DEPÉRET and FOURTAU's Lower Miocene beds were truly Middle Miocene because of their fossils. He placed the gritty beds occurring above the basalt to the East of Cairo, together with part of the Petrified Forest in the Lower Miocene, not on fossil evidence, but on account of lithological characters, plus the fact that the fossil wood occurs at the base of the Miocene in Moghara.

Recent studies on the geology of Gebel el Nassuri and Gebel el Ankabiya (SHUKRI and AKMAL, 1953, pp. 249–250) and Gebel Oweibed (SHUKRI and EL AYOUTI, 1956) in the Cairo-Suez district, assign a Middle Miocene age to the Marine Miocene sediments of the Cairo-Suez belt mainly on account of the workers' failure to find any break in these deposits. In addition, the megafossils as studied by SAID and YALLOUZE (1954, pp. 62–63) are either Vindobonian or fall into such a long range of time that they are of little use.

In the peninsula of Sinai, Miocene strata occupy large areas in the West and South-West. They include from base to top the Miocene Clays,

Grits, and Marls, and towards the top the Gypsum Series consisting of gypsum beds, alternating with intergypseous marls (Moon and Sadek, 1925, p. 11). Limestones may occur at various levels in the succession. Burdigalian, "Schlier" and Vindobonian beds have been reported, while the presence of Upper Miocene strata has been considered as a mere possibility (Moon and Sadek, 1921, pp. 28 30).

However, the existence of the Burdigalian Stage has not yet met with full acceptance. Picard (1943) has denied its presence in Egypt on account of various arguments, the absence of genuine Burdigalian guide fossils was stressed in particular. Recently, Farag and Shata (1957, p. 323), have reported at Bir Haleifiya and Gebel Zeita area (East coast Gulf of Suez), the presence of a mixture of definite marine Upper Oligocene (Aquitanian) and Lower Miocene (Burdigalian) megafossils in the lowest beds of their Oligo-Miocene series.

LOCALITY DETAILS

This investigation involves the study of samples from Gebel Gharra, G. Atâqa (Eastern Desert) and G. Gushia (Sinai) (pl. 1).

Gebel Gharra (also written G. Garra) is located at about $7\frac{1}{2}$ km North of Iweibid Station which is 40 km West of Suez. It is also known as Gebel U' Jerat al Yassara according to Macfadyen (1930, p. 4). It should not, however, be confused with the G. Garra which is some 50 km West of Assouan in the Libyan desert.

Barthoux (1922, pp. 82, 83) gives the succession at G. Gharra and adds that it is the locality where the basal formations of the series with the rare echinoid *Echinolampas pignatarii* Stefanini, are best developed. He assigned this basal part to the Burdigalian and considered the overlying Miocene strata to belong to the Schlier and the Vindobonian.

The section of G. Gharra as here represented (pl. 1) was sampled by Mr. R. W. Pooley, formerly Chief Paleontologist of the Anglo-Egyptian Oilfields Ltd. Sampling (P 1367–P 1386) started on the North-East end of this Gebel and was continued along Sadl el Gâmûs (P 1337–P 1366). This paper deals in detail only with the following *Miogypsina* samples: P 1337, P 1342, P 1347, P 1349 and P 1360.

As for Gebel Attaka, also written G. Atâqa, which lies in the Eastern Desert, its samples (FS 470–FS 473) were collected by the author from a cliff about 0.5 km West of the road to Ras Gharib and some 18 km South from the gate of the Port of Adabiya.

As regards Gebel Gushia (also written G. el Gushiya) which lies in Sinai, some 27 km NW of Abou Zenima, at about the latitude of km 92 on the road to Tor, the author's sampling started in Wadi el Burqa at about 6 km from Wadi Gharandel in the Eocene which underlies the main Miocene section. Samples FS 285–FS 287, here investigated in detail, are from the base of the Miocene series.

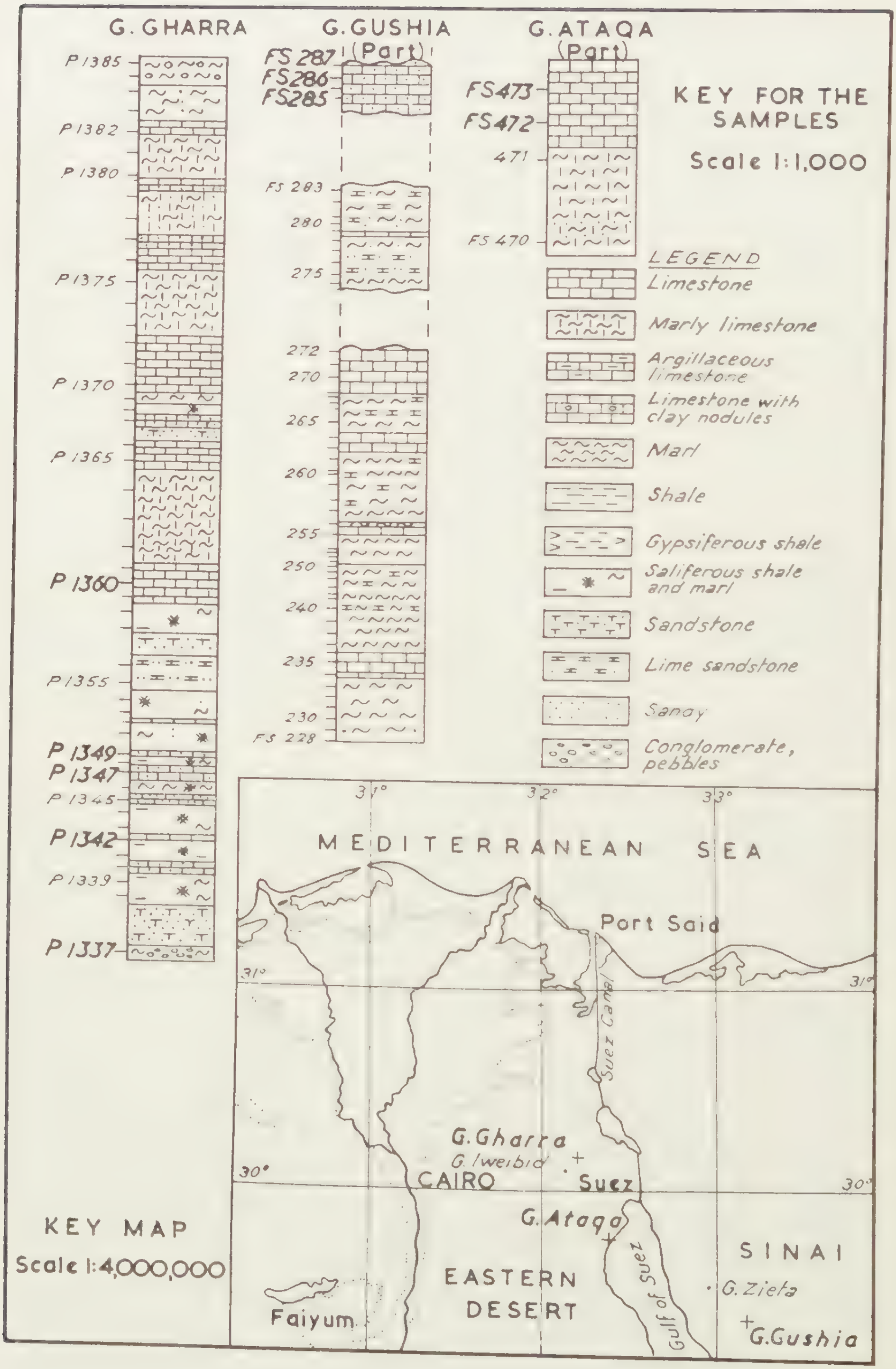
G. GHARRA
G. GUSHIA (Part)
G. ATAQA (Part)
KEY FOR THE SAMPLES
Scale 1:1,000
LEGEND
Limestone
Marly limestone
Argillaceous limestone
Limestone with clay nodules
Marl
Shale
Gypsiferous shale
Saliferous shale and marl
Sandstone
Lime sandstone
Sandy
Conglomerate, pebbles
P 1385
P 1382
P 1380
P 1375
P 1370
P 1365
P 1360
P 1355
P 1349
P 1347
P 1345
P 1342
P 1339
P 1337
FS 287
FS 286
FS 285
FS 283
280
275
272
270
265
260
255
250
240
235
230
FS 228
FS 473
FS 472
471
FS 470
MEDITERRANEAN SEA
Port Said
Suez Canal
G. Gharra
G. Iweibid
CAIRO
Suez
G. Ataqa
Gulf of Suez
SINAI
G. Zieta
G. Gushia
EASTERN DESERT
Faiyum
KEY MAP
Scale 1:4,000,000

PLATE 1

GENERAL CONSIDERATIONS

Miogypsina specimens were collected from the original sample whenever it was possible, alternatively they were picked from the washed residues obtained by the conventional method of washing using sodium hydroxide and hydrogen peroxide.

As for the thin sections, these were prepared in the usual way, using instead of Canada Balsam the more practical Rosenbusch cement which is a mixture of Canada Balsam and shellac (GLAESSNER, 1947, p. 47).

As for the illustrations, a camera lucida was used for the preparation of the drawings, which had then to be retouched on account of some distortion. Besides, the photomicrographs were taken with a Leitz camera fitted on an ordinary binocular microscope using slow films (Selochrome). Retouching was made with gouache or with soft pencils, depending whether the paper of the prints was glossy or mat.

GLOSSARY OF MORPHOLOGICAL TERMS

In this study a number of characters used by DROOGER (1952) in his study of the American Miogypsinidae, were investigated (pl. 2). Their symbols and their definitions are given below:

T_t : is the maximum thickness of the test.

D_I : is the largest diameter of the proloculum including half the wall thickness.

D_{II} : is the largest diameter of the deuteroconch including half the wall thickness.

X : is the number of spirally coiled chambers excluding the two embryonic chambers (DROOGER, 1954a, p. 230) in individuals with a single spiral.

$200\alpha/\beta$: is the degree of symmetry of the protoconchal nepionic spirals.

α : is the arc length of the circumference of the proloculum underlying the smaller spiral.

β : is the arc length of this circumference underlying both protoconchal spirals.

γ : is the angle formed by the apical-frontal line through the centre of the protoconch and the line connecting the centres of the embryonic chambers; it is measured from the apex and its value is positive when the principal auxiliary chamber (or the bigger one, II′, when there are two) is directed towards the frontal margin or the main development of the equatorial chambers, and negative when this chamber is oriented towards the apex. When the individual values of a sample occur on either side of the 180° mark, all the values are made either positive or negative in order to avoid wrong means (DROOGER, written communication). In such cases this is best done by considering the whole scale either as negative or as positive. Thus, $\gamma = +90°$ may become

$-270°$ if the whole scale is negative and alternatively $\gamma = -90°$ may become $+270°$ if the whole scale is considered positive.

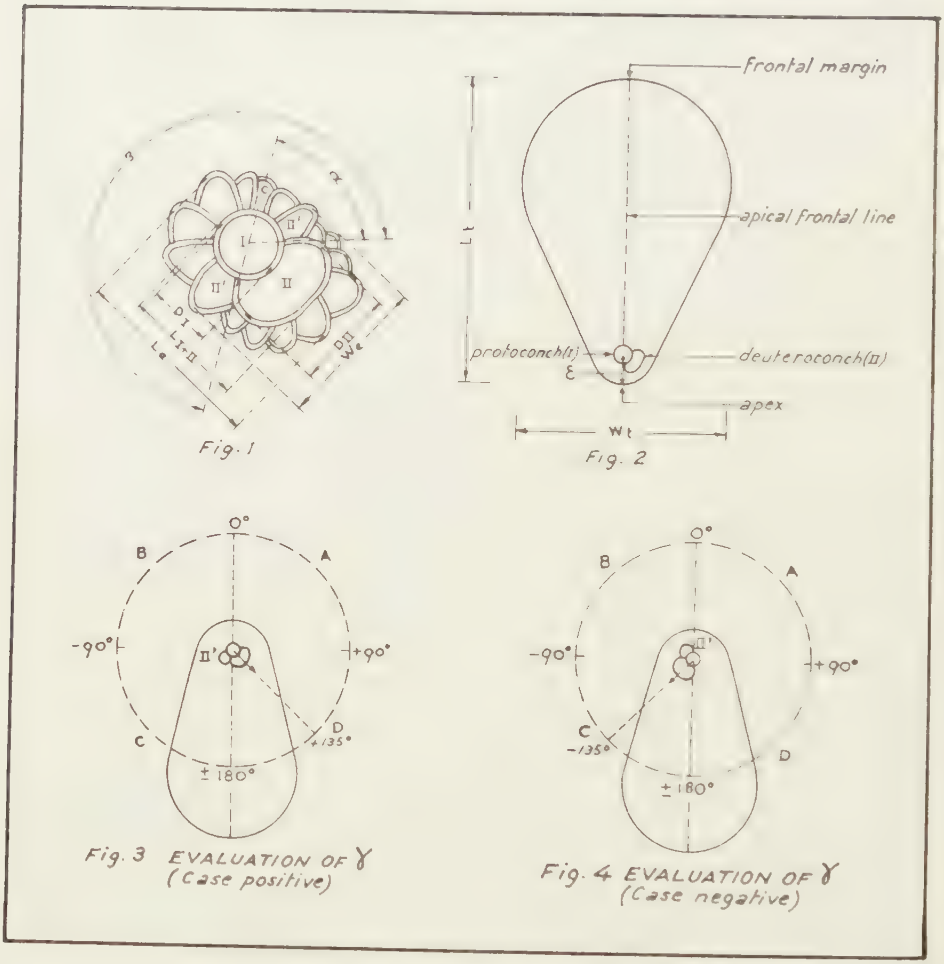

PLATE 2

In addition to the above characters the following ones were also used (pl. 2):

L_t : is the maximum length of the test measured along the apical-frontal line.

W_t : is the maximum width of the test measured along a line at right angles to the apical frontal line.

L_{I+II} : is the common length of both the protoconch and the deuteroconch passing through their centres and including all the thickness of their walls.

ε : is the distance from the centre of the protoconch to the apex.

L_e : is the maximum length of the embryonic and nepionic chambers measured along the extension of the line connecting the centres of the protoconch and the deuteroconch. It includes half the thickness of the walls of the end-chambers.

W_e : is the maximum width of the embryonic-nepionic chambers in a direction at right angles to L_e. It includes also half the thickness of the walls of the end-chambers.

L_eW_e: is the product of L_e by W_e which represents approximately the area of the embryonic–nepionic stages.

TECHNIQUES

Measurements were made on oriented thin sections by means of an ocular micrometer reading to 0.005 mm.

Estimation of α, β and γ was obtained either by making use of photomicrographs, or by very carefully drawing the lines determining the angles corresponding to γ and to the arcs α and β directly on the ground side of the slide by means of a small plastic ruler and a fine picking needle; these lines are then copied with a sharp pencil under the microscope and transferred to a transparent sheet of paper where they may be extended so as to allow the proper measurement of the angles under consideration by means of an ordinary protractor. Both of these methods, when checked, gave comparable results.

There is another easy method for estimating all these angles which makes use of the cross-hairs and the ordinary graduated revolving stage of the microscope (teste DROOGER).

SYSTEMATICS

Order FORAMINIFERA

Family MIOGYPSINIDAE

Genus **Miogypsina** SACCO, 1893

Subgenus **Miogypsina** SACCO

Miogypsina (Miogypsina) cushmani VAUGHAN

Pl I, figs. 21–30; Pl. III, figs. 3–6, 8, 9

Miogypsina cushmani VAUGHAN, 1924, Geol. Soc. Amer., Bull., vol. 35, pp. 802, 813, pl. 36, figs. 4–6; DROOGER, 1952, Study of Amer. Miogypsinidae, Acad. Thesis Utrecht, pp. 38, 56, pl. 2, fig. 40–44; DROOGER, 1954, K. Nederl. Akad. Wetensch. Proc., ser. B, vol. 57, No. 5, pp. 586, 589; DROOGER and MAGNÉ, 1959, Micropaleontology, vol. 5, No. 3, pp. 277, 278.

Dimensions: L_t : 1.3–1.9 mm W_t : 1.1–1.6 mm T_t : 0.5 mm.

Locality : Gebel Gharra (Cairo–Suez Road), P 1360.

Remarks : This species shows, according to DROOGER's scale (1952, p. 54), a tendency towards *Miogypsina intermedia* DROOGER on account of the arithmetic mean of $200\alpha/\beta$, since its value of 76.9 is relatively low and approaches the region of the exemplum intercentrale (abbreviated as ex.interc.) introduced by DROOGER (Ibid., p. 1) for the samples near the border line of two adjoining species, which are in this case *M. cushmani* and *M. intermedia*.

Miogypsina (Miogypsina) intermedia DROOGER

Pl. I, figs. 11–20; Pl. III, figs. 1, 2, 7, 10–12; Pl. IV, figs. 1–12

Miogypsina intermedia DROOGER, 1952, Study of Amer. Miogypsinidae, Acad. Thesis Utrecht, pp. 35, 55, pl. 2, figs. 30–34, pl. 3, fig. 4; DROOGER, 1954, K. Nederl. Akad. Wetensch., Proc., ser. B, vol. 57, No. 5, pp. 586, 589; DROOGER, 1955, K. Nederl. Akad. Wetensch., Verh., Afd. Natuurk., ser. 1, vol. 21, No. 2, pp. 25–27, pl. 1, figs. 1–5; DROOGER and MAGNÉ, 1959, Micropaleontology, vol. 5, No. 3, p. 277.

Dimensions: L_t : 1.–2.6 mm W_t : 1.–2.3 mm T_t : .3–.96 mm.

Localities : Gebel Gharra (P 1337, 1342), G. Atâqa (FS 472, 473) and G. Gushia (FS 285–287).

Remarks : This species shows some tendency towards *Miogypsina globulina* in G. Gushia (FS 285–287), because in these samples the arithmetic mean of $200\alpha/\beta$ is relatively low and as such close to the region of *M*.ex.interc. *globulina-intermedia*. In G. Gharra (P 1342) and G. Atâqa (FS 473), however, *Miogypsina intermedia* shows some tendency towards *M. cushmani* by approaching *M.* ex. interc. *intermedia-cushmani*. As for G. Atâqa sample FS 472, *Miogypsina intermedia* would occupy there, as far as evolution is concerned, an intermediate position between the two former cases if DROOGER's scale (1952, p. 54) is accepted.

As for the *Miogypsina* species of sample P 1337, tentatively identified as *M. intermedia* on the basis of DROOGER's scale (1952) for the mean value of $200\alpha/\beta$, it is seemingly somewhat different in its general character from the other *Miogypsina* samples which were assigned in this study to *M. intermedia*. It represents an exemplum intercentrale occurring just at the border line between *Miogypsina intermedia* and *M. globulina* and, as such, seems to show some resemblance to the latter species. This may still more be appreciated knowing that lately DROOGER (1959) identified a *Miogypsina* sample (Colma, CM 9) with a mean value for $200\alpha/\beta$ reaching 49 as *Miogypsina globulina*, although originally (DROOGER, 1952) the maximum M $200\alpha/\beta$ for this species was 45. However, no emphasis, either statistic or systematic, need be put on the *Miogypsina* assemblage of sample P 1337, because of its somewhat unsatisfactory quality and quantity.

Subgenus Miogypsinoides YABE and HANZAWA

Miogypsina (Miogypsinoides) complanata SCHLUMBERGER mauretanica BRONNIMANN

Pl. I, figs. 1–10; Pl. II, figs. 1–13

Miogypsina (*Miogypsinoides*) *complanata* SCHLUMBERGER var. *mauretanica* BRONNIMANN, 1940, Schweiz. Pal. Abh., vol. 63, art. 1, p. 77, pl. 7, figs. 7–14, pl. 8, fig. 1, pl. 9, figs. 1–2, 13, pl. 11, figs. 9–17, p. 78, textfig. 18, p. 79, textfigs. 10–20.

Dimensions:

macrospheric: L_t : .82–2 mm W_t : .86–2 mm T_t : .32–.6 mm

microspheric : L_t : 1.3–2.48 mm W_t : 1.36–1.92 mm.

Locality : Gebel Gharra (P 1337, 1347, 1349).
Remarks : Drooger (1954b, p. 589), in his investigation of *Miogypsina* in Morocco, has found that *M. complanata* var. *mauretanica* was sometimes used by Bronnimann himself for *Miogypsinoides* assemblages very widely diverging in character. As used here the type *mauretanica* is considered to be represented by the assemblage of Morocco sample 90/91, the characters of which as given by Drooger (1954b, p. 589), are as follows:

Sample	Character	N	R	M	σM
90/91	X	31	9–15	11.4	± 0.29
	γ	31	– 30°– + 160° (via ± 180°)	– 118°	± 7.1

All our specimens belonging to this species have the surface covered by pustules. They were fully investigated, although their seemingly anomalous occurrence amid a fairly highly developed *Miogypsina* s.s. sequence, is not yet well understood.

Miogypsina (*Miogypsinoides*) *complanata mauretanica* starts to occur in G. Gharra in sample P 1337, accompanied by a number of *Miogypsina* s.s. referred to *M. intermedia* with some resemblance with *M. globulina*. However, this *Miogypsinoides* is very abundant in samples P 1347 and P 1349. It is worth pointing out that a single specimen of *Miogypsina* s.s. collected in the sample P 1346, just below the afore-mentioned levels, has a value of 63.3 for $200\alpha/\beta$ and 38° for γ. It is referred to *Miogypsina intermedia* showing, as sample P 1342, some tendency towards *M. cushmani* by approaching *M.* ex. interc. *intermedia–cushmani*.

While attempting to identify the *Miogypsinoides* assemblages of G. Gharra, a tentative grouping of some of the Mediterranean types assigned to *M. complanata* was done on the basis of the arithmetic means of X. This may serve as a start for a more extensive and detailed investigation which should also include other characters and forms.

Type	Samples		N	M_x	σM_x	d/σd
Low M_x	Morocco 90/91 (Drooger, 1954b, p. 589)		31	11.4	± 0.29	0.79
	Italy (Bric del Duca) (Drooger, 1954a, pp. 231–232)		20	11.2	± 0.38	
	Egypt	P 1347	19	11.1	± 0.37	
		P 1349	32	10.8	± 0.23	
		P 1337	4	10.75	± 0.478	
Moderate M_x	France (Christus) (Drooger *et al.*, 1955, p. 19)		15	13.9	± 0.74	0.5
	Morocco 95 (Drooger, 1954b, p. 589)		6	13.3	± 0.58	
High M_x	Italy (Villa Giuseppina) (Drooger, 1954a, p. 231)		30	19.9	± 0.4	

The specimens of Saint Étienne d'Orthe (Landes), originally described (Schlumberger, 1900) to have an embryonic spiral of about 20 chambers, represent the type of the species.

As to the differences in the group with low M_x, if sample P 1349 is considered as the minimum instead of P 1337, which is very small, $d/\sigma d$ is still insignificant, being only 1.6.

Comparisons between the arithmetic means of the different types are as follows:

TAB

Statistical data for a number of characters investigated in the samples of *Miogypsina* s.s.

Locality	Sample	200α/β N	200α/β R	200α/β M	200α/β σ_M	γ N	γ R	γ M	γ σ_M	ε (mm) N	ε (mm) R	ε (mm) M	ε (mm) σ
G. Gharra	P 1360	13	50–96	76.9	±3.49	8	0–76°	31.5°	±9.02	8	.24–.40	.32	±.
	P 1342	11	48–83	63.4	±3.50	10	22–50°	37.9°	±3.41	11	.18–.3	.256	±.
G. Atâqa	FS 473	13	37–96.4	62.1	±3.9	11	19–51°	35.45°	±2.82	10	.22–.3	.253	±.
	FS 472	5	44–92	60.5	±8.3	4	14–31°	25.75°	±3.7	5	.225–.4	.305	±.
G. Gushia	FS 287	10	30–74.5	51.–	±4.2	10	16–82°	28.8°	±6.05	7	.24–.27	.255	±.
	FS 286	15	28–75	50.3	±3.7	13	10–47°	26.6°	±3.3	10	.16–.3	.24	±.
	FS 285	8	25–65	50.1	±4.2	8	5–45	23	±4.8	8	.19–.31	.25	±.
G. Gharra	P 1337	4	33–60	45.7	±5.9	4	−48–+20°	−14°	±9.9	4	.15–.23	.176	±.

TAB

Statistical data for a number of characters investigated in the samples of *Miogypsina* (*Miogypsinoides*) *complanata* Schlumberger *mauretanica* Bronnimann from Gebel Gharra.

Sample	X N	X R	X M	X σ_M	γ N	γ R	γ M	γ σ_M	ε (mm) N	ε (mm) R	ε (mm) M	ε (mm) σ
P 1349	32	8–13	10.8	±.23	25	−84– −195°	−127.2°	±5.9	30	.17–.3	.244	±.
P 1347	19	8–14	11.1	±.37	19	−85– −204°	−136.3°	±7.57	24	.2–.35	.262	±.
P 1337	4	10–12	10.75	±.478	3	−129– −151°	−139°	±6.42	4	.22–.26	.245	±.

Type	Status	Samples	d/σd
Low M_x	max.	Morocco 90/91	2.7
Moderate M_x	min.	Morocco 95	
Moderate M_x	max.	France (Christus)	7.7
High M_x		Italy (Villa Giuseppina)	

D_I (mm)			D_{II} (mm)				L_{I+II} (mm)				Determination
R	M	σ_M	N	R	M	σ_M	N	R	M	σ_M	
145–.21	.172	±.0053	12	.2–.29	.22	±.0074	10	.3–.4	.342	±.0108	Miogypsina cushmani (with tendency to be an ex. interc. intermedia-cushmani)
12–.18	.146	±.0049	12	.17–.23	.203	±.0056	12	.25–.37	.302	±.009	Miogypsina intermedia (with a tendency to be an ex. interc. intermedia-cushmani)
08–.185	.15	±.008	13	.14–.27	.216	±.009	11	.20–.35	.306	±.011	
14–.2	.162	±.011	5	.15–.23	.202	±.014	5	.29–.4	.338	±.021	Miogypsina intermedia
13–.16	.147	±.006	4	.17–.23	.197	±.012	8	.26–.33	.30	±.008	Miogypsina intermedia (with a tendency to be an ex. interc. globulina-intermedia)
11–.18	.14	±.006	6	.13–.27	.215	±.02	10	.23–.38	.30	±.014	
12–.17	.144	±.006	8	.16–.22	.188	±.007	8	.24–.35	.298	±.010	
11–.14	.125	±.006	4	.12–.15	.14	±.007	4	.2–.26	.23	±.013	Miogypsina intermedia (ex interc. intermedia-globulina)

D_I (mm)			D_{II} (mm)				L_{I+II} (mm)				T_t (mm)			
R	M	σ_M	N	R	M	σ_M	N	R	M	σ_M	N	R	M	σ_M
1–.15	.12	±.002	22	.1–.16	.128	±.0035	25	.19–.26	.218	±.0038	6	.3–.5	.44	±.03
1–.155	.123	±.0028	19	.1–.16	.129	±.004	19	.195–.26	.227	±.0044	6	.4–.6	.51	±.03
11–.15	.131	±.008	3	.13–.145	.138	±.0044	3	.21–.26	.23	±.013	—	—	—	—

It appears from the above data that the difference between the various types of *M. complanata* s.l. is either usually or nearly always significant, whereas each type by itself includes forms whose maximum and minimum average values are insignificantly different. Subdivision into separate species would be quite possible (see also Papp, 1959).

(To be continued)

Plate I

Drawings of the embryonic-nepionic stage in median sections neglecting the stolons and the thicknesses of the walls.

Figs. 1–10, 21–26 about × 33, other figs. about × 30.

Figs. 1–10 *Miogypsina (Miogypsinoides) complanata* Schlumberger *mauretanica* Bronnimann from G. Gharra sample P 1349.

Figs. 11–20 *Miogypsina intermedia* Drooger showing some tendency towards *M.* ex. interc. *intermedia-cushmani* from G. Gharra sample P 1342.

Figs. 21–30 *Miogypsina cushmani* Vaughan showing some tendency towards *M.* ex. interc. *intermedia-cushmani* from G. Gharra sample P 1360.

Plate II

Miogypsina (Miogypsinoides) complanata Schlumberger *mauretanica* Bronnimann from Gebel Gharra.

Figs. 1–6, 9 about × 19; all other figs. × 32

From sample P 1349: Figs. 1–4, 6 external views; fig. 7 embryonic-nepionic apparatus; fig. 8 horizontal section in a microspheric form; figs. 10, 11 horizontal sections in macrospheric forms; fig. 13 vertical section.

From sample P 1347: Fig. 5 external view; fig. 9 horizontal section in a macrospheric form; fig. 12 vertical section.

Plate III

All figs. × 32, except fig. 3, × 36.

Miogypsina intermedia Drooger showing some tendency towards *M.* ex interc. *intermedia- cushmani*, from G. Gharra sample P 1342. Figs. 1,7 horizontal sections; figs. 10–12 embryonic-nepionic stages.

Miogypsina cushmani Vaughan with some tendency towards *M.* ex. interc. *intermedia-cushmani*, from G. Gharra sample P 1360. Figs. 3–6, 8, 9 embryonic-nepionic stages.

Miogypsina intermedia Drooger showing some tendency towards *M.* ex. interc. *globulina-intermedia* from G. Gushia sample FS 287. Fig. 2 horizontal section.

Plate IV

Figs. 2, 4, 5, × 24; all other figs. × 48

Miogypsina intermedia Drooger showing some tendency towards *M.* ex. interc. *globulina-intermedia* from G. Gushia. Fig. 1 embryonic-nepionic stage (sample FS 285); figs. 2, 6 horizontal sections (sample FS 287); figs. 3, 8, 9 embryonic-nepionic stages (sample FS 287).

Migypsina intermedia Drooger from Gebel Ataqa. Fig. 4 horizontal section (sample FS 473); figs. 5, 7 horizontal sections (sample FS 472); figs. 10–12 embryonic-nepionic stages (sample FS 473).

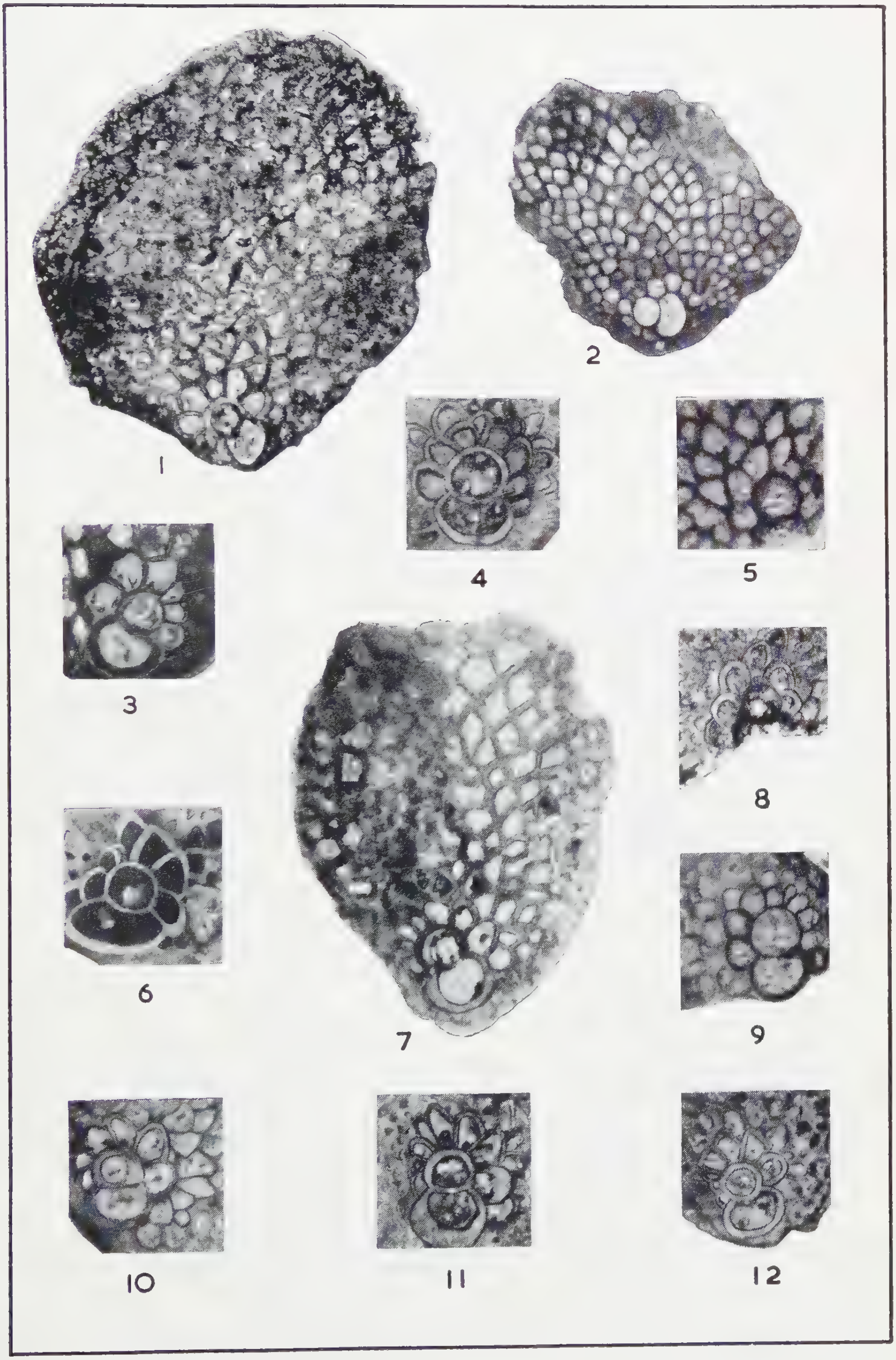
1
2
3
4
5
6
7
8
9
10
11
12

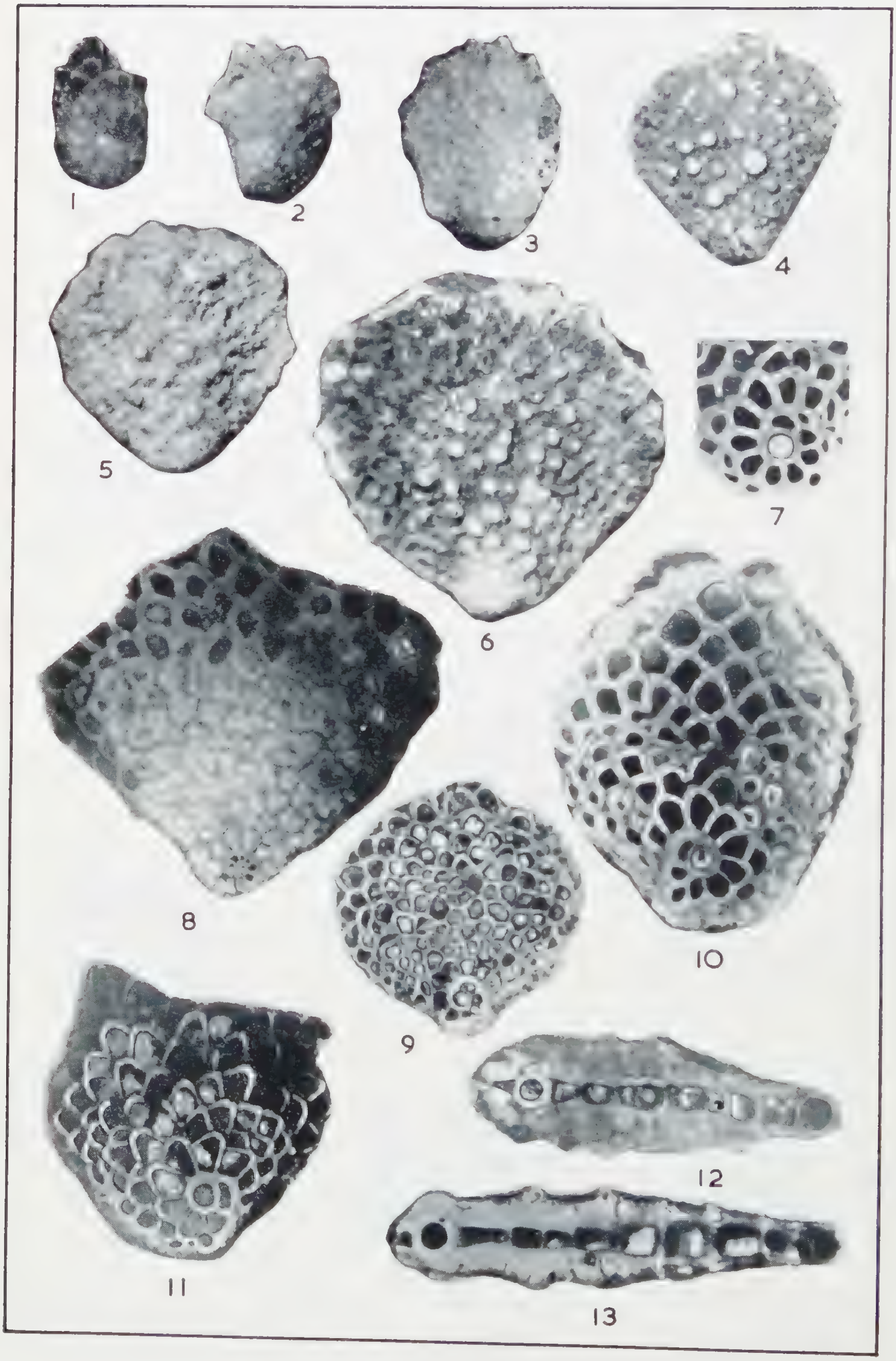
1
2
3
4
5
6
7
8
9
10
11
12
13

PLATE I

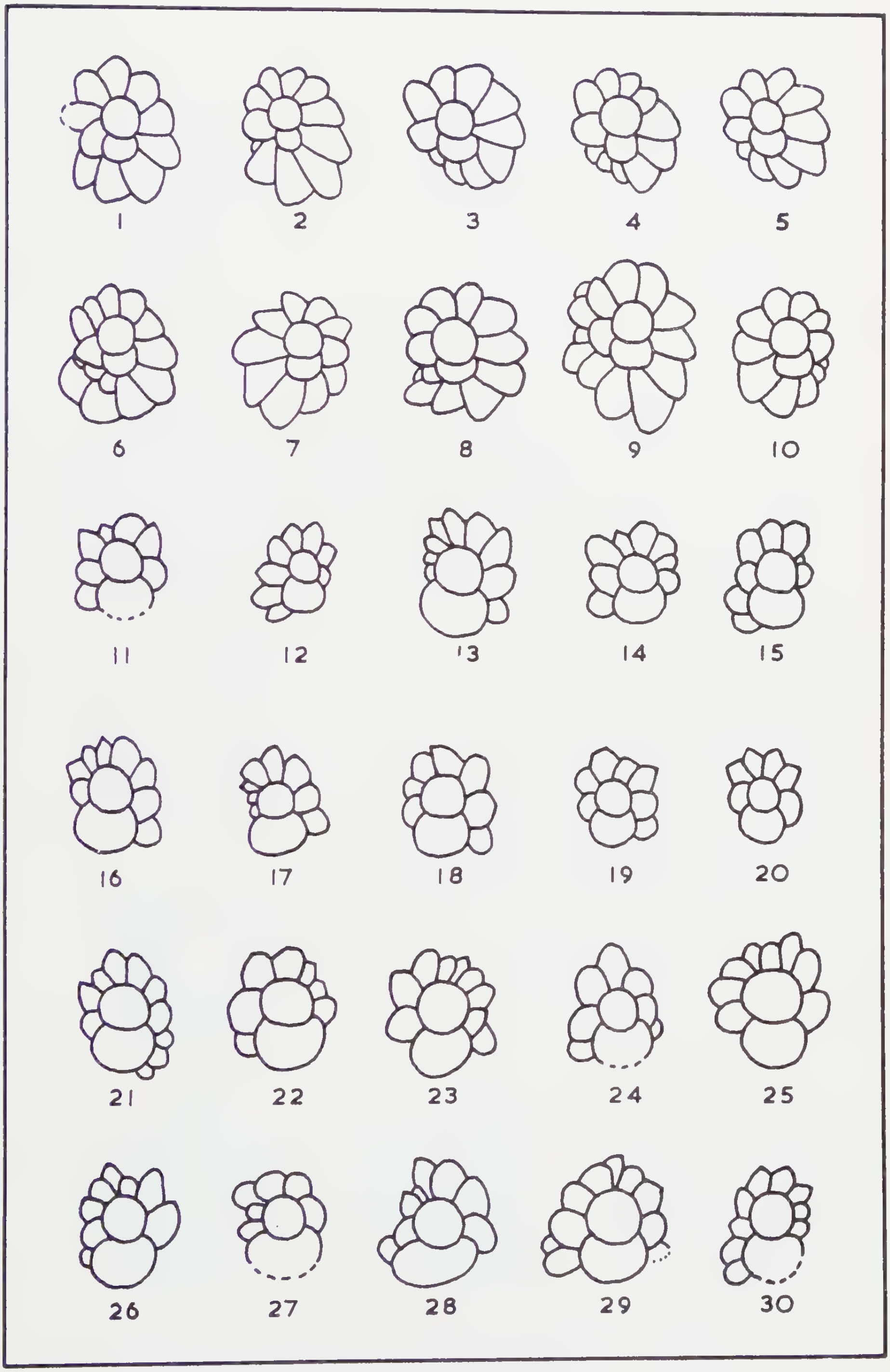
1
2
3
4
5
6
7
8
9
10
11
12
13
14
15
16
17
18
19
20
21
22
23
24
25
26
27
28
29
30

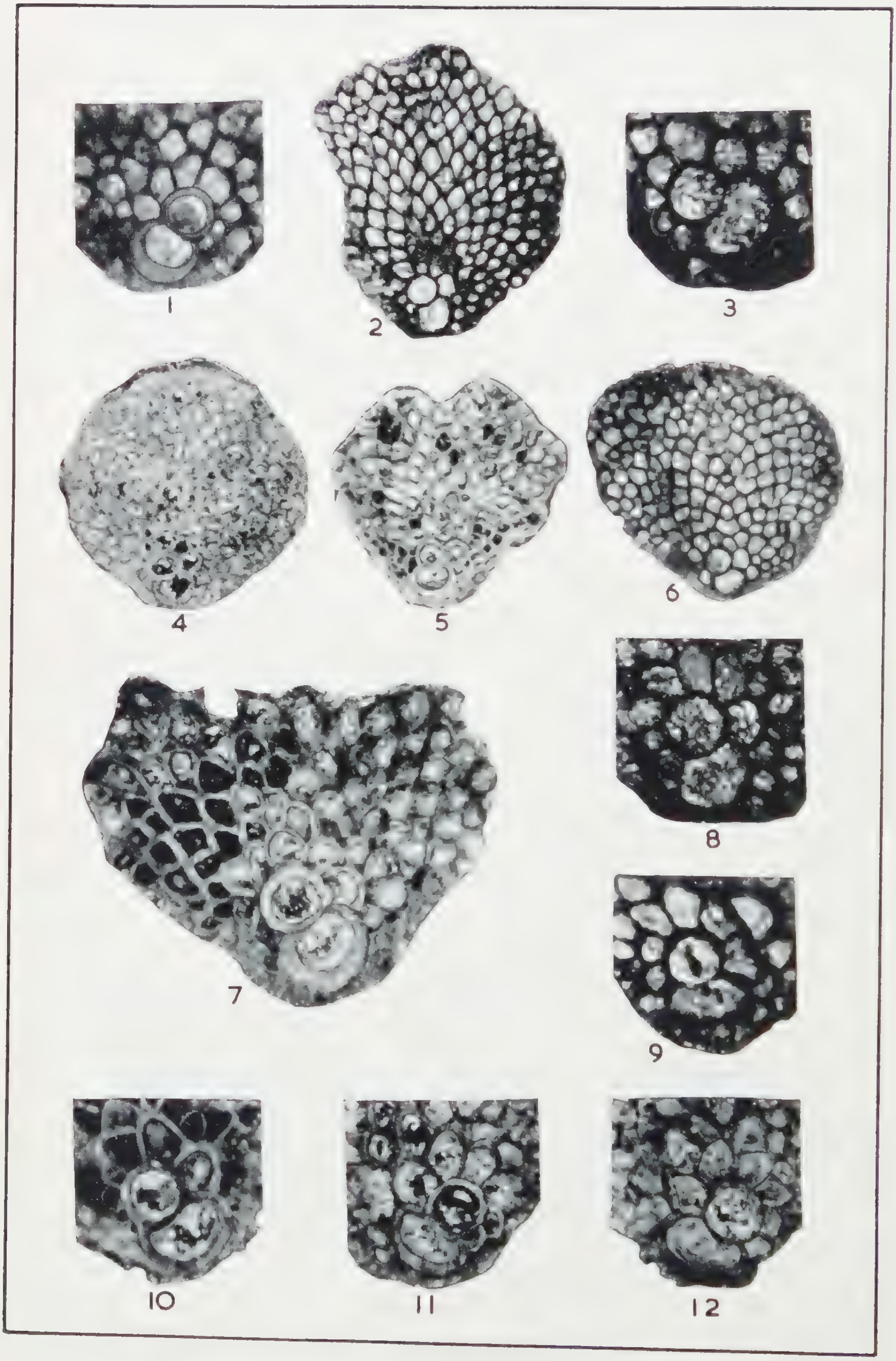
1
2
3
4
5
6
7
8
9
10
11
12

PALEONTOLOGY

CONTRIBUTION TO THE STUDY OF *MIOGYPSINA* s.l. FROM EGYPT. II

STATISTICAL INVESTIGATIONS

BY

F. J. SOUAYA

(Communicated by Prof. G. H. R. VON KOENIGSWALD at the meeting of June 24, 1961)

PRELIMINARY OBSERVATIONS

Besides the observed range (R), the arithmetic mean (M) and its standard error (σ_M) which are shown on tables 1 and 2, we also computed the standard deviation (σ) and its standard error (σ_σ) as well as the coefficient of variation (V) and its standard error (σ_V).

Amongst the characters investigated for the assemblages of *Miogypsina* s.s., the values γ and $200\alpha/\beta$ show consistently the highest coefficients of variation which have the following respective ranges: 26.43–142 with $R\sigma_V$: ± 5.6–$\pm 71.$– and 15.8–30.7 with $R\sigma_V$: ± 3.1–± 9.9. However, L_{I+II} followed by D_I, D_{II} and finally ε have usually relatively low coefficients of variation. Their respective ranges and those of their standard error are as follows: 6.66–15.3 with $R\sigma_V$: ± 2.09–± 4.4, 10.2–20 with $R\sigma_V$: ± 2.19–± 4.4, 9.65–22.7 with $R\sigma_V$: ± 1.97–± 6.6 and 5.8–22.5 with $R\sigma_V$: ± 1.56–± 7.9.

Although in statistic works coefficients of variation for pure or homogeneous samples are lower than the ones mentioned above, it is extremely important to realize first the limits of precision of this study before making any comment.

The determination of the degree of symmetry of the protoconchal spirals depends primarily on the recognition of the closing chamber. Although it is quite improbable that this chamber is an artifice of grinding because its genuine presence has been observed by various workers such as TAN SIN HOK, BRONNIMANN, DROOGER and the author himself, it remains, however, true that it is sometimes difficult to distinguish it for certain, and it may even become nearly impossible to recognize it at all. It follows that in certain cases a fairly high degree of inaccuracy in the absolute values of $200\alpha/\beta$ of certain individuals is liable to occur.

As for γ, the estimation requires as complete specimens as possible for the proper determination of the apical-frontal line. This condition could not always be fulfilled because of the material available. Besides,

it was sometimes impossible to draw a straight line through the apex, the middle of the frontal side and the centre of the proloculum. An approximation was then made for this apical-frontal line, thus introducing possible substantial errors in the absolute individual values of γ. Furthermore, whenever the two principal auxiliary chambers are of the same size or nearly so, the proper orientation and determination of γ is at least somewhat doubtful if not precluded, thereby accounting possibly for some additional error of estimation.

As for ε, which is here used as an expression of the position of the embryonic nepionic stage with reference to the periphery at the apex, it is sometimes difficult or even nearly impossible to choose a point which represents the apex accurately. Consequently, the distance ε measured may be inaccurate on account of the arbitrariness in making this choice. Besides, inconspicuous wearing of the test is a factor which has a non-determinable influence on the precision of the values of ε.

Apart from the abovementioned sources of error and the actual limits of precision set by the means used in making the various measurements, it was found that appreciable differences can be introduced whether the measurement of a certain characteristic such as D_I, D_{II}, L_{I+II} etc. . . ., is made on one side or the other of the thin sections.

Thus, on account of some subjectiveness in certain determinations and the practical difficulties of accurate observations caused by the thin sections, "the ways and means of measurement", it is only reasonable to expect inaccurate results, which should be interpreted with keen discernment. Consequently, all the abovementioned coefficients of variation should not be taken necessarily as an indication of impure samples and should not be considered either as translating only inherent differences in variability because the errors of observation, interpretation, approximation and measurements are appreciable, and may possibly be in certain cases, considerable.

Despite this serious inconvenience, it appears from this study in *Miogypsina* s.s. that taxonomic characters such as D_I and L_{I+II} which refer to the embryonic stages are important on account of their little variability within each species. This is particularly true for L_{I+II} in the case of *Miogypsina intermedia*, which shows a tendency towards *M. globulina* in Gebel Gushia where its value 0.30 mm is exactly the same in the samples FS 285, FS 286 and FS 287.

Besides, although $200 \times \beta$ and particularly γ have given high coefficients of variation, and while it is still desirable to develop a more refined technique to secure more accurate data than the ones here used, it remains true, however, that the arithmetic mean of $200 \times \beta$ increases with evolution and that it can still be maintained as an important specific character. As for γ, it seems to have a comparatively low arithmetic mean ranging for most samples only between 23° and 38° in the species which belong to the sequence of *M. intermedia*–*M. cushmani* (except sample P 1337).

Furthermore, the arithmetic means of L_{I+II}, D_I, and possibly γ, seem to show some increase in value with evolution.

With respect to *Miogypsinoides*, the characters investigated, viz.: X, γ, ε, D_I, D_{II}, L_{I+II} and T_t, have the following respective ranges for their coefficients of variation: 8.8–12.5 with $R\sigma_V$: ± 1.56–± 3.1; 5.0–14.7 with $R\sigma_V \pm 1.81$–± 3.3; 6.9–13.5 with $R\sigma_V \pm 1.6$–± 2.4; 9.1–12.2 with $R\sigma_V \pm 1.2$–± 4.3; 6.6–13.8 with $R\sigma_V \pm 1.97$–± 2.73; 8.6–10 with $R\sigma_V$: ± 1.23–± 4.1; and 15.8–18.4 with $R\sigma_V \pm 4.5$–± 5.3.

These coefficients of variation are, as a whole, fairly low, except possibly for the maximum thickness of the test (T_t) which is based on the measurements made on 5 or 6 specimens only.

Moreover, it is interesting to point out that the arithmetic means of all the characters measured are appreciably close.

FREQUENCY CURVES

Curves based on the theoretical and observed frequencies were drawn for all the characters studied in the various samples.

A number of comparative diagrams are shown on plates 3 and 4 to illustrate briefly some relationships and trends.

Thus, it may be observed that $200\alpha/\beta$, ε, D_I and, to a lesser extent L_{I+II}, tend to increase with evolution in the sequence of *Miogypsina* s.s. considered here.

Besides, the characters of *Miogypsinoides* in the samples statistically investigated are apparently closely related and would suggest the same population.

The comparison between the theoretical and observed frequency distributions obtained for the characters studied in the assemblages of *Miogypsina* s.s. and *Miogypsinoides* was made using the Chi Square Test (χ^2) although the number of specimens in both the classes and the samples was usually small. The various results obtained are shown in tables 3 and 4 respectively. Samples which did not lend themselves for the detailed analysis of a particular character on account of their small size, their fragmentary condition or their poor preservation, were not included in these tables.

From an examination of the results presented on table 3 for the *Miogypsina* s.s. samples, it appears that the small values of χ^2 obtained for the characters investigated in the samples shown, may well be considered to be due to the hazard of sampling, and that there is good agreement between the theoretical and the observed frequencies.

Besides, each of the sets of samples, those from G. Atâqa (FS 472–FS 473) and those from G. Gushia (FS 285–FS 287), might be considered to belong to a single population as it is suggested from χ^2 for some of the characters investigated.

As regards the samples of *Miogypsinoides*, the differences between the

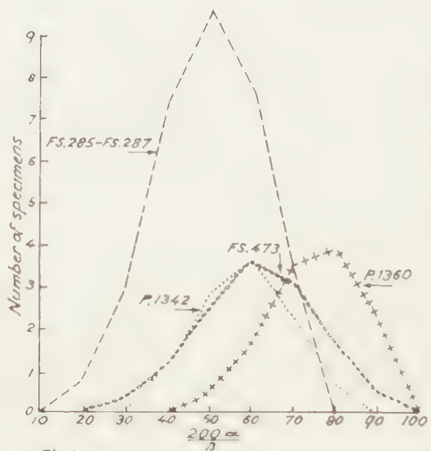

Fig. 1 COMPARATIVE DIAGRAM FOR THE CALCULATED FREQUENCY CURVES FOR 200α/β IN THE SAMPLES OF MIOGYPSINA S.S.

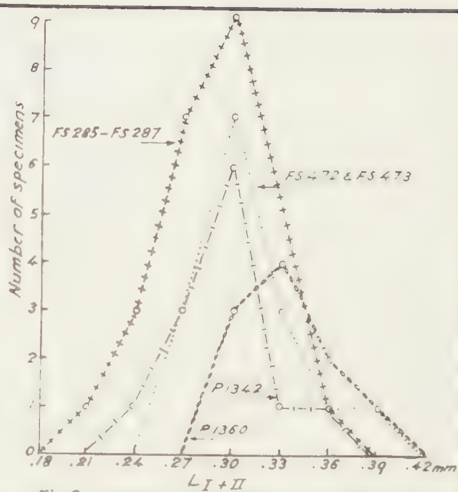

Fig. 2 COMPARATIVE DIAGRAM FOR THE OBSERVED FREQUENCY CURVES FOR L_{I+II} IN THE SAMPLES OF MIOGYPSINA S.S.

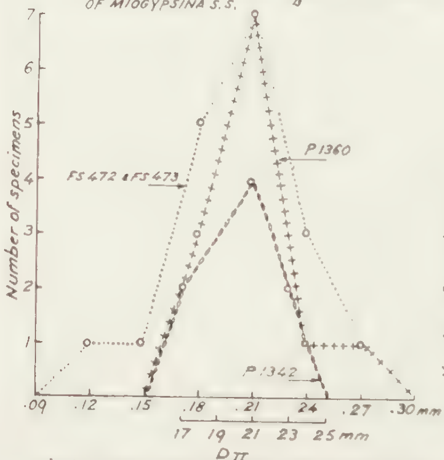

Fig 3 COMPARATIVE DIAGRAM FOR THE OBSERVED FREQUENCY CURVES FOR D_{II} IN THE SAMPLES OF MIOGYPSINA S.S.

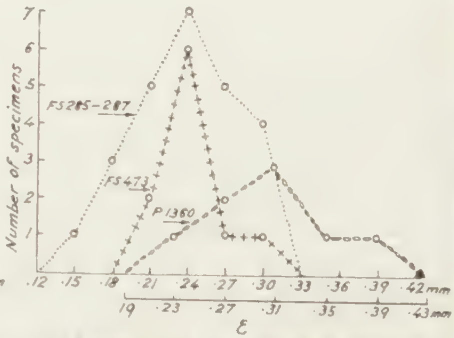

Fig 4 COMPARATIVE DIAGRAM FOR THE OBSERVED FREQUENCY CURVES FOR ε IN THE SAMPLES OF MIOGYPSINA S.S.

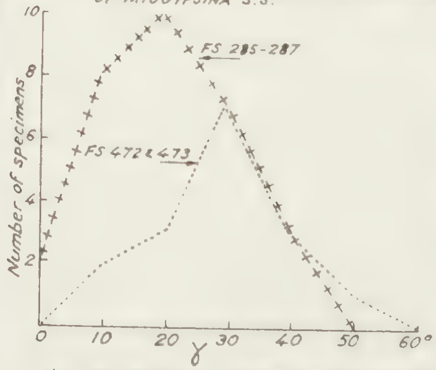

Fig 5 COMPARATIVE DIAGRAM FOR THE OBSERVED FREQUENCY CURVES FOR γ IN G GUSHIA AND G. ATAQA.

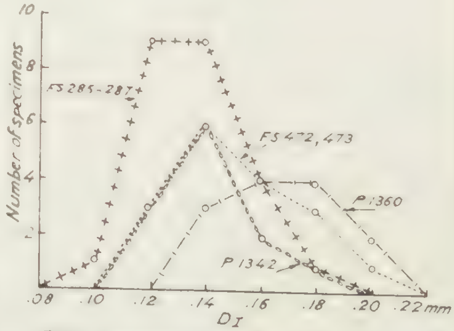

Fig 6 COMPARATIVE DIAGRAM FOR THE OBSERVED FREQUENCY CURVES FOR D_I IN THE SAMPLES OF MIOGYPSINA S.S.

PLATE 3

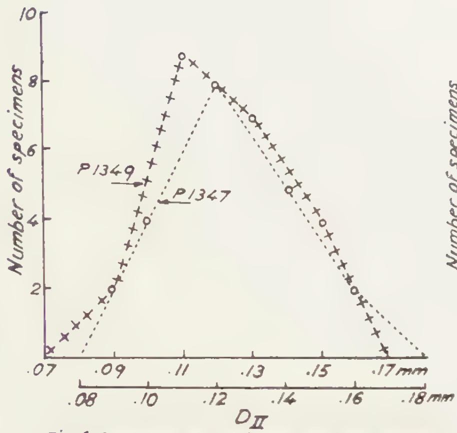

Fig. 1 COMPARATIVE DIAGRAM FOR THE OBSERVED FREQUENCY CURVES FOR D_{II} IN THE SAMPLES OF MIOGYPSINOIDES.

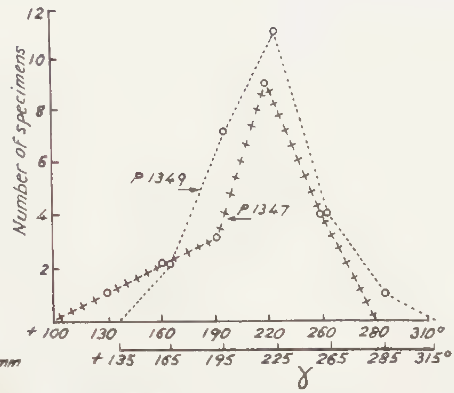

Fig. 2 COMPARATIVE DIAGRAM FOR THE OBSERVED FREQUENCY CURVES FOR γ IN THE SAMPLES OF MIOGYPSINOIDES.

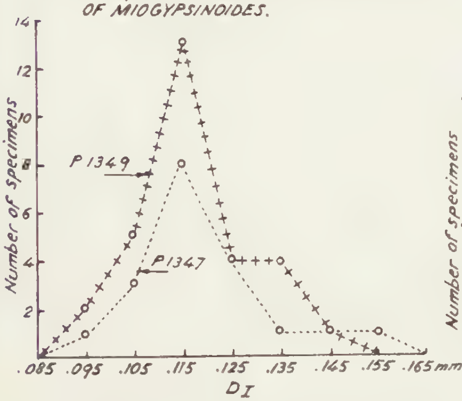

Fig. 3 COMPARATIVE DIAGRAM FOR THE OBSERVED FREQUENCY CURVES FOR D_I IN THE SAMPLES OF MIOGYPSINOIDES.

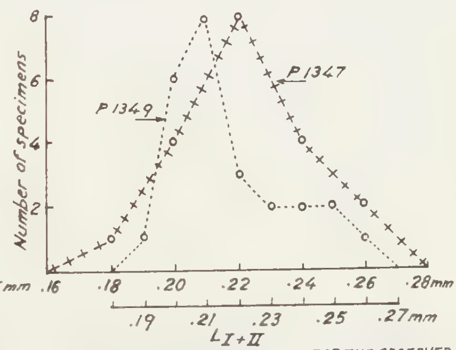

Fig. 4 COMPARATIVE DIAGRAM FOR THE OBSERVED FREQUENCY CURVES FOR L_{I+II} IN THE SAMPLES OF MIOGYPSINOIDES.

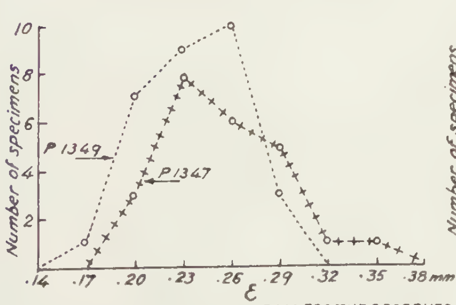

Fig. 5 COMPARATIVE DIAGRAM FOR THE OBSERVED FREQUENCY CURVES FOR ε IN THE SAMPLES OF MIOGYPSINOIDES.

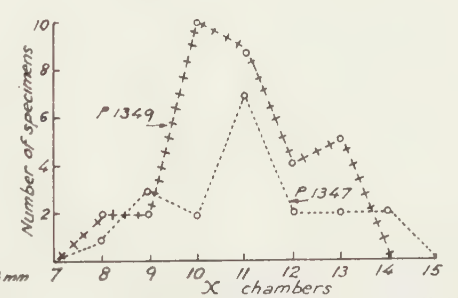

Fig. 6 COMPARATIVE DIAGRAM FOR THE OBSERVED FREQUENCY CURVES FOR X IN THE SAMPLES OF MIOGYPSINOIDES.

PLATE 4

TABLE 3

Comparison of the distributions of the *Miogypsina* s.s. samples

Character	Pl.	Fig.	Sample	N	Class Interval	v	χ^2	P
$200\alpha/\beta$	3	1	P 1360	13	10	2	0.98	$\neq$0.61
			P 1342	11	10	2	3.55	0.14–0.22
			FS 473	13	10	4	4.8	$\neq$0.3
			FS 285–287	33	10	3	6.26	$\neq$0.10
			FS 287	10	10	2	4.71	$\neq$0.10
			FS 286	15	10	3	5.61	0.10–0.20
γ	3	5	FS 473	11	10°	2	5.4	.05– .08
			FS 472–473	15	10	2	6.6	.05– .08
			FS 285–287	30	10	2	5.4	.05– .08
ε	3	4	P 1360	8	.04 mm	2	1.31	$\neq$0.5
			FS 473	10	.03	1	4.1	$\neq$0.05
			FS 285–287	25	.03	3	2.12	$\neq$0.5
D_{I}	3	6	P 1360	13	.02 mm	1	3.0	.08
			P 1342	12	.02	1	1.8	$\neq$ .20
			FS 472–473	17	.02	2	2.9	$\neq$ .20
			FS 285–287	24	.02	2	2.2	$\neq$ .30
D_{II}	3	3	P 1360	12	.03 mm	1	3.99	$\neq$ .05
			P 1342	12	.02	1	0.62	.40– .50
			FS 472–473	18	.03	3	5.08	.17
L_{I+II}	3	2	P 1360	10	.03 mm	1	1.62	.20– .30
			P 1342	12	.03	2	2.07	$\neq$ .37
			FS 472–473	15	.03	2	5.88	$\neq$ .05
			FS 285–287	26	.03	3	3.18	.30– .40

TABLE 4

Comparison of the distributions of the *Miogypsinoides* samples of G. Gharra

Character	Pl.	Fig.	Sample	N	Class Interval	v	χ^2	P
X	4	6	P 1349	32	1 ch.	3	4.5	0.2
			P 1347	19	1	4	4.73	0.3
γ	4	2	P 1349	25	30°	2	5.09	.08
			P 1347	19	30	2	6.6	.05– .03
ε	4	5	P 1349	30	.03 mm	2	2.27	$\neq$ .3
			P 1347	24	.03	3	3.96	$\neq$ .26
D_{I}	4	3	P 1349	29	.01 mm	3	6.10	$\neq$ .10
			P 1347	19	.01	4	6.94	$\neq$ .14
D_{II}	4	1	P 1349	22	.02 mm	1	3.50	.05– .10
			P 1347	19	.02	1	1.55	$\neq$ .20
L_{I+II}	4	4	P 1349	25	.01 mm	5	7.92	$\neq$ .16
			P 1347	19	.02	2	1.51	$\neq$ .5

v = degrees of freedom.
χ^2 = quadratic contingence.
P = probability ("seuil de signification").

observed and theoretical frequencies for all the characters studied and shown in table 4, are insignificant, except for the character γ in sample P 1347 where this difference may be significant. This divergence may be explained by the fact that the latter sample includes a number of approximate values on account of some incomplete specimens, the apical-frontal line of which is liable to be inaccurate.

CORRELATION AND REGRESSION

Numerous scatter diagrams were plotted in order to investigate the relations between the various characters studied. However, only those which show significant correlations are shown in plates 5–9. As for the numerical results they are shown in tables 5 and 6.

It is evident that in the *Miogypsina* s.s. samples, there is positive correlation, which may be fairly or highly significant for $D_I \cdot D_{II}$, $D_I \cdot \varepsilon$, $200\alpha/\beta \cdot L_{I+II}$ and $200\alpha/\beta \cdot \varepsilon$. In certain cases, however, this correlation,

TABLE 5

The coefficients of correlation and regression for some characters in the *Miogypsina* s.s. samples

Characters Y·X	Pl.	Fig.	Sample	N	r	R_e	R_1	R_2	P	b_{yx}	S_y
$D_I \cdot D_{II}$	5	3	P 1360	13	+.57	+.554	+.03	+.853	>.02	+.419	.014
	5	4	P 1342	13	+.36	+.347	−.245	+.758	>.05	+.36	.017
	5	1	FS 472–473	18	+.51	+.499	+.057	+.789	>.02	+.403	.023
	5	2	FS 285–287	17	+.778	+.7685	+.474	+.916	<.001	+.6045	.016
$D_I \cdot \varepsilon$	5	6	P 1360	8	+.70	+.675	−.011	+.935	>.02	+.270	.013
	5	5	P 1342	11	+.85	+.835	+.50	+.959	<.01	+.387	.009
	6	1	FS 472–473	15	+.56	+.55	+.066	+.833	=.02	+.246	.016
	6	2	FS 285–287	18	+.69	+.68	+.336	+.874	<.001	+.276	.012
$D_I \cdot 200\alpha/\beta$			P 1360	13	+.37	+.357	−.245	+.757	>.05	+.0017	.016
			FS 472–473	17	+.32	+.29	−.19	+.691	>.05	+.0015	.018
$200\alpha/\beta \cdot L_{I+II}$	6	3	P 1360	10	+.72	+.701	+.159	+.929	<.01	+275.54	8.556
	6	6	P 1342	11	+.40	+.384	−.263	+.804	>.05	+181.24	9.318
	6	5	FS 473–472	15	+.51	+.497	−.003	+.810	<.05	+447.2	12.04
			FS 473	10	+.11	+.104	−.558	+.691	>.05	+ 66.—	11.88
	6	4	FS 472	5	+.83	+.798	−.197	+.989	=.02	+326.44	9.13
			FS 287	8	+.12	+.116	−.641	+.762	>.05	+ 60.9	10.99
			FS 285–287	29	−.23	−.226	−.545	+.158	>.05	− 89.86	12.32
$200\alpha/\beta \cdot \varepsilon$	7	3	P 1360	8	+.666	+.639	−.066	+.932	>.02	+161.97	8.66
			P 1342	4	+.21	+.176	−.94	+.974	>.05	+ 73.1	16.10
	7	2	FS 472–473	15	+.57	+.556	+.084	+.838	<.02	+178.52	11.48
			FS 285–287	27	−.10	−.098	−.462	+.291	>.05		
$200\alpha/\beta \cdot \gamma$	7	6	P 1342	9	+.60	+.576	−.105	+.904	=.05	+.714	9.04
			FS 472–473	15	+.40	+.388	−.149	+.758	>.05	+.37	9.19
	7	5	FS 285–287	31	+.37	+.356	+.019	+.640	<.05	+.347	12.91

See note on table 6

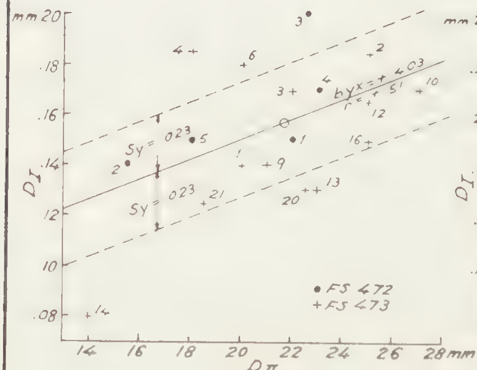

Fig. 1 D_I / D_{II} RELATIONSHIP IN SAMPLES FS 472 AND FS 473.

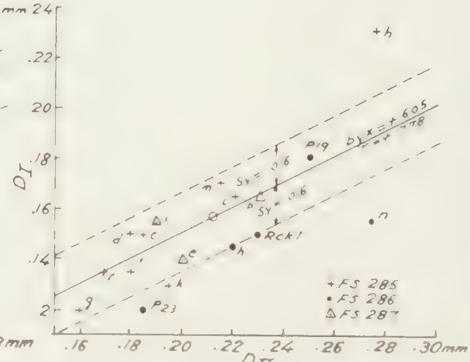

Fig. 2 D_I / D_{II} RELATIONSHIP IN SAMPLES FS 285 TO FS 287.

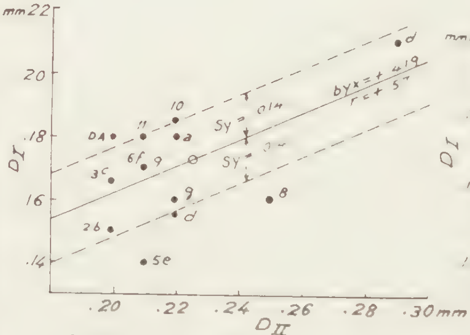

Fig. 3 D_I / D_{II} RELATIONSHIP IN SAMPLE P 1360.

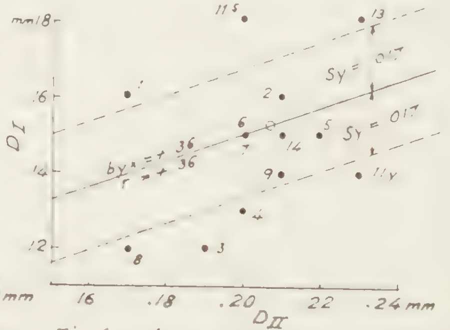

Fig. 4 D_I / D_{II} RELATIONSHIP IN SAMPLE P 1342.

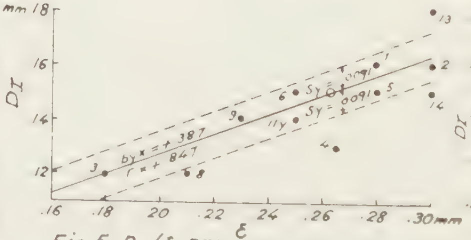

Fig. 5 $D_I / \mathcal{E}$ RELATIONSHIP IN SAMPLE P 1342

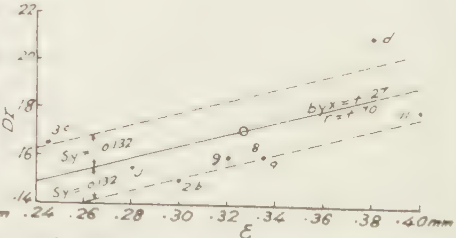

Fig. 6 $D_I / \mathcal{E}$ RELATIONSHIP IN SAMPLE P 1360.

PLATE 5

although appreciable, is insignificant as may be seen from the accompanying table. Besides, the samples from G. Gushia gave, in contrast with the other samples, negative values for the correlation of $200\alpha/\beta \cdot L_{I+II}$ and $200\alpha/\beta \cdot \varepsilon$. This deviation from the general tendency of positive correlation between these characters as exhibited by most of the samples examined, is however, statistically insignificant and may possibly be explained by the presence in the samples of G. Gushia, of some inaccurate values of $200\alpha/\beta$ on account of the fairly poor state of preservation of the *Miogypsina* assemblage.

In addition, it may be worth pointing out here the appreciable but insignificant or little significant positive correlations existing between $200\alpha/\beta \cdot D_I$ and $200\alpha/\beta \cdot \gamma$.

On account of the fairly broad security intervals (R_1 R_2) most of the abovementioned correlations give little reliable information about the correlation in the population except for some particular cases as in G. Gushia samples for $D_I \cdot D_{II}$ and $D_I \cdot \varepsilon$.

TABLE 6

The coefficients of correlation and regression for some characters in the *Miogypsinoides* samples

Characters Y·X	Pl.	Fig.	Sample	N	r	R_e	R_1	R_2	P	b_{yx}	S_y
$D_I \cdot L_t$			P 1349	18	−.24	−.233	−.629	+.254	>.05		
			P 1347	17	+.14	+.136	−.362	+.578	>.05		
$D_I \cdot D_{II}$	7	4	P 1349	19	+.76	+.75	+.47	+.903	<.001	+.517	.0080
	8	4	P 1347	19	+.65	+.64	+.28	+.853	>.001	+.395	.0085
$D_I \cdot L_{I+II}$	8	5	P 1349	22	+.788	+.781	+.548	+.888	<.001	+.5256	.0072
	8	3	P 1347	19	+.656	+.646	+.282	+.855	<.01	+.366	.0087
$D_I \cdot L_eW_e$	8	2	P 1349	29	+.48	+.474	+.142	+.716	<.01	+.2352	.0108
	8	1	P 1347	19	+.51	+.50	+.073	+.782	<.02	+.2346	.0095
$\varepsilon \cdot D_I$			P 1349	28	+.19	+.1856	−.197	+.522	>.05		
			P 1347	18	+.03	+.029	−.438	+.484	>.05		
$\gamma \cdot D_I$	9	1	P 1349	25	+.42	+.41	+.031	+.72	>.02	+1097.9	27.—
	9	2	P 1347	19	+.55	+.54	+.129	+.80	=.01	+1650	27.6
$D_I \cdot X$			P 1349	29	−.129	−.127	−.469	+.246	>.05	−.0017	.0122
	8	6	P 1347	19	−.55	−.54	−.803	−.127	=.01	−.0037	.0093
$\gamma \cdot X$	9	3	P 1349	26	−.52	−.51	−.756	−.165	<.01	−11.37	24.91
	9	4	P 1347	19	−.62	−.61	−.804	−.131	<.01	−12.92	26.68

N = number of specimens
r = coefficient of correlation
R_e = approximate coefficient of correlation of the population
R_1, R_2 = lower and upper limits of the interval of security
P = probability
b_{yx} = coefficient of regression (of Y on X)
S_y = standard error of estimate for Y.

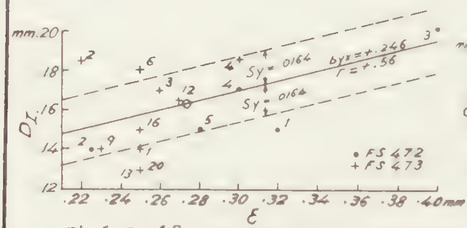

Fig. 1 $D_I/\mathcal{E}$ RELATIONSHIP IN SAMPLES FS 472 AND FS 473.

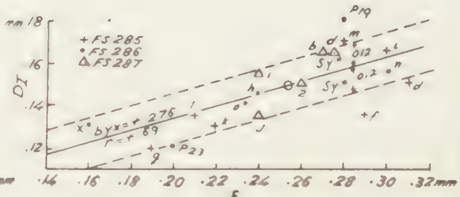

Fig. 2 $D_I/\mathcal{E}$ RELATIONSHIP IN SAMPLES FS 285 TO FS 287

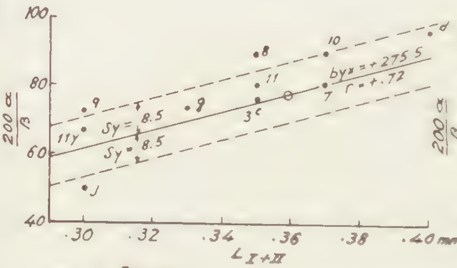

Fig. 3 $\frac{200\alpha}{\beta}/L_{I+II}$ RELATIONSHIP IN SAMPLE P 1360.

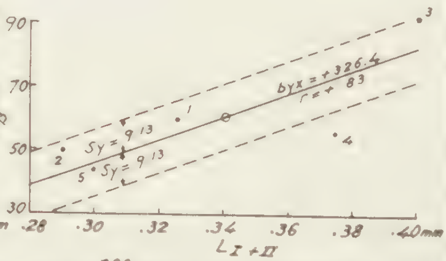

Fig. 4 $\frac{200\alpha}{\beta}/L_{I+II}$ RELATIONSHIP IN SAMPLE FS 472.

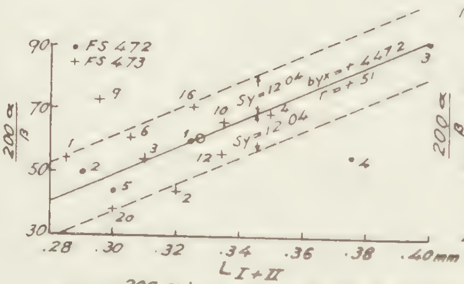

Fig. 5 $\frac{200\alpha}{\beta}/L_{I+II}$ RELATIONSHIP IN SAMPLES FS 472 AND FS 473.

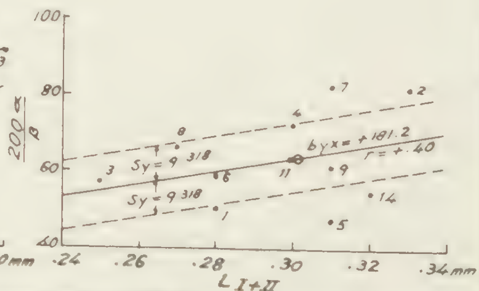

Fig 6 $\frac{200\alpha}{\beta}/L_{I+II}$ RELATIONSHIP IN SAMPLE P 1342.

PLATE 6

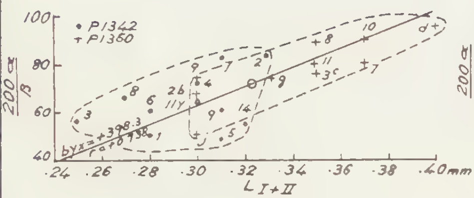

Fig. 1 $\frac{200\alpha}{\beta} / L_{I+II}$ RELATIONSHIP IN SAMPLES P1342 AND P1360.

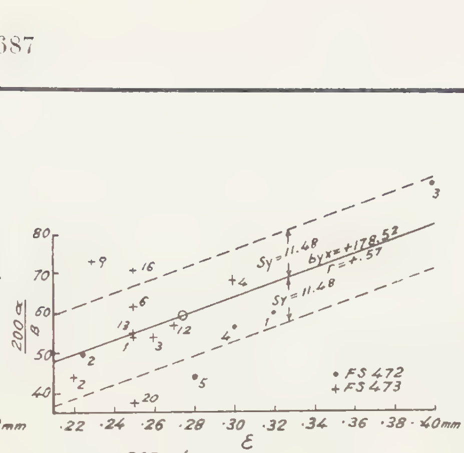

Fig. 2 $\frac{200\alpha}{\beta} / \varepsilon$ RELATIONSHIP IN SAMPLES FS 472 AND FS 473.

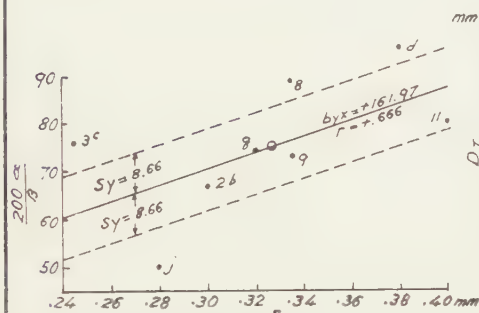

Fig. 3 $\frac{200\alpha}{\beta} / \varepsilon$ RELATIONSHIP IN SAMPLE P1360.

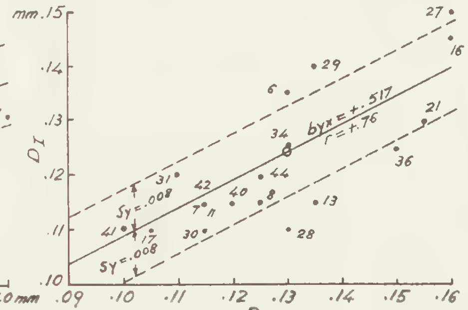

Fig. 4 D_I / D_{II} RELATIONSHIP IN SAMPLE P1349.

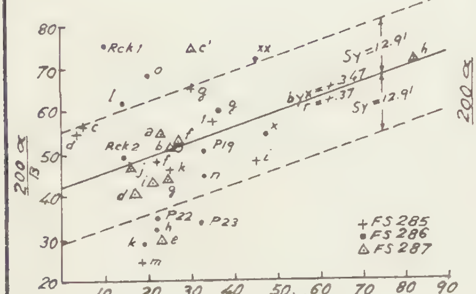

Fig. 5 $\frac{200\alpha}{\beta} / \gamma$ RELATIONSHIP IN SAMPLES FS 285 TO 287.

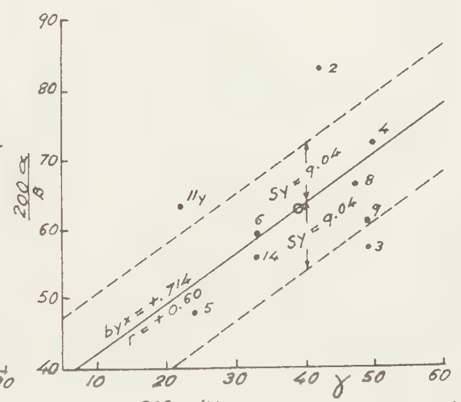

Fig. 6 $\frac{200\alpha}{\beta} / \gamma$ RELATIONSHIP IN SAMPLE P1342.

PLATE 7

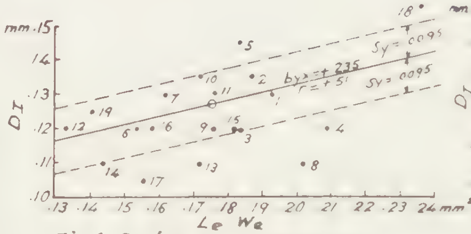

Fig. 1 D_I / $L_e W_e$ RELATIONSHIP IN SAMPLE P 1347.

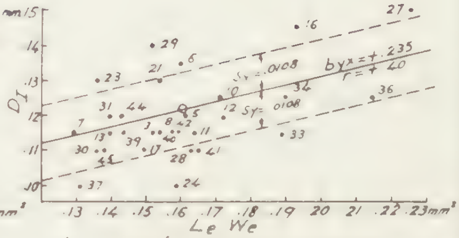

Fig. 2 D_I / $L_e W_e$ RELATIONSHIP IN SAMPLE P 1349

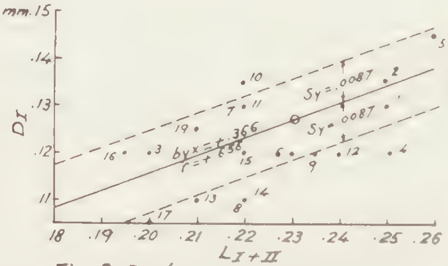

Fig. 3 D_I / L_{I+II} RELATIONSHIP IN SAMPLE P 1347.

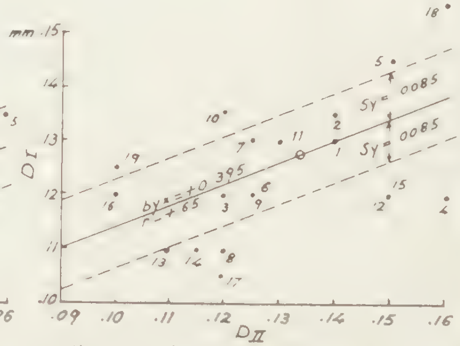

Fig. 4 D_I / D_{II} RELATIONSHIP IN SAMPLE P 1347.

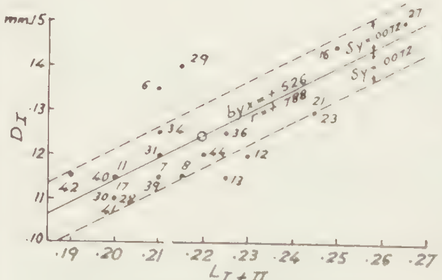

Fig. 5 D_I / L_{I+II} RELATIONSHIP IN SAMPLE P 1349.

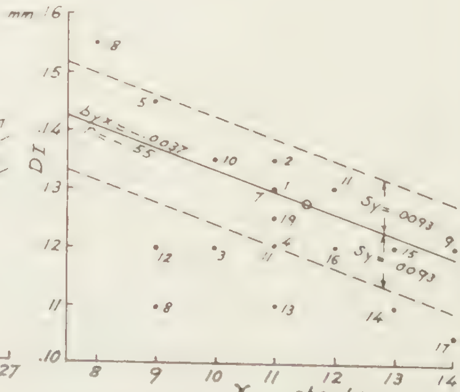

Fig. 6 D_I / X RELATIONSHIP IN SAMPLE P 1347.

PLATE 8

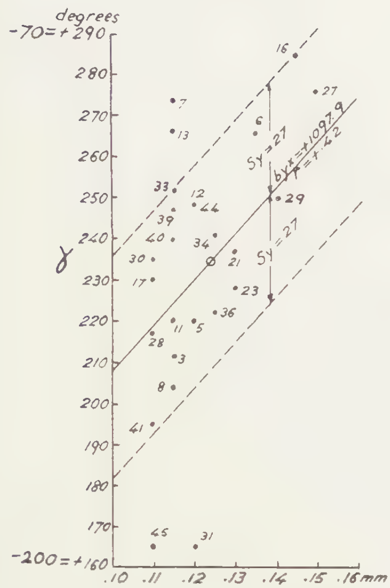

Fig. 1 γ/D_I RELATIONSHIP IN SAMPLE P1349.

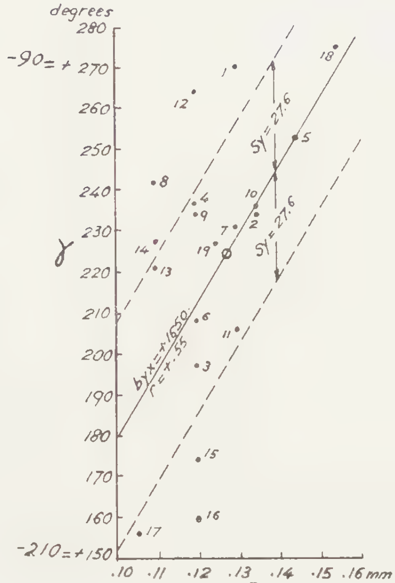

Fig. 2 γ/D_I RELATIONSHIP IN SAMPLE P1347.

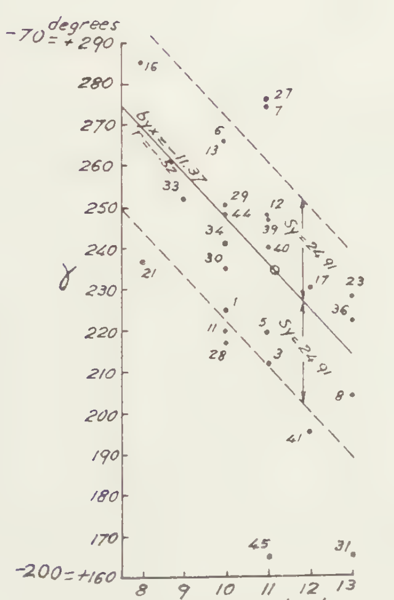

Fig. 3 γ/X RELATIONSHIP IN SAMPLE P1349.

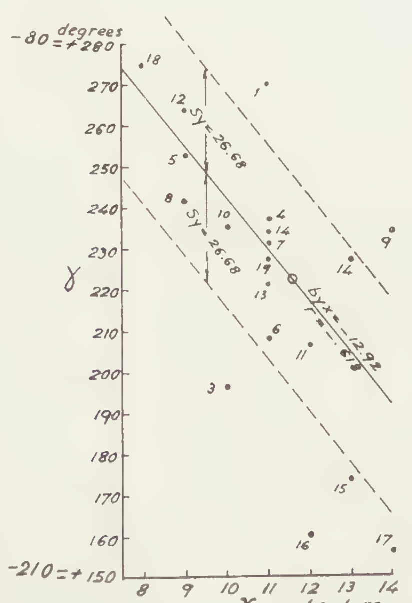

Fig. 4 γ/X RELATIONSHIP IN SAMPLE P1347.

PLATE 9

As regards the samples of *Miogypsinoides* investigated, it is apparent that significant positive correlations exist for $D_I \cdot D_{II}$, $D_I \cdot L_{I+II}$, $D_I \cdot L_eW_e$ and $\gamma \cdot D_I$. There is also for $\varepsilon \cdot D_I$, some positive correlation, which is, however, insignificant. As ε includes approximately $\frac{1}{2}$ D_I, this correlation would probably have been more evident if the determination of D_I and particularly ε, had been more accurate.

Moreover, it is interesting to note the significant negative correlations existing for $D_I \cdot X$ and $\gamma \cdot X$.

As for the relation between D_I and L_t, it proved to be of no significance.

From the values of R_1 R_2 presented in table 6, it may be inferred that the correlations obtained for $D_I \cdot D_{II}$ and $D_I \cdot L_{I+II}$ give an indication from fair to good about the correlation in the population; in the case of $D_I \cdot L_eW_e$, $\gamma \cdot D_I$ and $\gamma \cdot X$, this indication is, however, rather slight.

COMPARISON OF THE ARITHMETIC MEANS

Various comparisons were made between the arithmetic means of the characters investigated in the samples of *Miogypsina* s.s. and *Miogypsinoides*, in order to evaluate statistically the existing similarities and differences. The results obtained are shown in tables 7 and 8.

It is evident that there is no significant difference between the maximum and minimum means of ε, D_I, D_{II} and L_{I+II} in the samples identified as *Miogypsina intermedia* (excluding P 1337). However, in this series there exists a difference which is rather significant between the maximum and minimum values of the means of γ and $200\alpha/\beta$: this difference may be somewhat influenced by the approximate evaluation of these characters and may as well translate the tendencies which are shown by the end members of this group, namely to *Miogypsina cushmani* and *M. globulina*.

As for the *Miogypsina* s.s. sample P 1337 which lies just at the border line between *M. intermedia* and *M. globulina*, its mean values for $200\alpha/\beta$ and D_I are not significantly different from the low values of the above considered group of samples. However, they are somewhat significantly different ($P > .02$) from the high values. In the case of ε, the closest values of these samples are sometimes significantly different from those of P 1337, whereas their highest values are nearly always significantly different. As for γ, L_{I+II} and D_{II}, their means in P 1337, are different from those of the other samples identified as *M. intermedia*. This may be expected on account of sample P 1337 representing possibly the extreme variation of the *Miogypsina intermedia* species.

It may also be interesting to point out that there is no significant difference between the arithmetic means of all characters investigated in the samples of G. Atâqa as well as in those of G. Gushia: a fact which suggests that each set of samples belongs to a single homogeneous population.

As for the differences between the arithmetic means of *Miogypsina*

cushmani and the nearest corresponding values obtained for *M. intermedia* in the samples examined, it appears that in the case of $200\alpha/\beta$, ε and L_{I+II}, this difference is significant and may lend support to the identification of these two species. However, such a difference is insignificant for D_I and D_{II}. As for γ, it is well to point out that in the sample P 1360 which has been identified as *Miogypsina cushmani*, the mean value of this character falls within the range of the mean values of γ of the group of samples identified as *M. intermedia*.

As regards the samples of *Miogypsinoides*, they probably all belong to the same homogeneous population of *Miogypsinoides complanata mauretanica*, since there is no significant difference between the average

TABLE 7

Comparison of the arithmetic means of some characters in the *Miogypsina* s.s. samples

Char.	Locality	Sample	Determination	M	N	t	d/σ_d	P
$200\alpha/\beta$	G. Garra	P 1360	M. cushmani	76.9	13		2.72	=.007
		P 1342	M. intermedia	63.4	11			
	G. Garra	P 1342	M. intermedia	63.4	11		2.32	>.02
	G. Gushia	FS 285	M. intermedia	50.1	8			
	G. Atâqa	FS 472	M. intermedia	60.5	5	0.19		>.1
		FS 473	M. intermedia	62.1	13			
	G. Gushia	FS 285	M. intermedia	50.1	8	0.14		>.1
		FS 287	M. intermedia	51.—	10			
γ	G. Garra	P 1342	M. intermedia	37.9°	11	2.42		>.02
	G. Gushia	FS 285	M. intermedia	23.1	8			
	G. Atâqa	FS 472	M. intermedia	25.7°	4	1.8		=.10
		FS 473	M. intermedia	35.4	11			
	G. Gushia	FS 285	M. intermedia	23.1°	8	0.66		>.10
		FS 287	M. intermedia	28.8	10			
ε	G. Garra	P 1360	M. cushmani	.32 mm	8		2.57	=.01
	G. Atâqa	FS 472–473	M. intermedia	.27	15			
	G. Atâqa	FS 472–473	M. intermedia	.27 mm	15	1.69		<.10
	G. Gushia	FS 286	M. intermedia	.24	10			
D_I	G. Garra	P 1360	M. cushmani	.17 mm	13	0.9		>.10
	G. Atâqa	FS 472	M. intermedia	.16	5			
	G. Atâqa	FS 472	M. intermedia	.16 mm	5	1.79		≠.10
	G. Gushia	FS 286	M. intermedia	.14	9			
D_{II}	G. Garra	P 1360	M. cushmani	.22 mm	12		1.2	>.10
		FS 473	M. intermedia	.216	13			
	G. Atâqa	FS 473	M. intermedia	.216 mm	13	2.1		≠.05
	G. Gushia	FS 285	M. intermedia	.188	8			
L_{I+II}	G. Garra	P 1360	M. cushmani	.342 mm	10		2.9	.04
	G. Atâqa	FS 472–473	M. intermedia	.316	16			
	G. Atâqa	FS 472–473	M. intermedia	.316 mm	16		1.	>.10
	G. Gushia	FS 286	M. intermedia	.30	10			

See note on table 8.

values of all characters in the various samples investigated, except possibly for the maximum difference of $M\varepsilon$ which is just on the border of significance.

TABLE 8

Comparison of the arithmetic means of some characters in the samples of *Miogypsina* (*Miogypsinoides*) *complanata* SCHLUMBERGER *mauretanica* BRONNIMANN

Character	Locality	Sample	M	N	t	d/σ_d	P
X	G. Gharra	P 1347	11.1	19	0.39		>.1
		P 1337	10.7	4			
γ	G. Gharra	P 1347	— 136°	19		0.96	
		P 1349	— 127	25			
ε	G. Gharra	P 1337	.245 mm	4			
		P 1347	.262	24		1.	
		P 1349	.244	30		2.1	
D_I	G. Gharra	P 1347	.123 mm	19			
		P 1349	.12	29		0.90	
		P 1337	.131	4		1.78	
D_{II}	G. Gharra	P 1347	.129 mm	19			
		P 1349	.128	22	0.18	0.19	
		P 1337	.138	3	0.98	1.0	
L_{I+II}	G. Gharra	P 1347	.227 mm	19			
		P 1349	.218	25	1.51	1.55	
		P 1337	.23	3	0.96	1.09	

M = mean t = the Gosset's parameter
d = difference between the means
σ_d = standard error of the difference between the means.

COMPARISON OF THE VARIANCES

Comparison was made between the variances of the characters investigated in the various samples. Some of the results are shown on tables 9 and 10.

From table 9, it appears that a comparison between the maximum and minimum variances for the characters $200\times\beta$, D_I and L_{I+II} in the samples identified as *Miogypsina intermedia* resulted in values for F lower than the corresponding Snedecor's F for P = 0.05. This indicates that there is little divergence between these samples and permits the hypothesis that all these samples as far as the variance of all these characters are concerned, may belong to the same population.

Still considering the samples identified as *Miogypsina intermedia*, there is also some significant divergence which is not very high, between the variances of the samples P 1342 and FS 473 for the character D_{II}. For γ a similar conclusion can be drawn for samples P 1337 and FS 472-473, and as to ε for FS 287 and P 1337.

Not much importance, however, should be given now to ε and its variance, since their evaluation implies a certain degree of inaccuracy which may engender erroneous interpretation.

As regards the variances of the various characters investigated in sample P 1360 identified as *Miogypsina cushmani*, it appears that they may fall in the range of variation of the variances of the group of samples identified as *M. intermedia*, as it is the case for the characters $200\alpha/\beta$, D_I and D_{II} or show insignificant difference from them as for L_{I+II}. In the case of γ and ε, however, significant divergence exists between their variance in P 1360 and at least some of the samples of *M. intermedia*. Although this should be considered with some caution as γ in sample P 1360 was estimated from fairly incomplete specimens and ε may involve some error of approximation, it remains worth-while pointing this out.

TABLE 9

Comparison of the variances of some characters in the *Miogypsina* s.s. samples

Char.	Sample	Identification	N	σ^2	Σ^2	F	Snedecor's F P=.05	Snedecor's F P=.01
$200\alpha/\beta$	P 1360	M. cushmani	13	148.35	160.22			
	P 1342	M. intermedia	11	134.79	148.27	1.08	2.91	
	FS 472	M. intermedia	5	345.96	432.96	2.91	3.48	
	P 1337	M. intermedia	4	104.01	138.68	3.1	9.12	
γ	P 1360	M. cushmani	8	651.78	744.33			
	P 1342	M. intermedia	10	116.64	129.47	5.75	3.30	5.635
	FS 472–473	M. intermedia	15	95.65	102.35	1.26	2.65	
	P 1337	M. intermedia	4	396.5	527.3	5.1	3.34	5.56
ε	FS 472	M. intermedia	5	.0024	.0030			
	P 1360	M. cushmani	8	.0026	.0029	1.0	4.12	
	FS 287	M. intermedia	7	.00022	.00026	11.15		8.28
	P 1337	M. intermedia	4	.00157	.0021	8.	4.76	9.78
D_I	FS 472–473	M. intermedia	17	.000441	.000467			
	P 1337	M. intermedia	4	.00017	.000226	2.06	8.70	
	P 1360	M. cushmani	13	.000368	.000398	1.76	8.74	
	FS 472–473	M. intermedia	17	.000441	.000467	1.17	2.61	
	FS 285–287	M. intermedia	24	.000289	.000300	1.55	2.12	
D_{II}	P 1337	M. intermedia	4	.00021	.00028			
	P 1360	M. cushmani	12	.00062	.00068	2.43	8.76	
	P 1342	M. intermedia	12	.00038	.00042	1.62	2.83	
	FS 473	M. intermedia	13	.001225	.001323	3.15	2.80	4.43
	P 1337	M. intermedia	4	.00021	.00028	4.72	8.74	
L_{I+II}	P 1337	M. intermedia	4	.00067	.0009			
	P 1360	M. cushmani	10	.001156	.00128	1.4	8.81	
	FS 472–473	M. intermedia	15	.000961	.00103	1.24	3.03	
	FS 285–287	M. intermedia	26	.00109	.00113	1.09	2.35	
	P 1337	M. intermedia	4	.00067	.0009	1.25	19.45	

See note on table 10.

In the case of the samples of *Miogypsinoides*, the comparisons between the variances of the various characters are shown in table 10. They revealed no significant difference. It may thus be suggested that all these *Miogypsinoides* samples belong to the same population homogeneous with respect to the variability of all the characters investigated.

TABLE 10

Comparison of the variances of some characters in the samples of *Miogypsina* (*Miogypsinoides*) *complanata mauretanica*

Character	Sample	N	σ^2	Σ^2	F	Snedecor's F P = .05
X	P 1349	32	1.8225	1.877		
	P 1347	19	2.6569	2.804	1.49	1.93
	P 1337	4	.9025	1.200	2.33	8.68
γ	P 1349	25	895.8	931.6		
	P 1347	19	1085.7	1145.9	1.23	2.06
	P 1337	3	123.2	184.8	6.2	19.43
ε	P 1349	30	.00088	.000918		
	P 1347	24	.00126	.001314	1.43	1.92
	P 1337	4	.000289	.000384	3.41	8.65
D_I	P 1347	19	.000158	.000167		
	P 1349	29	.000121	.000125	1.33	2.—
	P 1337	4	.000256	.000340	2.71	2.945
D_{II}	P 1349	22	.000282	.000295		
	P 1347	19	.000317	.000334	1.13	2.13
	P 1337	3	.000085	.000127	2.62	19.43
L_{I+II}	P 1347	19	.000384	.000405		
	P 1349	25	.000365	.000379	1.07	2.06
	P 1337	3	.000529	.000793	2.09	3.40
T_t	P 1349	6	.006626	.007951		
	P 1347	5	.006416	.007699	1.03	5.05

σ^2 = variance of the sample
Σ^2 = variance of the population
F = Snedecor's parameter

COMPARISON OF THE COEFFICIENTS OF CORRELATION

This comparison was restricted to the coefficients that showed some significance, or at least were appreciable.

It was done with the help of the parameter:

$$z = \frac{1}{2} \log_e \frac{1+r}{1-r}.$$

It is apparent from table 11 that all the coefficients of correlation investigated in the samples of *Miogypsina* s.s. showed no significant differences, and it may be suggested that all these samples, whether

TABLE 11

Comparison of the coefficients of correlation of some characters in the *Miogypsina* s.s. samples

Correlation Y·X	Sample	Identification	N	r	R_1'	R_2'	d_z	$\sigma_{z_{1,2}}$	1.96 σ_z
$D_I \cdot D_{II}$	P 1360	M. cushmani	13	+0.57					
	FS 285–287	M. intermedia	17	+0.77	+.474	+.789	.39	.41	.804
	FS 472–473	M. intermedia	18	+0.51			.48	.37	.727
$D_I \cdot \varepsilon$	P 1360	M. cushmani	8	+0.70					
	P 1342	M. intermedia	12	+0.85			.387	.57	1.117
	FS 472–473	M. intermedia	15	+0.56	+.50	+.833	.625	.44	.862
	FS 285–287	M. intermedia	18	+0.69			.218	.38	.745
$200\alpha/\beta \cdot L_{I+II}$	P 1360	M. cushmani	10	+0.72					
	P 1342	M. intermedia	11	+0.40			.488	.51	.9996
	FS 472	M. intermedia	5	+0.83	+.16	+.80	.77	.79	1.5484
	FS 472–473	M. intermedia	15	+0.51			.627	.76	1.4896
$200\alpha/\beta \cdot \varepsilon$	P 1360	M. cushmani	8	+.666	+.08	+.84	.15	.53	1.04
	FS 472–473	M. intermedia	15	+.57					
$200\alpha/\beta \cdot \gamma$	P 1342	M. intermedia	9	+.60					
	FS 472–473	M. intermedia	15	+.40	+.019	+.64	.272	0.50	0.98
	FS 285–287	M. intermedia	31	+.37			.034	0.67	0.67

TABLE 12

Comparison of the coefficients of correlation of some characters in the samples of *Miogypsina (Miogypsinoides) complanata mauretanica*

Correlation Y·X	Sample	N	r	R_1'	R_2'	d_z	$\sigma_{z_{1,2}}$	1.96 $\sigma_{z_{1,2}}$
$D_I \cdot D_{II}$	P 1349	19	+.76	+.47	+.85	.22	.35	.69
	P 1347	19	+.65					
$D_I \cdot L_{I+II}$	P 1349	22	+.79	+.55	+.86	.28	.33	.65
	P 1347	19	+.66					
$D_I \cdot L_e W_e$	P 1349	29	+.48	+.14	+.72	.04	.31	.61
	P 1347	19	+.51					
$\gamma \cdot D_I$	P 1349	25	+.42	+.13	+.72	.17	.32	.63
	P 1347	19	+.55					
$D_I \cdot X$	P 1349	29	−.13	−.13	−.47	.49	.31	.61
	P 1347	19	−.55					
$\gamma \cdot X$	P 1349	26	−.52	−.17	−.76	.045	.32	.63
	P 1347	19	−.62					

r = coefficient of correlation.

R_1', R_2' = lower and upper limits of the overlap of two or more security intervals.

$\sigma_{z_{1,2}}$ = standard deviation of the difference between the two values of z.

TABLE 13

Comparison of the coefficients of regression for some relations in the *Miogypsina* s.s. samples

Relation $Y \cdot X$	Sample	Identification	N	r	b_{yx}	d_b/σ_{d_b}
$D_I \cdot D_{II}$	FS 285–287	M. intermedia	17	+.77	+.6045	
	P 1360	M. cushmani	13	+.57	+.4189	0.81
	P 1342	M. intermedia	13	+.36	+.36	0.19
	FS 285–287	M. intermedia	17	+.77	+.6045	0.79
$D_I \cdot \varepsilon$	P 1342	M. intermedia	11	+.847	+.387	
	P 1360	M. cushmani	8	+.70	+.270	0.41
	FS 472–473	M. intermedia	15	+.56	+.246	0.15
	P 1342	M. intermedia	12	+.847	+.387	0.58
$200\alpha/\beta \cdot L_{I+II}$	P 1360	M. cushmani	10	+.72	+ 275.5	
	P 1342	M. intermedia	11	+.40	+ 181.2	0.56
	FS 472–473	M. intermedia	15	+.51	+ 447.2	1.42
	P 1360	M. cushmani	10	+.72	+ 275.5	1.07
	FS 472	M. intermedia	5	+.83	+ 326.4	0.67
$200\alpha/\beta \cdot \varepsilon$	P 1342	M. intermedia	4	+.21	+ 73.1	
	P 1360	M. cushmani	8	+.666	+ 161.9	0.26
	FS 472–473	M. intermedia	15	+.57	+ 178.5	0.15
	P 1342	M. intermedia	4	+.21	+ 73.1	0.32
$200\alpha/\beta \cdot \gamma$	P 1342	M. intermedia	9	+.60	+.714	
	FS 285–287	M. intermedia	31	+.37	+.347	0.58

TABLE 14

Comparison of the coefficients of regression for some relations in the samples of *Miogypsina* (*Miogypsinoides*) *complanata mauretanica*

Relation $Y \cdot X$	Sample	N	r	b_{yx}	d_b/σ_{d_b}
$D_I \cdot D_{II}$	P 1349	19	+.76	+.517	
	P 1347	19	+.65	+.395	0.77
$D_I \cdot L_{I+II}$	P 1349	22	+.79	+.526	
	P 1347	19	+.66	+.366	1.15
$D_I \cdot L_e W_e$	P 1349	29	+.48	+.2352	
	P 1347	19	+.58	+.2346	.005
$\gamma \cdot D_I$	P 1349	25	+.42	+ 1097.8	
	P 1347	19	+.55	+ 1650.–	.71
$D_I \cdot X$	P 1349	29	−.129	−.0017	
	P 1347	19	−.55	−.0037	.91
$\gamma \cdot X$	P 1349	26	−.52	− 11.37	
	P 1347	19	−.62	− 12.92	.28

d_b = difference between the two coefficients of regression

σ_{d_b} = standard deviation of the difference between the two coefficients of regression.

called *M. intermedia* or *M. cushmani* belong either to the same population homogeneous with respect to the correlation between $D_I \cdot D_{II}$, $D_I \cdot \varepsilon$, $L_{I+II} \cdot 200\alpha/\beta$, $\varepsilon \cdot 200\alpha/\beta$ and $\gamma \cdot 200\alpha/\beta$, or rather, as it seems to be the case here, to populations which show approximately the same correlations for these characters and would thus be similar in this respect on account of their belonging to the same evolutionary bioseries.

From table 12 it is evident that the samples of *Miogypsinoides* belong probably to the same population homogeneous with respect to all the investigated correlations as their respective coefficients are not significantly different.

COMPARISON OF THE COEFFICIENTS OF REGRESSION

This comparison was again restricted to the cases where the correlations were significant or at least appreciable.

As regards the samples of *Miogypsina* s.s. (table 13), it appears that there are no significant differences between the maximum and minimum values for the various coefficients of regression in the group of samples identified as *Miogypsina intermedia.* Besides, there is no significant difference between these values and those of sample P 1360 which is identified as *Miogypsina cushmani* showing some tendency towards *M. intermedia.*

As for the samples of *Miogypsinoides*, no significant differences were detected when comparing the coefficients of regression of the various relations investigated, as can be seen from table 14.

(To be continued)

PALEONTOLOGY

CONTRIBUTION TO THE STUDY OF *MIOGYPSINA* s.l. FROM EGYPT. III

GENERAL CONCLUSIONS

BY

F. J. SOUAYA

(Communicated by Prof. G. H. R. VON KOENIGSWALD at the meeting of June 24, 1961)

BIOMETRICS

The statistic use of the numerical data obtained during the investigation of a number of *Miogypsina* samples from the Eastern Desert (G. Gharra and G. Atâqa) and Sinai (G. Gushia) yielded interesting results despite the acknowledged arbitrariness in the evaluation of some characters and the unavoidable errors of measurements particularly those introduced by the use of thin sections.

It proved the relatively normal distribution of most of the observed values for *Miogypsina* s.l. and their insignificant difference from the theoretical calculated ones using the Chi-Square test.

As regards *Miogypsina* s.s., comparison between the variances and the coefficients of correlation and regression did not reveal, except possibly for the variability of γ and ε, appreciable significant differences between the various samples, which were identified in accordance with DROOGER's scale (1952, p. 54) for the range of the average values of $200\alpha/\beta$. This may indicate that all these samples either belong to the same population homogeneous with respect to the variability of most of the characters and the coefficients of the proven correlations and regressions, or rather, as seems to be the case here, to different populations fairly similar in this respect on account of some common sequence of evolution.

As for the comparison between the various arithmetic means, significant differences exist between some characters such as $200\alpha/\beta$, L_{I+II} and ε which would warrant, to a certain extent, the following determinations: *M. cushmani* with some tendency towards *M. intermedia*, *M. intermedia* with some tendency towards *M. cushmani*, *M. intermedia*, and *M. intermedia* with some tendency towards *M. globulina*. As for the sample P 1337 which is unsatisfactory in quality and quantity, it is tentatively kept in *M. intermedia* which it resembles somewhat in its average values for $200\alpha/\beta$, D_I and ε, but from which it differs in its mean values for γ, D_{II} and L_{I+II}: it is an exemplum intercentrale occurring just at the border line of *M. intermedia* and *M. globulina*.

As regards the insignificant differences between some arithmetic means of the *Miogypsina* s.s. samples investigated, they may suggest with the resemblance exhibited by the various coefficients of correlation and regression, as well as the similarity in the variability of most of the characters, some parentage between all these *Miogypsina* s.s. species which is translated by the various tendencies which they show towards each other.

In connection with the investigation of *Miogypsinoides complanata* Schlumberger, a brief preliminary analysis was made of three Mediterranean types, namely the ones with high, moderate and low arithmetic means of the spirally coiled nepionic chambers. It showed that each type is significantly different from the other with respect to this important characteristic.

As regards the *Miogypsinoides* samples of G. Gharra here under consideration, no significant differences were found between their arithmetic means, variances, coefficients of correlation and regression. This indicates that very probably all these samples belong to the same homogeneous population of *M. complanata* Schlumberger *mauretanica* Bronnimann.

Apart from these conspicuous results, it is well to point out that this research has also proved the importance of some characters which until now received little or inadequate attention.

In *Miogypsina* s.s., it was shown that the arithmetic means of D_I and L_{I+II} and possibly γ, ε and D_{II} tend to increase in value with evolution.

These considerations regarding D_I and D_{II} are in agreement with Bronnimann's ranges (1940, pp. 94 and 97) for *M. irregularis* and *M. mediterranea* as they are appreciably larger in the latter, which is seemingly a younger species. As regards D_I, this conclusion gives additional weight to Drooger's observation (1952, p. 11) about the mean value of the diameter of the protoconch increasing irregularly with time. It was also shown here that significant positive correlation exists between D_I and D_{II}.

Also, there exists some general tendency for a positive correlation which is sometimes significant, between $200\alpha/\beta$ and L_{I+II}, ε as well as γ.

As for the arithmetic means of $200\alpha/\beta$, which are believed to increase with evolution (Drooger, 1952), they show significant variations which are interpreted in accordance with Drooger's scale.

However, it is felt that this means of specific identification is not entirely satisfactory since it is based on a single character, the determination of the arithmetic means of which may well vary appreciably with the size of the samples used. In addition, its evaluation is often approximate and sometimes subjective and even doubtful.

Interested workers are urged here to attempt the study of the various species of *Miogypsina* s.s. with the aim to establish scales parallel to Drooger's for the ranges of the arithmetic means of $200\alpha/\beta$ and X, and based on other characteristics, so as to render specific determinations more certain and perhaps easier. In the choice of these characteristics

their degree of variation within each systematic unit is worth taking into account. In this connection it was found that L_{I+II} and D_I are fairly slightly variable in the species here under consideration.

Moreover, it is also felt that checking on the objectiveness of the scales already existing and the ones to be proposed, should be made by means of statistic methods using, of course, good judgement and a critical mind so that various specific destinctions should be based on significant differences.

Amongst the characteristics which may in the future prove to be of import, is the angle γ. γ was already found by DROOGER (1954b) to be approximately 90° in *M. mediterranea* and in *M. mediterranea* var. *excentrica*; its arithmetic mean is respectively negative and positive in *M. socini* and *M. irregularis* (DROOGER, 1954a). Here, the average values of γ were found to be small, ranging only between $-14°$ and $38°$ in the closely related forms investigated of *M. intermedia–M. cushmani*. Besides, the values of γ showed positive correlation with those of $200\alpha/\beta$ in G. Gharra (P 1342), G. Gushia (FS 285–FS 287) and G. Atâqa (FS 472–FS 473). This is somewhat significant in the two former localities, whereas in the last mentioned it is only appreciable.

In the *Miogypsinoides* samples (P 1349, P 1347 and P 1337), the arithmetic means of γ are high and range only between $-139°$ and $-127°$. They are insignificantly different from each other. Besides, there is a significant positive correlation between γ and D_I while a significant negative correlation exists between γ and X. This proves that in all probability γ is a fairly important characteristic.

However, for γ, as well as for all the other characteristics, a standardization of their exact meaning is needed, so as to secure relatively accurate and comparable values where approximation is avoided as much as possible.

In the case of γ, if no straight line can pass through the centre of the protoconch, the middle of the frontal margin and the apex, this may be substituted by a straight line which should pass through the centre of the protoconch parallel to the apical frontal line.

As regards the other characteristics investigated in the *Miogypsinoides* samples, namely X, ε, D_I, D_{II}, L_{I+II} and even the maximum thickness of the test, their arithmetic means are appreciably close and insignificantly different.

Besides, positive significant correlations were proved for $D_I \cdot D_{II}$, $D_I \cdot L_{I+II}$ and $D_I \cdot L_eW_e$. It is also interesting to mention that the regression lines in the above correlations for the samples P 1347 and P 1349 are close and even approximately parallel in the last case with the former sample which is older, occupying a relatively slightly higher position.

For similar studies in future it is here recommended to deal, if possible, with samples of an appreciable size as they are bound to yield, if properly investigated, a good estimation of the various characteristics. Moreover,

the coefficients of correlation observed are as such liable to give precise information about the correlation in the populations.

Furthermore, if thin sections are to be used it is possible that a mean of the observations on either side of each section may give in most cases more accurate results than the ones based on the measurements made on a single side only.

BIOSTRATIGRAPHY

From the examination of a number of samples from the basal Miocene beds of Gebel Gharra, G. Atâqa and G. Gushia, it was found that *Miogypsina* s.l. occurs in two biostratigraphic units, which were named Zone of *Operculina complanata* (DEFRANCE) and Zonule of *Miogypsina cushmani* VAUGHAN.

The Zone of *Operculina complanata* (DEFRANCE) is the lower unit. Its type locality is Gebel Gharra where it is about 55 metres thick and includes the samples P 1337–P 1349. It may belong to the Burdigalian Stage on account of the similarity of its *Miogypsina* s.s. representatives with those of Morocco (DROOGER, 1954b, p. 588) and South-Western France (DROOGER et al., 1955, pp. 25–27) which occur in the upper part of this stage. Its characteristics are as follows:

1) The significant and conspicuous presence of *Miogypsina intermedia* possibly showing a tendency either towards *M. cushmani* or *M. globulina*.

2) The possible significant presence of *Miogypsina* (*Miogypsinoides*) *complanata* SCHLUMBERGER *mauretanica* BRONNIMANN, *Operculina complanata* (DEFRANCE), *O. carpenteri* SILVESTRI, *Heterostegina heterostegina* (SILVESTRI) and *H. costata* D'ORBIGNY (type *H. granulatatesta* PAPP and KÜPPER).

3) The absence of *Neoalveolina melo* (FICHTEL and MOLL).

The occurrence in G. Gharra of *Miogypsina* (*Miogypsinoides*) *complanata mauretanica* which until now has never been recorded in Egypt, with *Miogypsina* s.s. is most unusual as it is held (DROOGER, 1956, p. 70) that nowhere in the Western Mediterranean area the two subgenera *Miogypsinoides* and *Miogypsina* s.s. are contemporaneous; it is said they succeeded one another. Lately however, EAMES and CLARKE (1957, p. 80) and BLOW (1957, p. 78) have each given seperate examples for the conjoint occurrences of *Miogypsinoides complanata* SCHLUMBERGER and *Miogypsina irregularis* (MICHELOTTI) in the Mediterranean region, although previously other associations of *Miogypsinoides* with *Miogypsina* s.s. were explained by reworking of the former (DROOGER, 1954).

It is thus realized that until additional occurrences from other Egyptian localities definitely prove the genuine existence of *Miogypsinoides* assemblages in such a part of the Miocene column, any stratigraphic conclusion based on their geological distribution will have to be considered tentative and provisional. Their genuine nature might be suggested on account of their excellent state of preservation, their apparently homogeneous

characters, their association with a fauna which indicates the same environment and the apparent absence at least in this part of Egypt, of marine Chattian or Aquitanian rocks to account for the presence of such assemblages by reworking. But, since *Miogypsina complanata* occurs here in arenaceous limestones, which may be quite sandy as in sample P 1347, the possibility still exists that this occurrence is not genuine, although its source rock cannot, for the time being, be pointed out, because transported fossils which may be very well preserved (BERTRANEU and MAGNÉ, 1952, p. 278), are said to be characteristic of allochtonous limestones (PETTIJOHN, 1949, p. 167). In this case, the interval (P 1347–P 1349) might represent a passage phase from the Burdigalian to the Vindobonian Stage. However, noteworthy here is the Oligo-Miocene of FARAG and SHATA (1957, pp. 300–343) in the area of Bir el Haleafiya–Gebel el Zeita in Sinai. It includes Oligocene fossils which were not considered by the two authors as "rolled", always associated with Lower and Middle Miocene ones; the lowest beds of this series contain there definite marine Upper Oligocene (Aquitanian) and Lower Miocene (Burdigalian) fossils. It might then have been possible that in the region of Gebel Gharra, forms such as *Miogypsina complanata* of the low M_x type which in the region of Turin is "Aquitaniano" and in the region of Bordeaux, Chattian? (DROOGER, 1954, p. 246), lived or rather survived in younger geological times on account of some special conditions. It may be also interesting to note that *Miogypsina* (*Miogypsinoides*) *complanata* SCHLUMBERGER *mauretanica* BRONNIMANN was previously, but doubtfully, recorded by BRONNIMANN (1940, p. 104) from the Burdigalian of Morocco, though later DROOGER (1954) explained by sub-marine sliding and the action of turbidity currents on Upper Oligocene sediments, the presence of *Miogypsina complanata* s.l. in relatively younger formations. The assemblages of *Miogypsina* (*Miogypsinoides*) *complanata mauretanica* as found in Gebel Gharra deserve attention especially in that their main occurrence, seemingly to the exclusion of any *Miogypsina* s.s., is in a small interval or horizon covered by the samples P 1347 and P 1349. However, a few specimens were recorded with *Miogypsina* s.s. in the basalmost part of the section, in sample P 1337, where reworking is not doubted. Until further field studies are made and until additional occurrences are found and investigated in order to comprehend the full and true meaning of this main occurrence of *Miogypsina complanata*, it will be provisionally designated as ? Subzone of *Miogypsina* (*Miogypsinoides*) *complanata mauretanica*, where *Operculina complanata* and *Heterostegina costata* (type *H. granulatatesta* PAPP and KÜPPER) may also be significant. The use of the biostratigraphic term horizon as defined by FIEGE (1951, p. 2590) might have been more appropriate in this case.

A second biostratigraphic subdivision is here also proposed in the Zone of *Operculina complanata* (DEFRANCE); it is named the Subzone of *Miogypsina intermedia* DROOGER. It is mainly characterized by the

development of *Miogypsina intermedia* DROOGER; *Operculina complanata* (DEFRANCE) and *Heterostegina heterostegina* (SILVESTRI) may also be significant. The samples of G. Gushia (FS 285–FS 287) may represent, with the sample P 1337 of Gebel Gharra, the basal part of this subzone, because *Miogypsina intermedia* here shows some tendency towards *M. globulina* (MICHELOTTI), while the samples of G. Atâqa (FS 472–FS 473) and particularly those of G. Gharra (P 1342–P 1346) occupy a higher position on account of their *M. intermedia*, showing some tendency towards *M. cushmani* which indicates a higher degree of evolution (DROOGER, 1952, p. 54). These various occurrences of *M. intermedia* may be considered to represent teilzones of the same biozone (FIEGE, 1951, pp. 2589–2591).

The Zonule of *Miogypsina cushmani* represents the highest occurrences of *Miogypsina* s.s. in G. Gharra where it includes the samples P 1359–P 1361. Its age may be Helvetian on account of *Miogypsina cushmani* VAUGHAN occurring in the lower part of the Helvetian in Morocco (DROOGER, 1954b, p. 588). It is mainly characterized by:

1) The significant and conspicuous presence of *Miogypsina cushmani* VAUGHAN which shows in G. Gharra a certain tendency towards *M. intermedia*.
2) The possible significant presence of *Operculina carpenteri* SILVESTRI and its related form of *Heterostegina* which is a new species to be described later and elsewhere.
3) The possible presence of significant but inconspicuous *Neoalveolina melo* (FICHTEL and MOLL).

This latter species occurs conspicuously in the upper part of the Miocene section of G. Gharra (P 1362–P 1383) where in the absence of *Miogypsina* s.l. it characterizes with *Neoalveolina melo curdica* REICHEL, *N. melo haueri* (D'ORBIGNY) and *Heterostegina costata* s.s., a zone which is named the Zone of *Neoalveolina melo* (FICHTEL and MOLL); its age is considered to be Vindobonian.

This Zonule of *Miogypsina cushmani* then appears to represent as far as its character is concerned, a transitional unit between the Zones of *Operculina complanata* and *Neoalveolina melo*.

PALEOECOLOGY

In the Aquitaine Basin, DROOGER (DROOGER et al., 1955, pp. 33, 34) remarks that the Miogypsinidae are most common in rather coarse sediments, mostly calcareous sands and absent or uncommon in silty to clayey deposits. Besides, individuals in great numbers are met with in otherwise sterile sands, whereas they occur less frequently in the shell beds of beach origin. On this basis, he concludes that Miogypsinae lived in near-shore, turbulent water of the neritic zone, though not in that part with considerable surf-action.

In Gebel Gharra as well as in G. Atâqa and G. Gushia, representatives

of the genus *Miogypsina* occur in more or less arenaceous limestones. They are accompanied by usually conspicuous *Amphistegina lessonii* D'ORBIGNY and possibly also by various species of *Operculina* and *Heterostegina*, namely *O. complanata* (DEFRANCE), *O. carpenteri* (SILVESTRI) and *H. costata* D'ORBIGNY (type *H. granulatatesta* PAPP and KÜPPER). These are indubitable proofs for a marine warm shallow environment (GALLOWAY, 1933, pp. 315, 420–421) where various members of the family Miliolidae viz: *Quinqueloculina contorta* D'ORBIGNY, *Q. crassa* D'ORBIGNY, *Q. laevigata* D'ORBIGNY, *Q. seminula* (LINNÉ), *Pyrgo bulloides* (D'ORBIGNY) and *Triloculina tricarinata* D'ORBIGNY have occasionally flourished possibly with "*Rotalia*" *beccarii* (LINNÉ), *Elphidium macellum* (FICHTEL and MOLL), *E. flexuosum* (D'ORBIGNY) and *E. crispum* (LINNÉ). In addition, the frequent occurrence in these deposits of thick walled Ostreas is an additional evidence for the above described environment and for the agitation of the sea waters (PETTIJOHN, 1949, p. 166 and TWENHOFEL, 1950, pp. 185–187). However, this agitation was most probably not violent to the tearing and breaking extent, since the *Ostrea* shells and the *Miogypsina* tests are fairly well preserved; besides, in sample FS 470 of G. Atâqa where shell debris are quite numerous, suggesting a microcoquina, not a single *Miogypsina* specimen was found although somewhat higher up where the conditions were relatively calmer, *Miogypsina* is common to abundant.

REFERENCES

BARRON, T., Lower Miocene Beds between Cairo and Suez. Geol. Mag., n.s., decade V, **1**, 603–608 (1904).

BARTHOUX, J., Chronologie et Description des Roches Ignées du Désert Arabique. Mém. Inst. Egypte, **5**, 1–262 (1922).

BERTRANEU, J. and J. MAGNÉ, Le Miocène Marin du Revers Septentrional du Bassin du Hodna (partie orientale). Soc. Geol. France, Bull., 6 ser., **2**, 275–281 (1952).

BLANCKENHORN, M. L. P., Neues zur Geologie und Paläontologie Aegyptens: III. Das Miocän. Zeitschr. d. Deutsch. g. Ges., **53**, 52–152 (1901).

BLOW, W. H., Transatlantic correlation of Miocene sediments. Micropaleontology, **3**, 77–79 (1957).

BRÖNNIMANN, P., Über die tertiären Orbitoididen und die Miogypsiniden von Nordwest-Morokko. Schweiz. Pal. Abh., **63** (1940).

CUVILLIER, J., Présence de Miogypsines dans le Miocène d'Egypte. Acad. Sci., C.R. Séances, **206**, 1035 (1938).

DROOGER, C. W., Study of American Miogypsinidae. Utrecht, Univ., Doct. Diss. (1952).

———, *Miogypsina* in Northern Italy. K. Nederl. Akad. van Wetensch., Proc., ser. B, **57**, 227–249 (1954a).

———, *Miogypsina* in Northwestern Morocco. Ibid., ser. B, **57**, 580–591 (1954b).

———, *Miogypsina* at Puente Viejo, Spain. Ibid., ser. B., **59**, 68–72 (1956).

———, J. P. H. KAASSCHIETER and A. J. KEY, The Microfauna of the Aquitanian-Burdigalian of Southwestern France. K. Nederl. Akad. Wetensch., Afd. Natuurk., Verh., ser. 1, **21** (1955).

——— and C. Socin, Miocene foraminifera from Rosignano, northern Italy. Micropaleontology, 5, 415–426 (1959).

Eames, F. E. and W. J. Clarke, The ages of some Miocene and Oligocene foraminifera. Micropaleontology, 3, 80 (1957).

Ellis, B. F. and A. R. Messina, Catalogue of Foraminifera. The American Museum of Natural History, Special Publ. (1940–1955).

Farag, I. and A. Shata, Stratigraphy of the Bir el Haleafiya-Gebel el Zeita Area (West Sinai Foreshore Province, Egypt). Fac. of Sc., Cairo Univ., Bull. 295–357 (1957).

Fiege, K., The Zone Base of Biostratigraphy. Am. Ass. Petr. Geol., Bull., 35, 2582–2596 (1951).

Fourtau, R., Notes sur quelques publications parues en 1899–1900 concernant la Géologie et la Paléontologie de l'Egypte. Inst. Egypte, Bull., ser. IV, 1, 165–171 (1900).

Galloway, J. J., A Manual of Foraminifera. The Principia Press, Inc., Bloomington (1933).

Glaessner, M. F., Principles of Micropaleontology. John Wiley & Son, Inc., New York (1947).

Hume, W. F., Explanatory Notes to accompany the Geological Map of Egypt. Surv. Dept., Cairo, 1–50 (1912).

Lamotte, M., Introduction à la Biologie Quantitative. Masson et Cie, Paris (1948).

Macfadyen, W. A., Miocene Foraminifera from the Clysmic Area of Egypt and Sinai. Geol. Surv. Egypt, Govt. Press, Cairo, 1–149 (1931).

Moon, F. W. and H. Sadek, Topography and Geology of Northern Sinai. pt. I – Session 1919–1920, Petr. Res. Bull. No. 10, Govt. Press, Cairo, pp. 1–154 (1921).

——— and ———, Preliminary Geological Report on Gebel Khoshera Area (Western Sinai). Petr. Res. Bull. No. 9, Govt. Press, Cairo, pp. 1–35 (1925).

Papp, A., Handbuch der stratigraphischen Geologie, 3, pt. 1, Tertiär (1959).

Pettijohn, F. J., Sedimentary Rocks. Harper & Bros., N.Y. (1949).

Picard, L., Structure and Evolution of Palestine, with comparative notes on neighbouring countries. Geol. Dept. Hebrew. Univ., Jerusalem, Bull., 4, No. 2–34 (1943).

Said, R. and M. Yallouze, Miocene Fauna from Gebel Oweibed, Egypt. Bull. Fac. Science No. 33, Cairo Univ., 61–81 (1955).

Schlumberger, C., Note sur le genre *Miogypsina*. Soc. Géol. France, Bull., ser. 3, 28, 327–333 (1900).

Shukri, N. M. and M. G. Akmal, The Geology of Gebel el-Nasuri and Gebel el Anqabiya district. Soc. Géogr. Egypte, Bull., 26, 243–276 (1953).

——— and M. K. El Ayouti, The Geology of Gebel Iweibid — Gebel Gafra area, Cairo-Suez District. Soc. Géogr. Egypte, Bull., 29, 67–109 (1956).

Simpson, G. G. and A. Roe, Quantitative Zoology. Numerical Concepts and Methods in the Study of Recent and Fossil Animals. McGraw–Hill Book Co., Inc., New York and London (1939).

Stainforth, R. M., Foraminifera in the Upper Tertiary of Egypt. Jour. Paleontology, 23, 419–422 (1949).

Twenhofel, W. H., Principles of Sedimentation. McGraw–Hill Co., New York, 2nd ed. (1950).

VULCANISM AND TECTONICS

BY

H. A. BROUWER

(Communicated at the meeting of September 30, 1961)

If there is magma in depth it may rise in the moving crust and win the struggle for space and the struggle with cold until it reaches the surface. The struggle for space of the magma in connection with earth movements must be judged by the subject matter of structural geology, such as fracturing, folding, normal and reverse faulting, overthrusting and underthrusting, upwarps, downwarps and drift of larger crustal blocks, faulting due to horizontal shear and deep-seated zones of décollement to accomodate the horizontal movements. The structural changes which have influenced the birth and lifetime of volcanoes may be extremely variable and the structures associated with volcanic activity may have been studied in some detail without solving the problem of the nature of the movements which brought the structure about. Tension, compression and shear have all been used to explain the origin of rift valleys. One should not expect to find simple tectonic controls of extrusive vulcanism if the origin of the structures is not yet understood, but from some examples given below it will appear that the distribution of volcanic activity may give directions for a judgment on the nature of the earth movements.

Steep fractures and faults under tensile stress offer favourable factors for the rise and escape of magma and fractures formed by tension may in a later stage of deformation close by compression. It becomes more and more evident that horizontal shifting along shear planes, developed by rotational stress acting in a horizontal plane, plays an important part in structural geology and if the fault planes are not tightly closed and reach the magma at depth, volcanic activity may be connected with them.

Andean chains

Except for their northern and southern extremities the Andean chains of South America are characterized by the absence of ultrabasic rocks, by repeated block-faulting, accompanied by the emplacement of acid plutonic bodies and by great outpourings of volcanic products. They belong to the thick shelled type of CHAMBERLIN [1]) in which vertical diastrophism

[1]) R. T. CHAMBERLIN, The building of the Colorado Rockies Journ. of Geol. XXVII, 248–251 (1919). Vulcanism and mountain making. A supplementary note, Journ. of Geol. XXIX, 166 (1921).

dominates over horizontal. The youngest phase of extrusive vulcanism during the general rise in late-Tertiary and post-Tertiary time, was connected with new structural lines, independent of the older structures. The distribution of young vulcanism is closely associated with recent tectonic depressions. There is a striking lack of young vulcanism in most of the NW–SE directed part of the mountain chain in north and central Peru (fig. 1). We suggest that this lack of vulcanism is connected with a passive

Fig. 1. Vulcanism in the northern Andean chains. 1. schematic representation of the zones with active volcanoes; 2. zone where volcanoes are lacking.

or active influence of the Brazilian mass, directed more or less normal to this part of the mountain chain and preventing the appearance of favourable fractures. I have pointed out [1] that relative tension may especially be expected near the bending points of moving geanticlines and this may explain the strong vulcanism in South Peru, where the direction of the mountain chain is still NW–SE, but here we are in the neighbourhood of the main bending point of the Andean chains where a tensional contribution can be expected.

[1] H. A. Brouwer, The horizontal movement of geanticlines and the fractures near their surface. Journ. of Geol 29, 560–577 (1921). The Geology of the Netherlands East Indies. New York, 61–65 (1925).

Alpine chains

The rise of ophiolites during the geosynclinal stage in alpine mountain ranges is reasonably explained as connected with tension during the geosynclinal downwarp while their eruption ceased during the compressional phases of severe folding and overthrusting. Horizontal movement is clearly dominant and the important thickening of the crust and the dip at low angles of the faults in mountains of the thin-shelled type may have influenced unfavourably the escape of magma to the surface, at least within the truly mountainous belt.

During the youngest rise, while deeper zones were affected, the faults may not have reached the magma at depth or compression may still have influenced unfavourably the rise of magma.

Japan

Numerous active and recently extinct volcanoes are found in the northern part of Japan, in Kyushu and in the Riu Kiu islands. The interjacent part of the orogenic belt in western Honshu is situated near the northern corner of the Philippine basin, which is considered to have participated in horizontal shifting movements in shear patterns which play an important part in these regions. In the Philippines and Taiwan there are indications of a tendency to more or less northward relative movements of the basin with regard to Asia and such a tendency would certainly affect the structures in western Honshu and Shikoku. As far as vulcanism in this part of Japan is concerned we observe its extinction first in a southern

Fig. 2. Vulcanism in Western Japan. 1. schematic representation of zones with active volcanoes; 2. zone with post-Tertiary extinct vulcanism and 3. zone with Miocene and Pliocene vulcanism.

zone with Miocene-Pliocene vulcanism and later in a northern zone with post-Tertiary extinct vulcanism. Active vulcanism occurs where forces exerted by the Philippine basin make a small angle with the orogenic belt and, as in the Andean chains of southern Peru, relative tension can be expected near the main bending point of the belt in Kyushu, as a contribution to the persistence of volcanic activity there.

Lesser Sunda islands

Another example of volcanic activity in orogenic belts retreating from a more stable mass has been described from the two rows of Lesser Sunda islands near Australia [1]) (fig. 3).

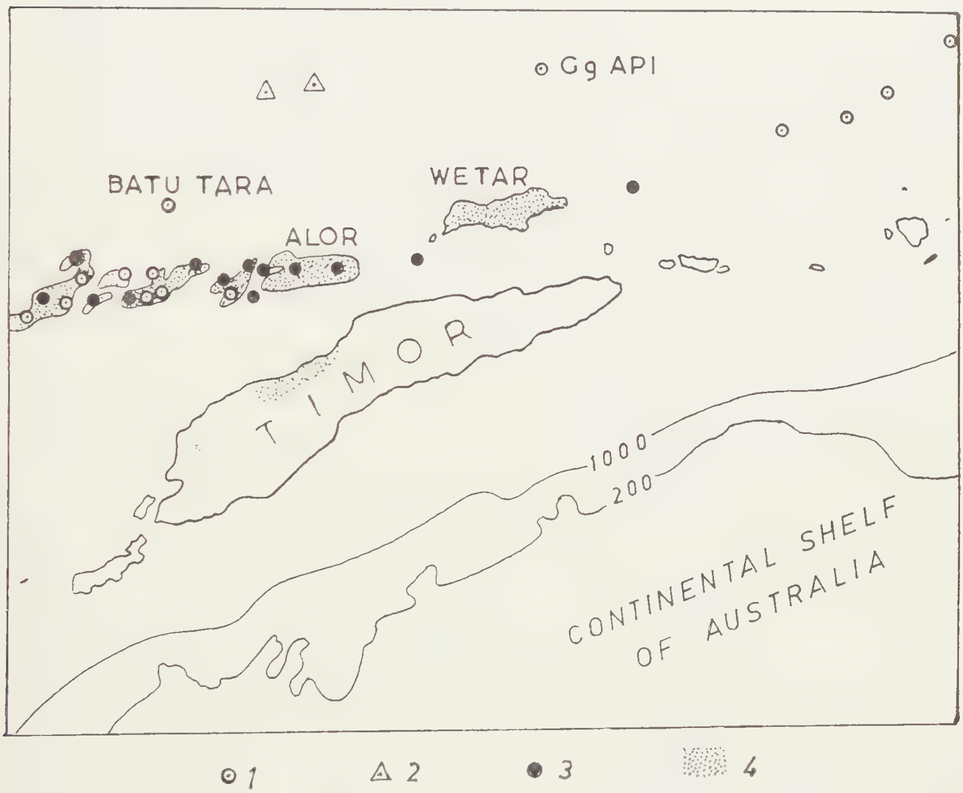

Fig. 3. Volcanism in the Lesser Sunda Islands near Australia. 1. active volcanoes (or groups); 2. active submarine volcanoes; 3. extinct volcanoes (or groups). 4. regions with partly Neogene volcanic rocks. Generally speaking the adaptation of the moving rows of islands is less complete and the volcanic activity has lasted longer in proportion to the distance from the Australian mass.

In the southern or Timor row old-Miocene vulcanism is indicated by the constituents of old-Miocene deposits north of the central basin in

[1]) H. A. Brouwer, Über Gebirgsbildung und Vulkanismus in den Molukken. Geol. Rundsch., VIII, 197 (1917). Geological Expedition to the Lesser Sunda islands IV, 397 (Amsterdam 1942).

Timor. The structure of this island is characterized by large overthrusts. Near the north coast the volcanic rocks are found in close association with young-Miocene and/or Pliocene rocks. These facts indicate that the site of volcanic action has retreated to the north in young-Tertiary time and died out completely before the end of the Tertiary. In the northern row of islands no older than young-Tertiary rocks and only fairly simple structures have been found. Volcanic products are found in the Miocene and volcanic action has lasted until the present time. On the islands Wetar and Alor, which are nearest to the southern row, volcanic rocks show a marked resemblance to rocks near the north coast of Timor and a general feature of the young volcanic activity in the northern row is that, proceeding from Wetar to the west or to the east first come regions where the morphology of the volcanic mountains shows that volcanic action became extinct later than in Wetar and still farther to the west and to the east volcanism is still active. The distribution of volcanic centres points to the existence of transverse or diagional fractures whch may be induced by longitudinal stretching of the moving row of islands. Active, partly submarine, vulcanism is found to the north of the northern row of islands. Generally speaking vulcanism lasted longer and the form of the moving rows of islands is less adapted to the front of the Australian mass (Australia with its submarine shelf) in proportion to the distance from the resistant body.

Recently [1]) somewhat similar relations have been suggested for Taiwan and neighbouring islands.

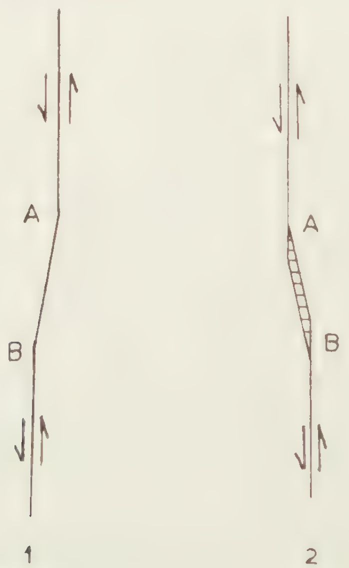

Fig. 4. Horizontal displacement on sinuous faults. Tension in the part A–B of 2.

[1]) BIQ CHINGCHANG, Circumpacific tectonics in Taiwan. Proc. 21st Intern. Geol. Congr. Norden. Part XVIII, 205 (1960).

Vulcanism and faults of lateral displacement

If the rock surfaces, which move past one another in a more or less horizontal direction, were pressed closely together, the rise of magma may be facilitated locally if the displacement takes place along sinuous or zigzag faults (fig. 4). In the North island of New Zealand such local tension has been applied to the eruption of ignimbrites by lowering of pressure, permitting release of gas [1]). The intensity and duration of vulcanism along the great fault scarp of the Sierra Nevada of California is greatest where the scarp is most irregular, while vulcanism is lacking where the scarp is straight [2]). This may also be connected with horizontal movements along fracture planes [3]). Tension joints forming an acute angle with the major fault plane, along which the horizontal movements took place, may account for subsidiary volcanic lines which cut diagonally across a major volcanic chain as in El Salvador and Nicaragua in Central America [3]).

Longitudinal lengthening in moving arcuate belts may be evidenced by the formation of gaping fractures or by horizontal movement on diagonal faults. In the Sunda arc for instance many volcanoes are arranged along diagonal lines. In the Sunda Strait between Java and Sumatra the greatest explosion of modern times took place at the island of Krakatau and there has been differential horizontal movement, the western part of Java moving to the south in relation to the southern part of Sumatra.

Crustal tension in broad swells

We have mentioned already a rise of orogenic belts in late-Tertiary and post-Tertiary time and the simultaneous growth of young volcanoes along structural lines which are independent of the older structures but the longer axis of these elongated swells and the major fractures will be directed more or less parallel to the strike of the older structures. Transverse and diagonal volcanic lines may also appear, as we have mentioned for moving arcuate belts.

General rise and dependence of the direction of fractures and volcanic lines upon the form of uplifted swells is also found in broad upwarps of the more stable masses. The balance of evidence with regard to the much debated origin of some conspicuous fault troughs accompanied by volcanic activity (e.g. Rhine Valley, East Africa) is in favour of the predominance of crustal tension in broad swells, uplifted by vertical forces. The place where the crust fractures will depend upon the distribution of maximal tensional stresses and on the varying resistance of the rocks against break.

---

1) R. H. Clark, Andesite lavas of the North Island, New Zealand. Proc. 21st Intern. Geol. Congr. Part XIII, 127 (1960).

2) E. A. Mayo, Rhyolite near Big Pine, California. Bull. Geol. Soc. Am. **55**, 592 (1944).

3) H. Williams, Problems and progress in volcanology. Eighth William Smith lecture. Quart. Journ. Geol. Soc. **CIX**, 313–314 (1953).

It becomes more and more evident that shearing and twisting have changed the position of areas of high stability and in connection with the distribution of volcanoes we must think of the possibility of compression next to rise by vertical forces. Upwarps with fractures and volcanic action are found in continents and ocean floors. We mention here an example (fig. 5) where the young, now extinct, vulcanism is arranged in a northern

Fig. 5. Volcanic regions in the upwarp of the Rhenish shield on both sides of the Rhine in West Germany; 1. Eifel; 2. Vogelsberg; 3. Rhön; 4. Kaiserstuhl; 5. Alb; 6. Ries. Black triangles indicate the dip of the shield. (Adopted from H. Cloos).

and a southern zone along fractures where these should be expected as a tensional feature during the upwarp of the large shield on both sides of the Rhine in West Germany [1]). That the magma reached the surface is considered to be connected with the stronger curvature of the shield in these zones. The curvature is also determinative for the direction and the volcanic productivity of the fractures.

The examples given in the preceeding pages may have shown that the diversity of volcanic environments needs not prevent to find simple tectonic controls.

[1]) H. Cloos, Hebung–Spaltung–Vulkanismus. Geol. Rundschau, **XXX**, 405–527 (1939).

ASTRONOMY

NOTE ON THE STRUCTURE OF THE SOLAR CHROMOSPHERE WITH SOME REMARKS ON THE ATHAY–THOMAS SPICULE MODEL

BY

OSAMU NAMBA [1]

(Communicated by Prof. M. G. J. MINNAERT at the meeting of October 28, 1961)

Abstract

Recent observations showing that the spicules emit practically all the visual line emission of the chromosphere ($h \gtrsim 1000$ km) require a reinterpretation of the chromospheric spectrum. Any spicule model combined with the spicule statistics should be able to explain the flash spectrum line intensities thus far obtained, which refer to the homogeneous chromosphere. With this condition, the spicule model developed in THOMAS and ATHAY's (1961) book is tested. It is found that the radiation of the K line in the upper chromosphere cannot be explained by this model, the assumed electron temperature ($\sim$ 50000 °K) being too high.

A new spicule model is suggested, in which the temperature is low (some 6000 °K) and the density is high (hydrogen content of the order of 10^{13} atoms per c.c.) through the chromosphere. This model is consistent with the COATES (1958) model derived from radio observations. The excitation of helium in the spicule is ascribed to the ultraviolet radiation from the hot, tenuous interspicular medium and from the corona. The broad profiles of the strongest chromospheric lines are explained in terms of "turbulence" and high opacity of the spicule.

1. *Introduction*

In recent years the concept has been developed that the solar chromosphere consists of *spicules* and *interspicular medium*. Many models of the inhomogeneous chromosphere have been presented. (Comprehensive description has been given by DE JAGER (1959) and by THOMAS and ATHAY (1961) and may be referred to.) While spicules have been observed mostly in the H_α line, recent observations obtained at eclipses (ATHAY and ROBERTS 1955, ATHAY and MENZEL 1956, HIEI 1961) and without eclipses (ATHAY 1958 and 1960) indicate that in the higher chromosphere all the line emission in the visual spectrum region comes only from spicules, the interspicular medium not contributing.

With respect to the lower chromosphere, we have but scanty knowledge of the spicular structure, though there is some indication that the spicules can be found down to a height of about 1000 km above the base of the chromosphere (MICHARD 1959). Lately, on a sequence of flash spectro-

---

1) Sterrewacht "Sonnenborgh", Utrecht. On leave from the Osaka University of Liberal Arts and Education, and the Institute of Astrophysics, University of Kyoto (Japan).

grams obtained at the 1958 eclipse in the South Pacific, HIEI (1961) could count the number of spicules down to $h \sim 1000$ km, using the following lines: H_α through H_8 of the Balmer series; Ca II H and K; Na D_1; He D_3, 4026 and 3888; Sc II 4247; Ca I 4227; and Sr II 4216 and 4078. According to him, in the higher chromosphere the number o spicules visible in light of the strongest lines increases rapidly with decreasing height and spicules become unresolved around $h \sim 5000$ km. But at about this height spicules begin to appear in the light of such medium strong lines as the Sr II lines, increase in number toward lower heights, and overlap one another at about $h \sim 3000$ km. In the weaker lines, spicules are visible at still lower heights. In this way, spicules were traced down to $h \sim 1000$ km in the Sc II and Ca I lines. Close correspondence in the spicular structure along the flash arc was found between a couple of adjecent lines such as the H_ε and Ca II H lines or the H_8 and He I 3888 lines.

Though HIEI's observation is the only available evidence for the spicular structure of the lower chromosphere, it is very likely that the spicules do exist through the chromosphere above $h \sim 1000$ km and that they emit the visual chromospheric spectrum, including the metal lines as well as the helium lines.

Although statistical studies of spicules have been made by several authors (cf., *e.g.*, THOMAS and ATHAY 1961, p. 57*ff*.), there are no available observations of line intensities emitted by the spicule proper. However, a large amount of intensity data have been accumulated from many eclipse expeditions. The data refer to the homogeneous chromosphere, unresolved into spicules and interspicular regions. Thus, if the above statement on the spicular structure through the whole chromosphere above 1000 km is to be accepted, one may require that any spicule model combined with the obtained spicule statistics should be able to explain these eclipse intensity data. Since the *Ca II H* and *K* lines are the strongest lines in the chromosphere, reaching the greatest height, it may be interesting to use these lines as a touchstone in examining models of the chromosphere.

Among many solar physicists, ATHAY, THOMAS and their colleagues have studied chromospheric problems with keen interest. Their efforts have recently been summarized in a monograph by THOMAS and ATHAY (1961) (hereafter referred to as *TA–61*). In view of their detailed treatment, the chromospheric model developed in this book may deserve special attention. We shall call this model the ATHAY–THOMAS, or briefly *AT*, *model*. (Note that this model is different from the old ATHAY–MENZEL–THOMAS model quoted by DE JAGER (1959, Section 26).)

In this note, we shall first demonstrate that the AT model cannot explain the observed K line intensity. The analysis of metallic lines leads one to a really cold and dense spicule model. The excitation of helium and the broad profiles of the strongest chromospheric lines will be reconsidered.

2. *Interpretation of the eclipse K line intensity on the* ATHAY–THOMAS *model*

The AT model of the chromosphere was derived from analyses of the hydrogen and helium spectra. In this model, a spicule is a relatively cold and dense mass of gas, embedded in the hot and tenuous interspicular medium. In the lower chromosphere ($1000 \lesssim h \lesssim 4000$ km) the spicule has an electron temperature $T_e \lesssim 11000$ °K, but in the upper chromosphere ($h \gtrsim 4000$ km) the temperature is as high as 4 to 5×10^4 °K and the density is of the order of 10^{11} particles per cm^3 (TA–61, Chap. 7 and 10). More particularly at $h \sim 6000$ km, within the spicule T_e is ~ 50000 °K and the electron density is $\log n_e \sim 11.0$ to 11.8, and spicules occupy about 1 to 0.1 per cent of the entire surface of the sun. (According to the model, in the lower chromosphere the helium lines are emitted by the interspicular medium.)

ATHAY (1960) estimated, on this model, the integrated absolute intensity of the K line, emitted by a 1–cm slice of the spicule body (diameter ~ 700 km), extending from $h \sim 6000$ km upward. The value thus obtained, $\log E \sim 13$, was compared with the intensity from the flash observations, $\log E \sim 14$. It was concluded that these two results agreed well. (The difference of a factor 10 is reduced if $n_e \sim 6 \times 10^{11}$ is used instead of 10^{11} as done by ATHAY.) However, apart from some errors in this estimate, such a comparison seems meaningless, because the observed intensity does not refer to the spicule body but to the averaged chromosphere as is clearly indicated (TA–61, p. 34) and the spicules cover only a small fraction of the solar surface. Here we shall develop our argument on a more accurate numerical basis.

For this purpose, we shall successively calculate the populations of some atomic levels according to the following scheme, and compare the finally deduced hydrogen content with that in the AT model:

$$\text{Observed K line intensity} \xrightarrow{(a)} n_U \xrightarrow{(b)} n_U{}^* \xrightarrow{(c)} n_L{}^*$$

$$\rightarrow n^*(\mathrm{Ca}^+) \xrightarrow[(d)]{} n^*(\mathrm{Ca}^{++}) \rightarrow n^*_{\text{calcium}} \xrightarrow[(e)]{} n^*_{\text{hydrogen}} .$$

n's denote number densities. U and L stand for the upper level ($4p^2\mathrm{P}^\circ_{1^1/_2}$) and the lower level ($4s^2\mathrm{S}_{^1/_2}$), respectively, while an asterisk refers to a spicule. The calculation refers to $h \sim 6000$ km, as ATHAY does. The steps are now briefly explained.

Step a: The integrated intensity of a flash spectrum line, $E(h)$, may be represented by a barometric formula with a constant logarithmic gradient β

$$E(h) = E(0)\, e^{-\beta h}, \tag{1}$$

where $E(0)$ refers to the base of the chromosphere. In a homogeneous chromosphere, the population of the upper level, n_U, of the line can then, approximately be derived from $E(h)$ through the equation

$$E(h) = N(h)\, h\nu A = n_U(h) \sqrt{2\pi R}\, \beta^{-^3/_2}\, h\nu A, \tag{2}$$

provided self-absorption is negligible (cf. UNSÖLD 1955, p. 618). In this equation, ν denotes the frequency of the line, A the spontaneous transition probability, and R the radius of the sun. When the chromosphere is not transparent in the line, eq. (2) gives a lower limit for the population of the upper level.

The High Altitude Observatory eclipse data (ZIRKER 1958; TA–61, p. 400) do not include the K line, but the H line. HOUTGAST (1957) gives the intensities for both the H and K lines. From a comparison of the two series of observations at the same eclipse (multiplying HOUTGAST's data by a factor 4π), we estimated the K line intensity: $\log E = 14.2$ at $h \sim 6000$ km in the H.A.O. intensity scheme. (HOUTGAST (1961) obtained $\log E = 14.13$ from the 1954 eclipse at Gotland.) We adopt $\beta = 0.7 \times 10^{-8}$ cm^{-1} also from HOUTGAST's data. (ZIRKER gives 0.68×10^{-8} to the H line.) $A_K = 1.5 \times 10^8$ is used after ALLEN (1955). From these data we obtain for the upper level of the K line,

$$n_U(6000) \sim 0.19 \text{ per cubic centimeter} \tag{3}$$

of the homogeneous chromosphere.

Step b: These excited atoms in reality concentrate in spicules which occupy a fraction of 1 to 0.1 per cent of the whole area of the sun at this height. For simplicity we shall assume 0.3 per cent which is valid within a factor 3. Then the corresponding population within a spicule will be

$$n_U{}^* \sim 60 \text{ cm}^{-3}. \tag{4}$$

Step c: At the high kinetic temperature $T_e \sim 50000$ °K, the emission of the K line is determined mainly by collisional transitions from the ground level, followed by spontaneous emission. The collision cross sections for the H and K lines were first calculated by JEFFERIES (1954) using a weak coupling approximation. For the K line he obtained a value of $9.9\ \pi a_0{}^2$ (a_0: the first BOHR radius). Recently VAN REGEMORTER (1960) revised the cross sections by taking into account strong coupling effects. We assume from the latter author's results a constant cross section $\bar{Q}_K = 35\ \pi a_0{}^2$. Then, for $n_e \sim 6 \times 10^{11}$ (the upper limit in the AT model), the population ratio is given as

$$\frac{n_U{}^*}{n_L{}^*} \simeq \frac{n_e C_K}{A_K} \sim 1.4 \times 10^{-3}, \tag{5}$$

where C_K is the collisional excitation coefficient

$$C_K = \bar{Q}_K \left\{ \left(\frac{8kT_e}{\pi m} \right)^{1/2} \left(1 + \frac{h\nu}{kT_e} \right) e^{-h\nu/kT_e} \right\} \sim 3.6 \times 10^{-7}. \tag{6}$$

ATHAY (1960) *guessed* this ratio to 1/20. The collisional excitation is more effective than the radiative one by a factor 20 (compare with eq. (12)), and then the excitation via recombination by a factor of about

100. (The departure from local thermodynamic equilibrium at $T_e = 50000°$ amounts to a factor 700.) Since the Ca^+ ions are mostly in the ground level, we have

(7) $$n_L^* \sim 4 \times 10^4 \sim n^*(Ca^+).$$

Step d: At $T_e \sim 50000$ °K the ionization of calcium is determined by a coronal-type ionization formula, in which collisional ionizations balance photoelectric recombinations. For later use we have computed the ionization equilibrium between Ca^+ (ionization potential = 11.87 eV) and Ca^{++} ions for a wide range of kinetic temperatures (Fig. 1). In this

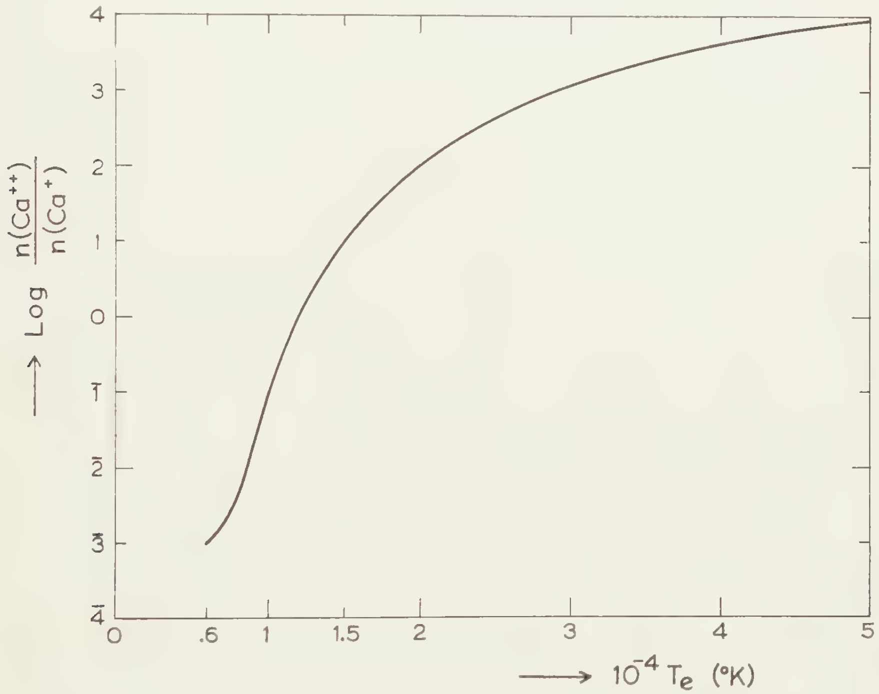

Fig. 1. Ionization equilibrium between Ca^+ and Ca^{++} in the chromosphere.

computation, the influence of the $4p\,^2P°$ level was taken into account. By a hydrogen-like approximation (cf. Burgess 1960), a constant cross section of 1 πa_0^2 was assumed for collisional ionizations. Recombination coefficients were based on Green's (1949) theoretical oscillator strengths for the continua of Ca^+. At low temperatures the ionization by ultraviolet radiation becomes predominating. For $\lambda \lesssim 1500$ Å a radiation temperature of 5000 °K was tentatively assumed according to the rocket measurements (De Jager 1955).

In the present case the ionization formula leads one to the ratio

(8) $$\frac{n^*(Ca^{++})}{n^*(Ca^+)} \sim 0.9 \times 10^4.$$

(In this step Athay's guess was right.) Since Ca^{++} has an ionization

potential of 51.21 eV, one can expect $n^*(Ca^{3+})/n^*(Ca^{++}) < 1$. Consequently, the total number density of calcium per unit volume of the spicule is estimated to be

$$n^*_{\text{calcium}}\,(6000) \sim n^*(Ca^{++}) \sim 4 \times 10^8. \tag{9}$$

Step e: Finally, introducing the hydrogen to calcium abundance ratio $H/Ca = 7.1 \times 10^5$, derived for the photosphere (Goldberg, Müller, and Aller 1960), we obtain the hydrogen content per cubic centimeter of the spicule

$$n^*_{\text{hydrogen}}\,(6000) \sim 3 \times 10^{14}. \tag{10}$$

This is the consequence from the AT model when we try to interpret the observed K line intensity on this model.

In the AT model, on the other hand, hydrogen is almost completely ionized ($n_p/n(H) \sim 10^4$) so that

$$n^*_{\text{hydrogen}} \simeq n_p \simeq n_e \sim 1 \text{ to } 6 \times 10^{11}. \tag{11}$$

Thus, we find a discrepancy of a factor 1000 between the AT model itself and what this model implies. If $n_e \sim 1 \times 10^{11}$ is used in *Step c* the situation becomes worse. Mistakes in Athay's estimate are found in *Steps b* and *c*.

Although our calculation is not entirely exact, one cannot escape from this great inconsistency. (The effect of self-absorption turned out to be unimportant, for the optical thickness of the spicule in the line center is about 0.7.) Causes for this contradiction can be found in reviewing the above processes. Among several uncertainties involved, one can pick up two main points: (1) the uncertainty in the spicule statistics and (2) the assumption of the high temperature $T_e \sim 50000$ °K.

As for the first point, according to several investigations, there is a considerable divergence in the estimated frequency of spicules at $h \sim 6000$ km (see, *e.g.*, TA–61, Fig. 3–12). The range of this divergence, however, does not seem to be greater than a factor of, say 30, so that the situation cannot be very much improved.

The second point, on the other hand, introduces a serious effect through *Step d*. If we could skip this step, that is to say, if $n^*(Ca^{++})/n^*(Ca^+) \lesssim 1$, the hydrogen content derived from the K line intensity would become close to that in the AT model. This implies that the probable kinetic temperature within the spicule should be much lower that the one assumed in this model. This conclusion seems to be a matter of course when we think of the very strong Ca II emission lines in the chromosphere, where the density of material is low. It may also be noted that in order to explain radio observations in millimeter and centimeter wavelength regions it was necessary to introduce a new model which was difficult to reconcile with the above quoted AT model (TA–61, Chap. 8).

The foregoing argument may directly be applied to any other model.

Although opinions still differ on whether the spicule is a relatively cold mass embedded in the hot, tenuous sub-coronal material or whether it is hotter than the surrounding medium, most of authors agree in ascribing high kinetic temperatures ($T_e \gtrsim 20000$ °K, say) to the spicule, at least, in the upper chromosphere. (Cf. DE JAGER 1959, Section 26; MICHARD 1959.) However, such hot spicule models would give rise to a similar difficulty as we met in the AT model.

3. *An alternative spicule model*

We shall now try to derive an alternative model which is adequate to interpreting the K line intensity from the flash spectrum. An upper limit for the kinetic temperature of the spicule may be found if it is required that the ratio $n^*(\mathrm{Ca}^{++})/n^*(\mathrm{Ca}^{+})$ should not exceed unity. With the aid of Fig. 1, one can place this limit at $T_e \sim 12000$ °K. Probably, the kinetic temperature within the spicule is close to 6000 °K, a value which has been found for the ionization and excitation of hydrogen in homogeneous models of the chromosphere (VAN DE HULST 1953, BÖHM-VITENSE 1955). What do we find if we assume a temperature of 6000 °K? We follow the same argument as before, *Steps a* and *b* being kept unchanged.

Step c: In this case almost all calcium atoms are in the singly ionized stage. The ratio of n_U^*/n_L^* decreases. The excitation by photospheric radiation becomes more important than the collision. The residual intensity of the Fraunhofer K line (0.02 of the continuum according to GOLDBERG, MOHLER, and MÜLLER 1959) with a dilution factor 2 may be assumed to be the radiation source. Since the intensity of the continuum in this spectrum region corresponds to the radiation temperature $T_r = 6600$ °K (GOLDBERG and PIERCE 1959), we estimate the excitation temperature $T_{ex} \sim 3600°$ for the K line. This determines the population ratio

$$\frac{n_U^*}{n_L^*} = \frac{g_U}{g_L} e^{-h\nu/kT_{ex}} \sim 0.78 \times 10^{-4}, \tag{12}$$

where g's are the statistical weight of the levels concerned. The collisional excitation with the assumptions $\bar{Q}_K = 35\ \pi a_0^2$ and $n_e \sim 1 \times 10^{11}$ adds only 2×10^{-6} to the above value in the present case.

Step d: As a result, from eq. (4) we obtain

$$n_L^* \sim 8 \times 10^5 \sim n^*(\mathrm{Ca}^+) \sim n^*_{\mathrm{calcium}}. \tag{13}$$

Step e: Finally the hydrogen content is found to be

$$n^*_{\mathrm{hydrogen}}\,(6000) \sim 6 \times 10^{11}. \tag{14}$$

With the value in (13), the optical thickness of a spicule in the line center can easily be estimated. The absorption coefficient in the center of the K line is given by

$$k_0 = \frac{\sqrt{\pi}\, e^2}{mc^2} \cdot \frac{\lambda^2 f}{\Delta\lambda_D} \sim 2.4 \times 10^{-13}. \tag{15}$$

Here λ is the wavelength of the K line ($=3934$ Å), f the oscillator strength ($=0.67$), and $\Delta\lambda_D$ the Doppler width. A "turbulent" velocity of 16 km/sec was assumed (see section 4). The optical thickness of a spicule with a diameter $D=1000$ km is, then,

$$\tau_0^* = k_0 n_L^* D \sim 20. \tag{16}$$

Such a large value of τ_0^* implies that our estimate of the hydrogen content in (14) is too small. A correct value may be close to 10^{13}.

The high opacity of a spicule in the centers of the H and K lines may be inferred from the ratio of the observed intensities of these lines, and from the smaller intensity gradients for these lines than those for the infrared triplet lines which share the upper level with the H and K lines. From the infrared lines, ZIRKER (1958) obtained $\beta \sim 1.3$ to 1.7×10^{-8} cm^{-1}.

A more accurate hydrogen content may be obtained from the intensities of some less strong lines appearing at somewhat lower heights. We choose the Sr II resonance line at λ 4078 Å due to the transition $5s^2\mathrm{S}_{1/2} - 5p^2\mathrm{P}^{\circ}_{1 1/2}$. From the data of HOUTGAST (1957) we adopt $\log E = 12.6$ and $\beta = 1.2 \times 10^{-8}$ at $h \sim 3000$ km (converted into the H.A.O. intensity units). For this transition $A = 1.3 \times 10^8$ (ALLEN 1955). By the same procedure as applied to the K line, we obtain the population of the upper level, $n_U = 1.3 \times 10^{-2}$ per unit volume of the homogeneous chromosphere, averaged over spicules and interspicular regions. Since spicules cover about 1 per cent of the total area of the sun at this height (TA–61, Table 3–3), we have the corresponding population $n_U^* \sim 1.3$ within the spicule. If a $T_{ex} \sim 4000$ °K can be assumed on the basis of the Utrecht Photometric Atlas (cf. ZIRKER 1958), we obtain the population of the ground level, which is practically equal to the total content of strontium:

$$n_L^* \sim 3.4 \times 10^3 \cdot n_U^* \sim 4.2 \times 10^3 \sim n^*(\mathrm{Sr}^+) \sim n^*_{\mathrm{strontium}}. \tag{17}$$

The optical thickness of the spicule in the center of the 4078 line turns out to be $\tau_0^* \sim 0.10$, so that self-absorption is negligible. From the abundance ratio H/Sr $= 2.5 \times 10^9$ (GOLDBERG, MÜLLER, and ALLER 1960), we are finally led to the hydrogen content within the spicule at $h \sim 3000$ km,

$$n^*_{\mathrm{hydrogen}}(3000) \sim 1.1 \times 10^{13}, \tag{18}$$

being consistent with the above estimate from the K line. (There is some indication that the density in the spicule varies little with height.) It may be noted that from BÖHM-VITENSE's (1955) analysis we have obtained a density of the same order of magnitude as this, when we tried to translate her model into an inhomogeneous model.

Since the electron density may be of the order of 10^{11}, most of hydrogen atoms must be neutral. This indicates that our assumption of $T_e \sim 6000$ °K is nearly correct.

Summarizing the above arguments, we may conclude that a spicule is a really cold and dense mass of gas. The kinetic temperature does not

exceed $T_e \sim 12000\,^\circ$K, it is perhaps about $6000\,^\circ$K. The density is of the order of 10^{13} per cubic centimeter. The change of physical conditions in the spicule with height may be small. (Note the abrupt rise in T_e at $h \sim 4000$ km in the AT model.) For the interspicular medium, with which the flash spectrum has nothing to do, we assume a hot and tenuous medium of gas for the reasons explained in subsequent sections.

Our spicule model sharply contrasts with many of the models thus far presented (cf. De Jager 1959, Section 26). But we are strongly supported by the Coates (1958) model which was derived solely from the radio data obtained at the wavelengths of 8.6 and 4.3 mm. In his model the spicule ($D = 1500$ km) has a constant electron temperature at $6400\,^\circ$K through the chromosphere and an electron density which varies slowly from 8.9×10^{10} at $h = 2000$ km to 2.2×10^{10} in the upper chromosphere. (The AT model could not explain satisfactorily the radio observations as mentioned before.) Indeed, his model and ours complement each other in the sense that his model gives the distribution of the electron temperature itself and the electron density, while our model furnishes the hydrogen content and some information about the electron temperature. Our model is also in harmony with the viewpoint that the spicule may be formed by *some* mechanism in the lowest, homogeneous part ($0 \lesssim h \lesssim 1000$ km) of the chromosphere, where the density lies in the range from 10^{15} to 10^{13} and the kinetic temperature in the range from 4000° to at most $8000\,^\circ$K (De Jager 1959, Section 19; TA–61, chap. 6 and 10).

The observed intensities of the flash spectrum lines may be explained as a combination of various effects such as the height distribution of spicules, change of the spicule size with height due to (collisional and radiative) interaction with the exterior media, self-absorption, and a possible change with height of physical conditions within the spicule.

4. *Excitation of helium and profiles of strong lines*

There are two important things we have left undiscussed thus far. The first is the problem of the excitation of helium, and the second the problem concerning the broad profiles of the strongest lines such as the H_α, H_β, H_γ, H and K, and He D_3 lines. These points have been thought to favor the high temperature model of the chromosphere. Now they should be explained on our cold spicule model. We shall briefly suggest possible directions in which the solution could be looked for.

Concerning the first point, the most probable source of the high excitation of helium will be the hard ultraviolet radiation from the corona and from the interspicular medium (Miyamoto 1947; Shklovsky and Kononovitch 1958). Miyamoto's original theory was rejected by Athay and Menzel (1956) for two main reasons: (1) a high opacity of the cold, homogeneous chromosphere does not allow the ultraviolet radiation from the corona to penetrate deeply into the chromosphere, and (2) the number of ultraviolet quanta from the corona being capable of ionizing helium

atoms is not sufficient to excite the visual He I lines to the observed intensities by two orders of magnitude (a singlet line at λ 6678 Å was used in the later argument in TA–61, p. 232*ff*. in place of the D_3 line in the original paper).

For the current inhomogeneous models of the chromosphere, with the hot and diffuse interspicular medium, the difficulty (1) is removed. As for the second argument, it can be shown that the interspicular medium of the chromosphere may contribute to the emission of hard ultraviolet radiation much more than the corona does. Consider, for example, the free-free emission from both regions. The intensity of the emission is proportional to $n_e^2\, T_e^{-1/2}\, e^{-h\nu/kT_e}$. Assume an electron density of 10^8 and a temperature 10^6 °K for the corona, and $n_e = 10^9$ and $T_e = 10^5$ °K for the interspicular medium. Comparing the contributions from the two media at a wavelength of 504 Å (ionization limit of He I), we find that the interspicular medium emits about 30 times more quanta than the corona does, per unit volume. With regard to the free-bound emission, the difference amounts even to 700. Although the distribution of electron density and temperature in the interspicular medium is not yet certain, it seems possible to interpret the emission of helium lines by the cold spicule as due to the effect of the ultraviolet radiation from the exterior media. (Cf. ALLEN 1961.) A model of the interspicular region should be established before one can reach the solution.

We may point out a second possibility: the collisional interaction between the cold spicule gas and the hot interspicular gas. Since the gas pressure in the spicule may be considerably higher than in the interspicular region, the spicule tends to expand. A strong interaction between the two kinds of gas masses can be expected. Helium atoms in the outermost layer of the spicule may be ionized by collisions with electrons from the hot surrounding. Magnetic fields, supposed to be present, may control this interaction to some extent. Probably, however, the ultraviolet radiation plays a more important part than this latter mechanism.

Now we turn to the problem how to explain the observed profiles of the strongest lines quoted above. The flat-topped, and often rectangular profiles with large half widths of these lines may be interpreted in terms of "turbulence" and self-absorption (cf., *e.g.*, UNSÖLD 1955, Section 142). When a constant source function, that is, the Planck function at an excitation temperature, $B(T_{ex})$, is assumed over a line through an emitting layer and the absorption coefficient is Dopplerian, the line profile may be represented by the well-known equation

$$I(\Delta\lambda) = B(T_{ex})\{1 - e^{-\tau(\Delta\lambda)}\} \text{ with } \tau(\Delta\lambda) = \tau_0\, e^{-\left(\frac{\Delta\lambda}{\Delta\lambda_D}\right)^2}. \tag{19}$$

Here $\tau(\Delta\lambda)$ denotes the optical thickness of the layer in the line at a distance $\Delta\lambda$ from the line center and τ_0 is the value at the center. Since the spicule has a rather small opacity in the D_3 line ($\tau_0^* \sim 0.2$ at

$h \sim 6000$ km), this line profile gives evidence for a "turbulent" velocity of 16 km/sec (TA–61, p. 71; cf. also UNSÖLD 1931 and CLUBE 1958). Combining this velocity with the observed half widths (TA–61, p. 71), we find, with the aid of the above formula, the optical thickness of the spicule in the centers of the H_α, H_β, H_γ, and K lines to be 18, 4.9, 4.0, and 20, respectively. The heights, which these line profiles refer to, lie in a probable range from 4000 to 7000 km and may be different for different lines (ATHAY 1958 and 1960).

The last mentioned value for the K line may be compared with (16). (The value in (16) should be increased.) It seems unnecessary, and even unnatural to introduce such a particular broadening mechanism into the K line as ATHAY (1960) suggested (gyration of Ca^+ ions about magnetic lines of force within a spicule). (Cf. also TA–61, p. 75*ff*.) The values for the Balmer lines are consistent with those expected from BÖHM–VITENSE's (1955) estimate for 2-level hydrogen atoms when the spicular structure is introduced.

Such large opacity of a spicule predicts, however, very flat-topped profiles of the strongest lines, much more conspicuous than those illustrated by ATHAY (1958 and 1960). In this respect, further and refined observations are highly desirable.

For a detailed consideration of line profiles, the assumption of a single value of the "turbulent" velocity for any element might be misleading. It is conceivable that *within* the spicule the gas has, besides the thermal motion, a small-scale mass motion. But the high opacity of the spicule in the strongest lines suggests that in these lines we are observing the rather thin outer layers of the spicule. If this is the case, one has to take into account several other effects such as (1) diffusion of the spicule gas into the interspicular medium ("thermal" character), (2) slow swirling of the spicule as a whole ("turbulent" character), and (3) inclination of the spicule axis with respect to the normal of the surface of the sun (important in the lower chromosphere; "turbulent" character). The variation of the source function across the emitting layer may exist and may be different in different lines.

5. *Conclusion*

In this note we have presented our chromospheric model in broad features and suggested how it could be developed further. The chromosphere may be depicted as a layer of the solar atmosphere, through which a large-scale circulation of matter and energy takes place between the photosphere and the corona. The spicule may be the feature by which matter and energy are supplied to the corona from below, and the interspicular regions are the medium where the hot material from the corona is slowly falling down. The former emits the visual spectrum of the chromosphere, and the latter may be the source of the far ultraviolet spectrum including the lines of multiply-ionized elements and the continuum. The lowest

part of the chromosphere ($0 \lesssim h \lesssim 1000$ km), where the spicular structure is no longer discernible, might be the layer in which the material from the corona, now cooled down, is mixed with the cold material stored there or supplied from below.

In relation to the spicules, which appear as the "fine mottles" on monochromatic images of the sun made in the H_α or K lines, the physical nature of the "coarse mottles" and the interrelation between these two formations in the chromosphere should also be investigated. (Concerning the coarse mottles, cf., *e.g.*, DE JAGER 1957 and 1959, Sections 21–24; KIEPENHEUER 1960; STEPANOV 1960; GIOVANELLI and JEFFERIES 1961.)

We intend to develop the spicule model suggested above into a more concrete model of the chromosphere. Observations of the spicular structure of the chromosphere with a high-resolution (both in geometrical and in spectroscopic sense) spectrograph are of fundamental importance and urgently needed.

Acknowledgments

The author wishes to express his cordial thanks to Professor C. DE JAGER and Professor M. G. J. MINNAERT, Director of the Utrecht Observatory, for helpful discussions about the chromospheric problems. His thanks are due also to Dr. J. HOUTGAST for information about the flash spectrum line intensities. The author's stay in Utrecht is supported by a fellowship from the Ministry of Education, Arts, and Sciences of the Netherlands.

REFERENCES

ALLEN, C. W., "Astrophysical Quantities", University of London, The Athlone Press. London. 1955.

———, Proc. 10th Int. Coll. Ap. Liège, "Les Spectres des Astres dans l'Ultraviolet Lointain", p. 241 (1961).

ATHAY, R. G., Ann. d'Ap., **21**, 98 (1958); *ibid.*, **23**, 250 (1960).

——— and W. O. ROBERTS, Ap. J., **121**, 231 (1955).

——— and D. H. MENZEL, Ap. J., **123**, 285 (1956).

BÖHM-VITENSE, E., Zs. f. Ap., **36**, 145 (1955).

BURGESS, A., Ap. J., **132**, 503 (1960).

CLUBE, S. V. M., M. N., **118**, 18 (1958).

COATES, R. J., Ap. J., **128**, 83 (1958).

DE JAGER, C., Ann. Géophys., **11**, 330 (1955).

———, Bull. Astr. Inst. Netherl., **13**, 133 (1957).

———, "Structure and Dynamics of the Solar Atmosphere", Handb. d. Phys., **52**, 80 (1959).

GIOVANELLI, R. G., and J. T. JEFFERIES, Australian J. Phys., **14**, 212 (1961).

GOLDBERG, L., O. C. MOHLER, and E. A. MÜLLER, Ap. J., **129**, 119 (1959).

———, E. A. MÜLLER, and L. H. ALLER, Ap. J. Suppl. Ser., **5**, No. 45 (1960).

——— and A. K. PIERCE, "The Photosphere of the Sun", Handb. d. Phys., **52**, 1 (1959).

GREEN, L., Ap. J., **109**, 289 (1949).

HIEI, E., Reported at the Annual Meeting of the Astronomical Society of Japan in May, 1961. Private communication (1961). Cf. Z. SUEMOTO and E. HIEI, Publ. A. S. Japan, **11**, 122 (1959).

HOUTGAST, J., Rech. Astr. Obs. Utrecht, 13, Part 3 (1957).
————, Bull. Astr. Inst. Netherl., No. 513 (1961).
JEFFERIES, J. T., Australian J. Phys., 7, 22 (1954).
KIEPENHEUER, K. O., Rendiconti S.I.F. XII Corso, "Radioastronomia Solare", 39 (1960).
MICHARD, R., Ann. d'Ap., 22, 547 (1959).
MIYAMOTO, S., Mem. Coll. Sci. Kyoto Univ., 25, 31 and 63 (with S. MATSUSHIMA), (1947).
SHKLOVSKY, I. S., and E. V. KONONOVITCH, Astr. Zhur., 35, 37 (1958) = Soviet Astr., 2, 32 (1958).
STEPANOV, V. E., Izv. Krim. Astr. Obs., 23, 184 (1960).
THOMAS, R. N., and R. G. ATHAY, "Physics of the Solar Chromosphere", Interscience Publ. New York. 1961.
UNSÖLD, A., Zs. f. Ap., 3, 77 (1931).
————, "Physik der Sternatmosphären", Springer-Verlag. Berlin. 1955.
VAN DE HULST, H. C., Chapter 5 in "The Sun", ed. G. P. Kuiper. Univ. Chicago Press. Chicago. 1953.
VAN REGEMORTER, H., M. N., 121, 213 (1960).
ZIRKER, J., Ap. J., 127, 680 (1958).

CONTENTS

PRINTED IN THE NETHERLANDS
DRUKKERIJ HOLLAND N.V., AMSTERDAM